

2
2000



LIBRARY
Michigan State
University

This is to certify that the

thesis entitled
The Integration of the Geographical Information System (GIS) and the Scientific Visualization (SVIS) for the simulation of the water runoff in a Watershed
presented by

Chia-Yii Yu

has been accepted towards fulfillment
of the requirements for

MS degree in *AE*

E.W. Parker Arlema

Major professor

Date *12/14/99*

PLACE IN RETURN BOX to remove this checkout from your record.
TO AVOID FINES return on or before date due.
MAY BE RECALLED with earlier due date if requested.

DATE DUE	DATE DUE	DATE DUE

**THE INTEGRATION OF THE *GEOGRAPHICAL INFORMATION SYSTEM* (GIS)
AND THE *SCIENTIFIC VISUALIZATION SYSTEM* (SVIS) FOR THE SIMULATION
OF THE WATER RUNOFF IN A WATERSHED**

By

Chia-Yii Yu

A THESIS

Submitted to
Michigan State University
in partial fulfillment of the requirements
for the degree of

MASTER OF SCIENCE

Department of Agricultural Engineering

1999

THE

Geo

mar

(GP

usec

map

GPS

wat

coll

Wa

imp

ABSTRACT

THE INTEGRATION OF THE *GEOGRAPHICAL INFORMATION SYSTEM (GIS)* AND THE *SCIENTIFIC VISUALIZATION SYSTEM (SVIS)* FOR THE SIMULATION OF THE WATER RUNOFF IN A WATERSHED

By

Chia-Yii Yu

The objective of the thesis is to develop a general design tool based on the Geographical Information System (GIS) for the simulation of water resource management. The Scientific Visualization System (SVIS), Global Positioning System (GPS), Differential Global Positioning System (DGPS), and Remote Sensing (RS) are used to produce three-dimensional GIS watershed maps of exceptional accuracy. The maps can be readily updated for changes in land use, landslides, and the stream system.

SVIS changes a two-dimensional GIS map into a three-dimensional GIS map. GPS and DGPS establish the precise three-dimensional position coordinates of the watershed, and thus correct the less accurate geo-referenced position database of GIS. RS collects the most recent land-surface information of the watershed.

The simulation of the water runoff on a vegetable farm in the Te-Chi Reservoir Watershed in Taiwan was used as an example to appraise the performance of the improved GIS design tool. The Watershed was assumed to be homogeneous.

Copyright by
CHIA-YII YU
1999

B.

N.

Ci

Co

M

Gu

da

the

ACKNOWLEDGEMENTS

I like to express my sincere gratitude to my major professor, Professor F.W. Bakker-Arkema for his never-ending support and guidance of this study.

My sincere thanks to my committee members, Dr. J. Bartholic and Dr. W. Northcott for their insight, guidance, and support in this study.

I thank Dr. Alocilja for providing early assistance in my Master Degree program.

I appreciate the assistance of several governmental agencies of the Republic of China (R.O.C.), i.e. the Institute of Botany of the Academia Sinica, the National Science Council, the Environmental Protection Agency, the Water Resources Bureau of the Ministry of Economic Affairs, and the Food Agency of the Taiwan Provincial Government for making available the water-quality, hydrological, and GIS reports and databases.

Finally, a very special thank you to my parents and fiancé Tsui-Ting Yang, for their never-ending love, support, encouragement, and guidance.

LIST C

LIST C

CHAP

CHAP

CHAP

TABLE OF CONTENTS

LIST OF TABLES -----	x
LIST OF FIGURES -----	xii
CHAPTER 1 INTRODUCTION -----	1
CHAPTER 2 OBJECTIVES -----	5
CHAPTER 3 LITERATURE REVIEW -----	6
3.1 GIS-SVIS of Watershed -----	6
3.2 Geographical Information System (GIS) -----	7
3.2.1 Geo-Referenced Data -----	7
3.2.1.1 Analog and Digital Maps -----	7
3.2.1.2 Geo-Referenced Data Input -----	9
3.2.1.3 Map Projections and Coordinates Systems -----	10
3.2.2 GIS Computer Systems Selection and Personal Training -----	11
3.2.3 Applications of GIS -----	11
3.3 Scientific Visualization System (SVIS) -----	12
3.4 Global Positioning System (GPS) and Differential Global Positioning System (DGPS) -----	14
3.4.1 GPS Fundamentals -----	14
3.4.1.1 GPS Satellites -----	14
3.4.1.2 GPS Ground-Control Stations -----	15
3.4.1.3 GPS Users -----	15
3.4.1.4 NAVSTAR GPS Performance -----	16

5.1 Hardware -----	33
5.1.1 GIS Digitizer System -----	33
5.1.2 GPS Receiver -----	34
5.2 Software -----	35
5.2.1 ArcView GIS 3.1 and Extension Programs -----	35
5.2.1.1 ArcView GIS 3.1 -----	35
5.2.1.2 ArcView Spatial Analyst -----	36
5.2.1.3 ArcView Tracking Analyst -----	37
5.2.1.4 ArcView 3D Analyst -----	37
5.2.1.5 ArcView Image Analysis -----	37
5.2.2 Microsoft Excel 97 -----	38
5.3 Methods -----	38
5.3.1 Digitizing the Te-Chi Reservoir Watershed GIS Maps -----	39
5.3.1.1 Preparing for Digitizing of a Watershed Map -----	40
5.3.1.2 Digitizing the Features of the Watershed Paper Map -----	42
5.3.1.3 Correcting the Digitizing Errors -----	42
5.3.2 Modifying GIS Maps by GPS, DGPS, and Relative Positioning Surveying -----	43
5.3.3 Processing Aerial Photographs by GIS -----	45
5.3.4 Simulating Water Runoff of A Watershed by GIS-SVIS -----	46
5.3.4.1 Hydrological Data and Software -----	47
5.3.4.2 Cell Runoff (mm) -----	49
5.3.4.3 Cell Sizes (m) -----	50
CHAPTER 6 RESULTS AND DISCUSSION -----	51

CH.

CH.

CH.

6.1 GIS Watershed Maps -----	51
6.1.1 Unmodified GIS Watershed Maps -----	51
6.1.2 Modified GIS Watershed Maps -----	53
6.1.3 Aerial Photographs Processed into GIS-SVIS Maps -----	58
6.2 GIS-SVIS Maps Illustrating Water Runoff -----	62
6.2.1 Slope-Type Factor -----	67
6.2.1.1 Slope Sun-Shade GIS-SVIS Map -----	69
6.2.1.2 Relative-Elevation GIS-SVIS Map -----	77
6.2.1.3 Sinkhole-Area and Relative-Elevation GIS-SVIS Map -----	78
6.2.1.4 Stream-Source Areas and Relative-Elevation GIS-SVIS Map -	80
6.2.1.5 Slope Flow-Length GIS-SVIS Map -----	80
6.2.2 Land-Use Factor -----	81
6.2.3 Slope-Type and Land-Use Factors -----	81
6.2.4 Calculation of Flow Rate -----	82
6.2.5 Flow Rate in the Drainage Area of the Chi-Chia-Wan Hydrological Station -----	87
6.2.5.1 Average Annual Runoff (Type A) -----	87
6.2.5.2 Medium Annual Runoff (Type B) -----	87
6.2.5.3 Maximum Daily Runoff (Type C) -----	88
6.2.5.4 Flow Rate Conclusion -----	88
CHAPTER 7 CONCLUSIONS -----	90
CHAPTER 8 RECOMMENDATIONS FOR FURTHER STUDY -----	91
CHAPTER 9 REFERENCES -----	92

APPE

Apper

Appe

Appa

App

App

App

Ap

APPENDICES	100
Appendix A. Table 5.2 The Annual Runoff Data over 27-Year Period in Seven Hydrological Stations in the Te-Chi Reservoir Watershed	101
Appendix B. Table 5.4 The Maximum Daily Runoff Data over 27-Year Period in Seven Hydrological Stations in the Te-Chi Reservoir Watershed	102
Appendix C. Table 6.1 The “aat.dbf” File of the Water Bodies Map of the Te-Chi Reservoir Watershed	103
Appendix D. Table 6.2 The “pat.dbf” File of the Vegetable Farm Map of the Te-Chi Reservoir Watershed	107
Appendix E. Table 6.3 The Registered Control Points and Modifications	109
Appendix F. Table 6.4 Statistical Program for the Modifications of the GIS Maps	111
Appendix G. Table 6.10 The Area and Location of the Sinkholes in the Te-Chi Reservoir Watershed	115

Table

LIST OF TABLES

Table 3.1 Specifications of the NAVSTAR and GLONASS Satellites -----	14
Table 3.2 Accuracy (95% probability) of NAVSTAR PPS and SPS -----	16
Table 3.3 Specifications of the Signal Systems of NAVSTAR GPS -----	17
Table 3.4 Wavelength and Frequency of Electromagnetic Radiation -----	23
Table 5.1 Specifications of the Digitized Paper Maps of the Te-Chi Reservoir Watershed -----	40
Table 5.2 The Annual Runoff Data Over 27-Year Period in Seven Hydrological Stations in the Te-Chi Reservoir Watershed -----	101
Table 5.3 Area Proportion of the Over 30% Slope -----	48
Table 5.4 The Maximum Daily Runoff Data Over 27-Year Period in Seven Hydrological Stations in the Te-Chi Reservoir Watershed -----	102
Table 6.1 The “aat.dbf” File of the Water Bodies Map of the Te-Chi Reservoir Watershed -----	103
Table 6.2 The “pat.dbf” File of the Vegetable Farm Map of the Te-Chi Reservoir Watershed -----	107
Table 6.3 The Registered Control Points and Modifications -----	109
Table 6.4 Statistical Program for the Modifications of the GIS Maps -----	111
Table 6.5 The Smallest Area of the Various Types of Land-Use in the Te-Chi Reservoir Watershed -----	62
Table 6.6 Average Annual Runoff (mm) (Type A) in Seven Drainage Areas in the Te- Chi Reservoir Watershed -----	66
Table 6.7 Medium Annual Runoff (mm) (Type B) in Seven Drainage Areas in the Te- Chi Reservoir Watershed -----	66
Table 6.8 Maximum Daily Runoff (mm) (Type C) in Seven Drainage Areas in the Te- Chi Reservoir Watershed -----	66
Table 6.9 Three Types of Area-weighted Runoff (mm) in the Te-Chi Reservoir Watershed -----	66

Table 6.10 The Area and Location of the Sinkholes in the Te-Chi Reservoir Watershed	115
Table 6.11 Predicted Flow Rate (m^3 /unit time) in the Drainage Area of Chi-Chia-Wan Hydrological Station	88

Figure

LIST OF FIGURES

Figure 4.1 Taiwan, Republic of China -----	29
Figure 4.2 The Te-Chi Reservoir Watershed in Taiwan, Republic of China -----	30
Figure 5.1 The GTCO AccuTab Surface-Lit LII Plus Digitizer System -----	33
Figure 5.2 The GTCO 16-button pointing device -----	34
Figure 6.1 The Unmodified GIS Map of Water Bodies in the Te-Chi Reservoir Watershed (Line and Polygon Features) -----	52
Figure 6.2 The Unmodified GIS Map of Vegetable Farm in the Te-Chi Reservoir Watershed (Point Feature) -----	54
Figure 6.3 The Unmodified GIS Map of Vegetable Farm in the Te-Chi Reservoir Watershed (Polygon Feature) -----	55
Figure 6.4 The Unmodified GIS Map of Water Bodies and Vegetable Farm in the Te-Chi Reservoir Watershed (Line and Polygon Features) -----	56
Figure 6.5 The GIS Map of the Cultivated Agricultural Areas in the Te-Chi Reservoir Watershed (Point Feature) -----	57
Figure 6.6 The Modified GIS Map of Water Bodies and Vegetable Farms in the Te-Chi Reservoir Watershed -----	59
Figure 6.7 The Aerial Photograph of the Te-Chi Reservoir and Its Surroundings -----	60
Figure 6.8 The Aerial Photograph of the Te-Chi Reservoir Processed by GIS-SVIS ---	61
Figure 6.9 The Annual Runoff in the Hydrological Stations of the Te-Chi Reservoir Watershed -----	63
Figure 6.10 The Locations of the Hydrological Stations in the Te-Chi reservoir Watershed -----	64
Figure 6.11 The GIS Map of the Hydrological Stations in the Te-Chi Reservoir Watershed -----	65
Figure 6.12 The GIS Map of Slope-Type in the Te-Chi Reservoir Watershed -----	68
Figure 6.13 The GIS-SVIS Map of Slope Sun-Shade at 4:20PM in the Te-Chi Reservoir Watershed -----	70

Figure

Figure 6.14 The GIS-SVIS Map of Slope-Type in the Te-Chi Reservoir Watershed ----	71
Figure 6.15 The GIS-SVIS Map of Relative Elevation in the Te-Chi Reservoir Watershed -----	72
Figure 6.16 The GIS-SVIS Map of Stream-Source Areas and Relative Elevations in the Te-Chi Reservoir Watershed -----	73
Figure 6.17 The GIS-SVIS Map of Flow-Length in the Te-Chi Reservoir Watershed --	74
Figure 6.18 The GIS Map of Land-Use in the Te-Chi Reservoir Watershed -----	75
Figure 6.19 The GIS-SVIS Map of Land-Use in the Te-Chi Reservoir Watershed -----	76
Figure 6.20 The GIS-SVIS Map of Area of Slope < 30% and Slope >= 30% in the Te-Chi Reservoir Watershed -----	83
Figure 6.21 The GIS Map of Area (Slope > 30%) of Cultivations, Roads, and Landslides in the Te-Chi reservoir Watershed -----	84
Figure 6.22 The Location of the Exemplified Vegetable Farm Area in the Te-Chi Reservoir Watershed -----	85
Figure 6.23 The Location of the Exemplified Vegetable Farm in the Te-Chi Reservoir Watershed -----	86

and th

digit

Heart

water

of wa

consi

effect

System

condi

Infor

(Den

data

resou

wate

entit

layer

wate

exec

1995

Chapter 1 INTRODUCTION

GIS-SVIS of a watershed integrates the Geographical Information System (GIS) and the Scientific Visualization System (SVIS) system with aerial photographs and digital images in order to represent the characteristics of a watershed (Raper, 1989; Hearnshaw and Unwin, 1994). GIS-SVIS improves on the traditional methods of watershed system assessment by its: (1) quick execution, (2) integration of different types of watershed information, (3) utilization of a variety of analysis tools, and (4) ability to consider the whole rather than part of the watershed, and (5) multi-dimensional display effect.

The *Watershed Geographical Information System* uses the *Watershed Information System* (which collects the transformed *Watershed Information*) to simulate a watershed's conditions. The *Watershed Data* is a collection of attributes of a watershed. *Watershed Information* is the raw watershed data used for analysis, evaluation, and decision-making (Denzer, 1993). The *Watershed Information System* transforms the raw watershed database into a systematic watershed database used in planning and managing of natural resources. The *Watershed Geographical Information Systems* comprise of: (1) a watershed geo-referenced database with information on the quantitative attributes and entities of a particular location, (2) a computer-based program for analyzing various layers of geo-referenced data and attribute-data of an entity, and for exploring the watershed relationships between entities, and (3) the list of personnel required for executing, operating, and maintaining GIS (Anonymous, 1997a; Congalton and Green, 1995; Dueker and Kjerne, 1989).

with

virtu

whic

(Kap

(Pier

Rang

Defer

devel

al., 19

dimer

i.e. th

and (3

points

twent

1996)

drastic

Avail

Drift

Ephen

broad

SVIS transforms a two-dimensional display of a GIS spatial database into a map with three-dimensional effect. The uniqueness of a GIS-SVIS display of a watershed is its virtual reality. SVIS is able to transform simulation data into a three-dimensional map which the human optic nerves and brain neurons can properly interpret (Denzer, 1993).

The Global Positioning System (GPS) is a satellite-based radio-navigation system (Kaplan, 1996). It is an improvement over older conventional radio-navigation systems (Pierce, 1946). There are two types of GPS: (1) the Navigational Satellites for Timing and Ranging (NAVSTAR) system developed and operated by the U.S. Department of Defense, and (2) the Global Orbiting Navigational Satellite System (GLONASS) developed and operated by the Ministry of Defense of the Russian Federation (Lowe et al., 1997). GPS permits land, sea, and airborne users to determine: (1) the three-dimensional position of the user, i.e. the latitude, longitude, and altitude, (2) the times, i.e. the satellite vehicle (SV) time, GPS time, and Universal Coordinated Time (UCT), and (3) the velocity of the user, by calculating the user-position change between two points over time or by computing the SV Doppler frequencies. Both GPS systems operate twenty-four hours a day, in all weather, and can be used anywhere in the world (Kaplan, 1996).

Differential Global Positioning System (DGPS) is a system for eliminating or drastically reducing the measurement errors caused by the effects of Selective Availability, Signal Bounce, Signal Noise, Ionosphere, Troposphere, Satellite Clock Drift, Code Measurement, Receiver Clock, Multipath Measurement, and Satellite Ephemerides (Bordin, 1996; Parkinson, 1996). A base station at a known location broadcasts the corrections of the errors (Capaccio et al., 1997). DGPS substantially

impro

sever

gover

certain

differe

(Cap

acqui

remot

obtain

collec

princi

electr

pictor

visua

imag

earth

the T

1996

adju

improves the accuracy of the GPS measurement. DGPS services are currently offered in several regions by private organizations for a subscription fee, and in some locations by governmental agencies free of charge. Consequently, as long as a DGPS service covers a certain area, a user can utilize a standard GPS receiver able to accept a particular differential input, and dramatically decrease or even eliminate the measurement errors (Capaccio et al., 1997).

Remote Sensing (RS) is a reconnaissance-from-a-distance technology which can acquire information on an object or phenomenon through the analysis of data collected by remote sensors (Avery and Berlin, 1992). RS is much different from *in situ sensing* which obtains information by physical contact of an object (Avery and Berlin, 1992). Data collection (Lee and Marsh, 1995) and data analysis (Ji and Mitchell, 1995) are two principle objectives of RS.

The quality of the RS data depends on the sensitivity of the remote sensors to electromagnetic energy i.e. light, heat, and radio waves, and determines the quality of the pictorial images of an object (Lee and Marsh, 1995). Data analysis depends on traditional visual interpretation or on complex computer processing of the RS photographs and images (Ji and Mitchell, 1995). RS can monitor a watershed's environment at any site on earth.

The Te-Chi Reservoir Watershed is a sub-watershed located at the headstream of the Ta-Chia-Chi river basin in the Central Mountain Range of Taiwan (Anonymous, 1996d). The multifunctional reservoir watershed is used for agriculture, tourism, flood adjustment, drinking-water supply, and hydroelectricity. The Te-Chi Reservoir

Management Committee is the chief authority. The Taiwan Power Company operates the Te-Chi Reservoir Dam and supplies hydroelectric power to the Ta-Chia-Chi river basin.

The total Te-Chi Reservoir Watershed area is 601.61 km² (232.28 mi²) (Anonymous, 1996d). Approximately 6.34% of the watershed area is used for agriculture (Anonymous, 1994c). The agricultural lands are mostly located along the Te-Chi Reservoir. The Reservoir has been subjected to bioenvironmental pollution for years (Anonymous, 1995c), and was therefore selected as the site for this GIS-SVIS-based water runoff study.

Chapter 2 OBJECTIVES

The objectives of this research are:

- (1) to develop GIS maps of the Te-Chi Reservoir Watershed.
- (2) to use the GIS maps for calculating the annual and maximum daily water-flow rates, and for developing the water-runoff maps in the Watershed.
- (3) to calculate the flow rates on a vegetable farm in a particular area of the Watershed.

Chapter 3 LITERATURE REVIEW

3.1 GIS-SVIS of A Watershed

Water resource conservation studies are important for a watershed because of the complicated nature of watershed-level environmental issues. GIS is essential to watershed simulation (Lyon and McCarthy, 1995). GIS systematically synthesizes watershed information and efficiently simulates specific geo-referenced data for analysis; it can be updated by remote sensing (Lee and Lunetta, 1995).

GIS, DGPS, and RS can be integrated to produce accurate and dynamical planes with the various properties of a specific area (Lyon and McCarthy, 1995). DGPS corrects the GIS watershed maps by the proper correction of signal measurement, and RS updates the map information by image-processing techniques. Thus, with a package of GIS, DGPS, and RS, a researcher is able to analyze in depth the water issues of a watershed.

SVIS, comprising a computer-aided graphical with human vision, supports the multi-dimensional display and the auto-animation of complex data sets. By integrating GIS and SVIS, the GIS dataset of a watershed can be displayed as a three-dimensional map (latitude, longitude, and altitude) or as a multi-dimensional map (latitude, longitude, altitude, and time...) (Anonymous, 1997c; Anonymous, 1996f). For example, for visualization the SVIS software "Data Explorer Visualization" (Anonymous, 1999) integrates the software programs ESRI's ARC/INFO, the ERDAS's IMAGE, and the Oracle Database, utilizing Digital Elevation Model (DEM), Digital Line Graphs (DLG) for the various output-model formats. By using the spatial effect of SVIS, the integration of GIS and SVIS becomes an excellent tool for watershed system analysis. A GIS-SVIS

system containing color differentiation and auto-animations is an excellent system-analysis and computation tool.

The following sections review the principles and interactions of GIS, SVIS, GPS, DGPS, and RS in order to simulate the water runoff in a watershed.

3.2 Geographical Information System (GIS)

Geographical information is of a dynamical nature because it synthesizes and updates the three information components of a region regarding: (1) space, (2) time, and (3) attributes (Chrisman, 1997). GIS is designed to input, store, update, manipulate, analyze, and illustrate all types of geo-referenced information by arranging systematically computer hardware, software, and geo-referenced data. Because of the ability of GIS of storing spatial information, analyzing geo-referenced data, and managing geo-referenced information in an integrated manner to display the area properties of a region, GIS is really a computer-based mapping system.

GIS requires knowledgeable, highly trained, and experienced personnel since it are not a fully automated system (Anonymous, 1997a).

3.2.1 Geo-referenced Data

3.2.1.1 Analog and Digital Maps

An expansive and adaptable definition of a map is “the physical or conceptual depiction of the characteristics of the Earth or other celestial body” (Robinson, 1976). Maps under this definition can be divided into two classes: (1) real or analog maps, and (2) virtual or digital maps. A real map is static and is a drawing or a scanned image. A virtual map is a data set stored in digital form; it is dynamic, and is more flexible than an

analog map for recording, examining, interrogating, and analyzing information over time (Lyon and McCarthy, 1995).

A GIS map is a digital map which represents locations on the Earth's surface in one or several coordinate systems, and which has been projected on a flat surface. The information provided includes spatial and descriptive information (Anonymous, 1997a). The spatial information describes the spatial relationships of the various geographical features of a region by topology; it can be represented as a point feature, as a line/arc feature, or as an area/polygon feature, and as a surface feature/entities of a region. Spatial and descriptive information is stored in graphical and tabular databases (Anonymous, 1997a). The link between a graphical database and its records in a tabular database is of a one-to-one link through a numerical identifier.

A point feature is represented: (1) by a discrete location with a shape too small to be shown as a line or area feature, and (2) by a point location without an area (Anonymous, 1997a).

A line/arc feature is a set of ordered coordinates which represent the linear shape of a map object when: (1) it is too narrow to be displayed as an area, and (2) it is a feature without width (Anonymous, 1997a).

An area feature represents a homogeneous area bounded by one or more arc features or by a set of polygons, and is measured in unit squared (Anonymous, 1997a).

A surface feature is a three-dimensional representation of geographic information, and is represented by a set of continuous data in which the map features are spatially continuous, i.e., there is an infinite set of values between any two locations. There is no clear or well-defined break between possible values of a surface feature. Models build

from regularly or irregularly spaced sample points on a surface can represent surfaces. Examples are the Grid model, the Lattice model, and the Triangulated Irregular Network (TIN) model (Anonymous, 1997a).

An entity is a collection of objects described by the same attributes. Entities are identified during the conceptual design phase of a database and an application design, and are represented by computerized cartographic-data structures.

The spatial relationships of a region are defined by its topology through mathematical procedures (Anonymous, 1997a). Connectivity (arc-node topology), area definition (polygon-arc topology), and contiguity (left-right arc topology) are three topological concepts employed in the analysis of spatial information.

Various geo-referenced data models are available in the literature to represent geographical information, e.g. the Coverage model, Image model, and Drawing model (Anonymous, 1997a).

3.2.1.2 Geo-referenced Data Input

There are many methods to input geo-referenced data, e.g., by map digitizing (Anonymous, 1996e), by map or aerial photography scanning (Anonymous, 1998b), by map tracking with DGPS, and by RS imagery and aerial photography (Anonymous, 1998c). Each process may encounter the following problems: (1) overlaying of two or more maps in the same region due to different map scales (Anonymous, 1996e), and (2) mistakes in the ground registration of the spatial database (Anonymous, 1997a). The specific features and the degree of accuracy of two maps at different scales are difficult to match up (Stevens, 1946). If the spatial database is not properly registered, a serious problem can occur during the latter stages of the analysis and assessment (Anonymous,

1996e). In addition, map digitizing can cause the wrong scale and symbols to be produced for displaying the desired details.

3.2.1.3 Map Projections and Coordinate Systems

Spatial data registration (multipurpose cadaster) requires a ground-based coordinate system so that the original data can be transformed and a fixed latitude/longitude relationship can be established (Anonymous, 1997a). Because of the curved surface of the Earth, a map projection is necessary to produce a flat map for a coordinate system of a particular spatial data registration (Synder, 1987).

A map projection is a mathematical technique for calculating the parallels and meridians on a map. The projection applies the mathematics of an ellipsoid, of a sphere (Latitude-Longitude), or of a flat coordinate system to develop (Chrisman, 1997): (1) a cylindrical projection, (2) a conical projection, and (3) an azimuthal (planar) projection. Several important projections such as the Mercator projection (Anonymous, 1996e), the US Quadrangle projection (Anonymous, 1996e), the Lambert Equal Area projection (Anonymous, 1996e), the Lambert Conformal projection (Anonymous, 1996e), the Robinson projection (Anonymous, 1996 b), and the Gnostic projection (Anonymous, 1996e) can be derived from the three basic projections. These map projections can be represented in a number of coordinate reference systems in specifying the ground registration of the spatial database. The coordinate reference systems include: (1) the Spherical coordinate system, (2) the two-dimensional Cartesian coordinate system, (3) the three-dimensional Cartesian coordinate system (Chrisman, 1997), (4) the State-Plane coordinate system (Anonymous, 1996e), (5) the Universal Transverse Mercator (UTM) coordinate system (Congalton and Green, 1995), and (6) the US Public Land Survey

coordinate system (Anonymous, 1996e). The correct selection of the map projection and the coordinate system is important in the registration of the geo-referenced database of a region because the GIS maps of different properties of a region cannot be overlaid if different map projections and coordinate systems are used (Muehrcke, 1986; Snyder, 1987; Thompson, 1988; Congalton and Green, 1995).

3.2.2 GIS Computer Systems Selection and Personnel Training

Not only should the characteristics of a geo-referenced data be well understood, the GIS computer system should be chosen carefully. Proper estimation of the hardware/software computing needs of the GIS-related research project is essential. In selecting the correct software, the following should be considered (Gupyill, 1988; Parker 1989): (1) the data input and editing should be simple, (2) the software should contain a cartographic analysis tool and should have modeling capability, (3) the software should run on different computer systems and operating systems, and (4) the software should be able to run under different hierarchical and relational database-management systems.

In selecting the hardware, the following should be considered (Gupyill, 1988; Parker 1989): (1) the size of the hard disk, (2) the clock speed and RAM of the computer, (3) the number of users, (4) the compatibility with input/output devices.

State-of-the-art GIS equipment and technology cannot be operated and properly maintained without well-trained personnel. Consequently, the staff occupies an essential place in a GIS system (Anonymous. 1997a).

3.2.3 Applications of GIS

The potential applications of GIS are broad. As long as a problem is associated with space, GIS is an excellent tool. In this research, GIS is applied to the simulation of

the water runoff in a watershed. The GIS maps can perform issue-settling tasks and undertake question-interrogating jobs.

3.3 Scientific Visualization (SVIS)

SVIS is important in environmental research. By representing numerical data in a visual format, SVIS can provide environmentalists and engineers with a better understanding of the results of their research. The human sense of sight intuitively reflects reality (Denzer, 1993).

SVIS assists GIS to: (1) create an exploratory spatial database by employing the Digital Terrain Model (DTM), the Digital Elevation Model (DEM), or other topographical database model (Anonymous, 1996f), and (2) use the exploratory spatial database to display a three-dimensional map (Anonymous, 1997c).

SVIS: (1) transforms symbolic data into geometric data and enables researchers to intuitively observe the results of simulation (Raper, 1989), (2) offers a method for seeing the unseen to enrich the process of scientific discovery and foster unexpected insights (Robinson, 1976), (3) allows the generation of images from complex multi-dimensional data sets (Anonymous, 1998b), and (4) allows the use of computer graphics (Domik, 1994), image processing (Anonymous, 1998b), computer vision (Hearnshaw, 1994), and computer-aided design (CAD).

The goal of SVIS is to provide new scientific insight through visual means. An estimated fifty-percent of the brain's neurons are associated with vision. SVIS in scientific computation aims at putting neurological machinery to work. Three-dimensional displays stimulate more neurons and therefore a larger portion of the brain in the problem-solving process. With two-dimensional contour maps, the mind must first

build a conceptual model of the relief before an analysis can be made. Considering the cartographic complexity of certain terrain, this is an arduous task for even the most dexterous mind. Three-dimensional displays simulate spatial reality, thus allowing the viewer to quickly recognize changes in elevation.

Some numerical models of watershed runoff movement require a large database (Domik, 1994). The most efficient way for researchers and analysts to study this information is to visually represent it. SVIS is used in many disciplines to interpret large, complex database sets and gain insight into the trends, patterns, dependencies, and missing data within a database (Worboys, 1995).

SVIS applied to GIS depends on psychological cues to create a natural three-dimensional display on a two-dimensional monitor. SVIS models do not result in photographs but in renditions (Keller and Keller, 1992). The process of generating a three-dimensional scene is termed rendering. To render a realistic scene, individuals rely on visual perspective cues and subtle changes in color and texture (Keller and Keller, 1992). Depth in a sense can result from feature obstruction and overlap, or from the addition of atmospheric attenuation such as fog or haze. Usually, the light intensity and clouds are measures of the relative distance within a scene. The presence of trees, or a seasonal characteristic such as snow, artificially enhances the sense of reality. A physiological cue, such as accommodation, convergence or the retinal disparity, can balance the three-dimensional image of a two-dimensional image (Domik, 1994).

SVIS is commonly used to model a terrain surface such as a watershed surface (Anonymous, 1994a). Most terrain algorithms are based on Fractal Geometry which in turn is based on the concept of Self-Similarity. Self-Similarity accounts for the change in

distance from a spatial feature; i.e., what appears at one scale is represented at the same or another scale (Domik, 1994). The Fractal Dimension of a surface can describe a landscape form. A fractal dimension is measured as a real number ranging between two and three, where two is for a perfectly smooth surface and three is for an infinitely variable surface.

3.4 Global Positioning System (GPS) and Differential Global Positioning System (DGPS)

3.4.1 GPS Fundamentals

NAVSTAR is based on a constellation of satellites that continuously transmit coded signals in two carrier frequencies L1 and L2 (Parkinson and James, 1996; Kromer and Landis, 1992). A GPS receiver should receive the navigational signals from at least four satellites in order to identify its three-dimensional position (latitude, longitude, and altitude) and its velocity in real time (Kaplan, 1996). A GPS system consists of: (1) the GPS satellites, (2) the GPS ground-control stations, and (3) the GPS users.

3.4.1.1 GPS Satellites

Table 3.1 Specifications of the NAVSTAR and GLONASS Satellites

GPS	NAVSTAR	GLONASS
No. of Space Vehicles	24	24*
Launch Base	Cape Canaveral, USA	Baikonur Cosmodrome, Kazakstan
No. of Orbital Planes	6	3
No. of Satellites Per Plane	4	8
Orbital Altitude (km)	20,200	19,130
Inter-orbital Plane Angle (Degree)	60	120
Orbital Inclination (Degree)	55	64.8
Period of Revolution	11hr, 58min, 00sec	11hr, 15min, 44sec

* Two space vehicles were decommissioned in 1996.

Data source: Lowe et al, 1997 and Kaplan, 1996

The GPS satellites send radio-navigation signals from space. Both the U.S. NAVSTAR and the Russian GLONASS GPS satellites orbit the Earth, and form a

nominal Operational Constellation. Each satellite transmits a signal at a specific frequency (Lowe et al., 1997). Some satellites have the same frequency but since they are located in antipodal positions in an orbit plane, or in different orbit planes, they do not appear at the same time in a user's view (Blanchard, 1996).

Table 3.1 describes the specifications of the U.S. and the Russian GPS satellites. Additional information on the satellites is given in Section 3.4.4.

3.4.1.2 GPS Ground-Control Stations

GPS ground control is provided by the tracking stations. A station measures the satellites' signals to compute their precise orbital position (ephemeris) and to correct the clock (Parkinson, 1996). The Master Control station transmits the satellites' ephemeris and clock offsets to the satellites which in turn incorporate the correction data into the radio signals to be sent to the GPS receivers (Kromer and Landis, 1992).

The NAVSTAR GPS satellites are controlled by the Master Control station located at Schriever Air Force Base, CO, U.S.A and four tracking stations located around the world (Kromer and Landis, 1992). The GLONASS GPS satellites are controlled by the Ground-based Control Complex (GCC) located at Moscow, Russia and a series of Command Tracking Centers (CTC) located at different locations in the Russia (Kuranov, 1995; Langley, 1995). The author employs the NAVSTAR system in this thesis because a GLONASS GPS receiver is not commercially available in the U.S.A.

3.4.1.3 GPS Users

A GPS system relies upon the precise distance measurement between the GPS user and the satellites (Anonymous, 1996a). Users determine their position on the earth

by accurately measuring the distance from four to twelve satellites. The satellites act as reference points and transmit their positions and time signals to the GPS user.

GPS technology consists of the GPS satellites, receivers, processors, and antennas, and can be used in navigating, positioning, timing, tracking, and mapping. A GPS receiver must receive at least four satellite signals to accurately compute the four dimensions of latitude, longitude, altitude, and time (Blanchard, 1996); the velocity of a user is calculated from his/her positions over an elapsed time period (Anonymous, 1996a).

3.4.1.4 NAVSTAR GPS Performance

The NAVSTAR GPS performance largely depends on the U.S. government actions and on the effects of atmospheric noise and bias.

The 1994 Federal Radionavigation Plan describes the type of NAVSTAR GPS services: (1) Precise Positioning Service (PPS), and (2) Standard Positioning Service (SPS). PPS cryptographic equipment is only available to designated U.S. governmental agencies, to the U.S. and Allied military, and to the civilian users specifically approved by the U.S. government. SPS is available to the users from all over the world without charge (Anonymous, 1995a).

Table 3.2 Accuracy (95% probability) of NAVSTAR PPS and SPS

NAVSTAR GPS Services	PPS	SPS
Horizontal Accuracy (m)	22	100
Vertical Accuracy (m)	28	156
Time Accuracy (nanosecond)	100	340

Source: U.S. Federal Radionavigation Plan, 1994

The U.S. Department of Defense degrades SPS accuracy in order to control the Selective Availability (SA) (See Section 3.4.1.6) (Parkinson, 1996) by adding a time-

varying bias (See Table 3.2). The SPS figures are 95% accurate; i.e. the equivalent of two-distance root-mean-square (2 drms) or twice the radial error standard deviation.

3.4.1.5 NAVSTAR GPS Satellite Signals

Table 3.3 represents the specifications of the signal systems of NAVSTAR. The NAVSTAR system broadcasts two microwave carrier-phase signals L1 and L2 (Parkinson and James, 1996; Kromer and Landis, 1992). The L1 signal contains the Navigation Message and the SPS code; the L2 signal provides the PPS code which enables the measurement of a physical error such as the ionospheric delay. In order to obtain specific information, the signals are modulated by three binary codes (Parkinson and James, 1996; Kromer and Landis, 1992): (1) a C/A (Coarse Acquisition) code, (2) a P (Precise) code, and (3) a Navigation Message.

Table 3.3 Specifications of the Signal Systems of NAVSTAR GPS

Signal Systems \ GPS Types	NAVSTAR
Carrier Phase Frequency: L1 (MHz)	1575.42
Carrier Phase Frequency: L2 (MHz)	1227.60
Signaling	CDMA*
Type of PRN Code	GOLD
Number of Code Elements (C/A Code, bit/millisecond)	1023
Number of Code Elements (P Code, bit/millisecond)	2.35×10^{14}
C/A Code Chipping Rate (Mbit/second)	1.023
P-Code Chipping Rate (Mbit/second)	10.23
Navigation Message (Chipping Rate, bit/sec)	50
Navigation Message (Modulation)	BPSK NRZ
Navigation Message (Total Length, second)	750
Navigation Message (Subframe Length, second)	6

1. k: frequency channel number (k=0,1,2...) with different channel spacing for L1 and L2.

2. FDMA: Frequency Division Multiple Access; CDMA: Code Division Multiple Access.

Data source: Axelrad and Brown, 1996; Parkinson and James, 1996; Filatchenkov, 1996; Kuranov, 1995; Raby, 1994.

The C/A code, a constantly changing Pseudo Random Noise (PRN) with a short chipping rate, is regarded as a Spoof code to modulate the L1 carrier phase of SPS in

order to acquire the P code (Parkinson and James, 1996). Each satellite is given a specific unencrypted C/A PRN code for identification, thus allowing any user of the system to decode and use the transmitted data. The U.S. Department of Defense de-synchronizes the satellite clock and thereby introduces an intentional error in the C/A code.

The P code, a constantly changing PRN at a long chipping rate, is an Anti-Spoofing code for modulating both the L1 and L2 carrier phase signals of PPS (Parkinson and James, 1996; Kromer and Landis, 1992). Because of its higher modulation bandwidth, the signal is significantly more precise than the C/A code. It is combined with an encrypted Y code, and thus a PPS user requires either a classified Anti-Spoofing Module for each receiver channel or a cryptographic decoding key.

The Navigation Message modulates the L1 carrier-phase signal mixed with C/A code signal, and contains data on a satellite's orbit, the clock correction, the ephemeris, the almanac, and other system parameters.

3.4.1.6 GPS Error Sources

Between space and a GPS receiver on the ground, the transmitted radio-navigational microwaves from the GPS satellites are affected by noises (Parkinson, 1996). Other sources of error are bias and human mistakes.

Specifically, the sources of the noise errors are: (1) the noise in the PRN code of the GPS satellites (Parkinson, 1996), and (2) the noise in the GPS receiver (Leick, 1995). The error in the PRN code is caused intentionally for security reasons. The noise error source in the GPS receiver is caused by the noise inherent in any electronic instrument measurement. The noise errors are: (1) selective availability, (2) signal bounce, (3) signal noise, (4) code measurement mistakes, and (5) receiver clock mismatch (Capaccio et al.,

1996 & 1997; Langley, 1997; Brodin, 1996; Misra et al., 1993 & 1996; Parkinson, 1996; Rossbach et al., 1996; Raby, 1994; Hartman et al., 1991; Doebelin, 1990).

The sources of the bias errors are: (1) selective availability, (2) satellite clock drift, (3) satellite ephemeride error, (4) ionospheric delay, (5) tropospheric delay, and (6) multipath reflection (Capaccio et al., 1996 & 1997; Langley, 1997; Brodin, 1996; Misra et al., 1993 & 1996; Parkinson, 1996; Rossbach et al., 1996; Raby, 1994; Hartman et al., 1991). According to the “1994 Federal Radionavigation Plan”, GPS policy requires some services to be degraded intentionally. The SA bias is an example of bias in the SPS information controlled by U.S. Department of Defense; it is introduced in the PRN code and is a time-varying bias. Each satellite signal has a different SA bias in the C/A code signal. This bias results in the NAVSTAR GPS SPS performance to be reduced from 30m to 100m.

The errors due to the tropospheric and ionospheric delays are caused by natural factors. The satellite ephemeride error, multipath reflection, and satellite clock drift are the result of instrumental factors. Natural factors are due to Instrumental factors and include: (1) the ephemeris error because a GPS receiver does not update the Navigation Message on time, thus causing the Almanac to be off, (2) the multipath error caused by a signal being reflected off a coarse surface near the GPS receiver and being received by the receiver, and (3) the error in the reading of the satellite clock (Capaccio et al., 1996 & 1997; Langley, 1997; Brodin, 1996; Misra et al., 1993 & 1996; Parkinson, 1996; Rossbach et al., 1996; Raby, 1994; Hartman et al., 1991).

The human error in obtaining the correct GPS information can be substantial and may be caused by incorrect computer operations at the control station or wrong selection of the geodetic datum at the receiver (Anonymous, 1996a).

3.4.2 DGPS Fundamentals

The fundamental purpose of DGPS is to correct the bias errors at a location with the corrected bias errors at a known position, such as a GPS receiver's location, or a base station.

By using two identical receivers simultaneously, one at a reference point with known location coordinates and the other at unknown location coordinates, the unknown location coordinates can be established because the differential positioning removes the error sources common to both receivers. Applying this positioning correction is restricted to a limited range. Both receivers should use the same GPS satellites during the measurement, and have identical Geometric Dilution of Precision (GDOP) indices in order to be identically affected by the bias errors (Capaccio et al, 1997).

The components of GDOP are (Anonymous, 1996a): (1) the Position Dilution of Precision (PDOP) or Spherical Dilution of Precision (SDOP) for displaying the measurement condition of the three-dimensional position, (2) the Horizontal Dilution of Precision (HDOP) for displaying the measurement condition of the latitude and longitude, (3) the Vertical Dilution of Precision (VDOP) for displaying the measurement condition of the altitude, and (4) the Time Dilution of Precision (TDOP) for displaying the measurement condition of the time.

Vector differences between a GPS receiver and the NAVSTAR GPS satellites magnify the GPS measurement errors. In a position fix, the volume of the envelope

formed by the unit-vectors pointing from a GPS receiver to the NAVSTAR GPS satellites, is inversely proportional to the GDOP (Anonymous, 1996a). The GDOP is computed from the geometric relationships between the position of a GPS receiver and the positions of the satellites (Hofmann-Wellenhof, 1992). For planning purposes, the GDOP is often computed from Almanac information and from the estimated position of the GPS satellites. It should be kept in mind that the estimated GDOP: (1) does not take into account obstacles which block the line-of-sight from the receiver to the satellites, (2) cannot be displayed on the screen of the receiver, and (3) is usually computed with using parameters calculated from the navigation-solution processes (Capaccio, 1997; Leick, 1995). Generally, the measurement errors from the satellite signals are multiplied by the appropriate GDOP term to estimate the position or time error (Parkinson, 1996). The various GDOP terms are computed using the navigation covariance matrix. While each of the GDOP terms can be individually computed, they are covariantly linked and thus are not independent of each other (Capaccio, 1997; Leick, 1995). This procedure is explained in section 5.3.3.

3.4.2.1 Carrier Phase Tracking vs. Code Phase Tracking for Surveying

The generator of a GPS receiver continuously produces a pre-determined PRN code (Leick, 1995). The code repeats the same 1023-chip PRN code sequence every millisecond. The signal generated by the GPS receiver can match the satellite signal either partially or in full. When the NAVSTAR satellite and receiver codes match, the signal is detected. The bandwidth (cycles) of the PRN code is so wide that even if the receiver generates the same code, the two are often not in sync. This results in an out-of-phase match, and may cause a 300 meters measurement error (Brodin, 1996; Armstrong,

1992). If a carrier phase is used instead of a code phase, the Carrier Phase Tracking system eliminates this problem.

The Carrier Phase Tracking technique uses a special device to track the L1 and/or the L2 carrier phase signals (Brodin, 1996). L1 has a bandwidth of 19 centimeters, and is smaller than the C/A code. Tracking and measuring the carrier phase signals improves the accuracy of a GPS receiver's measurements to +/- 1.0 mm (Brodin, 1996).

Carrier Phase Tracking does not provide improvement for the timing function. When modulating a carrier signal with a time-tagged binary code, the carrier signal does not carry a time-tag that distinguishes one cycle from another. Carrier-phase information contains information on the phase cycles and on the fractions of cycles over time. At least two identical GPS receivers are required for tracking the carrier phase signals simultaneously (Brodin, 1996).

The difference in the ionospheric delay at two GPS receivers must be small enough to insure that the carrier phase cycles are properly accounted for. This usually requires that two GPS receivers are located within a limited distance of each other to prevent this problem. The accuracy of the Carrier Phase Tracking of a measurement also depends on the location of the user (Capaccio et al., 1996 & 1997; Langley, 1997; Brodin, 1996; Misra et al., 1993 & 1996; Parkinson, 1996; Rossbach et al., 1996; Raby, 1994; Hartman et al., 1991).

With a carrier-tracking receiver, and using the Relative Positions surveying method, several positions can be measured within a limited range from one reference point. The surveying method is able to fix the positions of the points in relation to each other (Parkinson, 1996; Leick, 1995) and in relation to the location of the Control Points,

with an accuracy on the order of millimeters (Anonymous H, 1984; Clarke, 1963). See Section 5.3.3 for more detailed information.

3.5 Remote Sensing (RS)

3.5.1 Fundamentals of RS

3.5.1.1 Electromagnetic Spectrum

Table 3.4 Wavelength and Frequency of Electromagnetic Radiation

Name		Wavelength	Frequency
Gamma rays		< 0.1 nm	
X-rays		0.1 nm - 10 nm	
Ultraviolet (UV) light		10 nm - 0.4 μm	750 ~ 3,000 THz
Visible light		0.4 μm - 0.7 μm	430 ~ 750 THz
Infrared (IR) Waves	Near IR Waves	0.7 μm ~ 1.3 μm	230 ~ 430 THz
	Short Waves	1.3 μm ~ 3 μm	100 ~ 230 THz
	Intermediate Waves	3 μm ~ 8 μm	38 ~ 100 THz
	Thermal IR Waves	8 μm ~ 14 μm	22 ~ 38 THz
	Far IR Waves	14 μm ~ 1 mm	0.3 ~ 22 THz
Radio Waves		0.1 m ~ 100 km	0.3 THz ~ 30 kHz

Data source: Serway, 1992

The Electromagnetic Radiation (EMR) consists of energy propagated through space between the electric and magnetic fields. The EMR comprises the entire

electromagnetic spectrum; i.e. from cosmic rays, gamma rays, X-rays, ultraviolet light, visible light, infrared radiation, to radio waves (Serway, 1992) (See Table 3.4).

3.5.1.2 Wave Phenomena

When electromagnetic waves are radiated through space and encounter an object as small as a molecule of air, the radiation will either be reflected from the object, absorbed by the object, or transmitted through the object (Halliday et al., 1993). Thus, the total amount of radiation that strikes an object, i.e. the incident radiation, is equal to the reflected radiation plus the absorbed radiation plus the transmitted radiation (Ohanian, 1985)

In remote sensing, the reflected radiation is the critical part. It is the radiation that causes the human eye to see colors, infrared film to record vegetation, and radar images of the earth to be created and to become visual (Asrar, 1989).

3.5.1.3 Wave Descriptions

The frequency or wavelength of the EMR identifies the type of electromagnetic waves (see Table 3.4) (Serway, 1992). The velocity of electromagnetic waves is equal to the speed of light, i.e. 3×10^8 meters/sec (Ohanian, 1985).

The electric and the magnetic fields are important concepts used to mathematically describe the physical aspects of electromagnetic waves. The electric field vibrates in a direction transverse (i.e. perpendicular) to the direction of travel of an electromagnetic wave. The magnetic field vibrates in a direction transverse to the direction of an electromagnetic wave and transverse to the electric field. Polarization is defined as the orientation of the electrical field; it is usually described in terms of horizontal polarization and vertical polarization.

3.5.2 Aerial Photography

Due to the orientation of the optical axis of a RS camera with respect to the surface of the Earth at the time of film exposure, aerial photography can obtain: (1) a vertical airphoto taken with the camera's optical axis oriented in a vertical or nearly vertical angle to the local ground surface ($90^\circ \pm 3^\circ$), and (2) an oblique airphoto taken with the camera's optical axis tilted 20° or more from the vertical (Avery and Berline, 1992). An oblique photograph can be further classified as: (1) a high-oblique airphoto showing the each surface, the horizon, and a portion of sky, and (2) a low-oblique airphoto showing only the earth surface.

Aerial photography has two benefits: (1) it offers cartographers and planners detailed measurements, and (2) it provides observers information on land use and environmental conditions (Ulliman, 1995).

Although both GIS maps and aerial photos present an overlook of the earth, aerial photographs are not maps. A map is an orthogonal representation of the earth surface; it is directionally and geometrically accurate (at least within the limitations imposed by projecting a three-dimensional object onto two-dimensions). Aerial photographs display a high degree of radial distortion, and thus the topography is distorted (Ulliman, 1995). Measurements made from a photograph are not accurate until corrections are made of the distortion. Nevertheless, aerial photography is a powerful tool for studying the earth environment (Anonymous, 1998b).

Because GIS software can correct for radial distortion, aerial photographs are an excellent data source for many projects, especially for those which require spatial data of

a location at periodic intervals (Anonymous, 1998b). Typical applications include land use surveys and habitat analyses.

3.5.2.1 Basic Elements of Air Photo Interpretation

Aerial photographs are different from regular photos in three important aspects:

(1) objects are portrayed from an overhead and unfamiliar position, (2) infrared wavelengths are seen, and (3) photos can be taken at different scales (Wolf, 1983).

The following Interpretation Factors can assist interpreters in identifying objects in an aerial photograph (Wolf, 1983; Avery and Berline, 1992; Ulliman, 1995; Yu, 1997):

- (1) **Tone (hue or color):** tone relates to the relative brightness or color of the elements in a photograph. It is a basic interpretive element because without tonal differences, the other elements cannot be distinguished.
- (2) **Size:** the size of an object must be considered in the context of the scale of the photograph. The scale is essential for determining if an object is a small pond or a large lake.
- (3) **Shape:** shape relates to the general outline of an object. A regular geometric shape is usually an indicator of a man-made design.
- (4) **Texture:** the “smooth” or “rough” texture of the features of an image is an indication of a uniform and non-uniform wave-frequency reflection, and thus of a change in the tone in a photograph. Because texture is produced by a set of features which are too small to identify individually, texture recognition depends on the sense of sight in response to the extent of the roughness of a feature. Grass, cement, and water generally appear as "smooth", while a forest canopy appears as "rough".

- (5) **Pattern (spatial arrangement):** the pattern formed by objects in a photo can be recognized by its various spatial arrangements. A random pattern formed by an unmanaged area of trees and an artificial pattern formed by an evenly spaced row of trees in an orchard are two different spatial arrangements.
- (6) **Shadow:** shadow aids interpreters in determining the height of an object. However, shadow may also obscure an object.
- (7) **Site:** site refers to a particular topographical or geographical location on an aerial photograph. It is important identifying vegetation type and landforms.
- (8) **Association:** some objects are found “in association” in combination with other objects. The association of an object can provide useful insights about other objects.
- (9) **Stereo:** stereo shows the relative elevation of an object.
- (10) **Resolution:** resolution refers to the degree of detail shown in an aerial photograph.

3.5.2.1.1 Types of Aerial Photography

There are several types of aerial photography due to: (1) the type of film, (2) the lens resolution (line pairs/mm), (3) the filter type, and (4) the peripheral instrumentation (Avery and Berline, 1992). The various types are: (1) black and white photography, (2) infrared black-and-white infrared photography, (3) color infrared photography, (4) normal color photography, (5) panchromatic photography, and (6) special aerial photography, e.g., ultraviolet and additive-color.

3.5.2.1.2 Characteristics of Aerial Photography

People shoot an object or phenomenon in the various electromagnetic spectrums in order to record instant information. Aerial photography can (Avery and Berline, 1992; Anonymous, 1998b): (1) record an image of any earth-surface area, (2) show any feature of an object or phenomenon, and (3) display an object or phenomenon at any spatial resolution and geometric fidelity.

Aerial photographs can provide multispectral images of an area and overlapping areas, while GIS can analyze various levels of information provided by aerial photography (Anonymous, 1998b).

3.5.3 Remote Sensing and GIS

Remotely sensed images have some features which are ideal for a GIS data source because: (1) its regional view, (2) its repetitive looks at the same area, (3) its ability to scan over a broader portion of the spectrum than the human eye, (4) its focus on a specific bandwidth in an image, (5) its ability to look at a number of bandwidths simultaneously, (6) its ability to record signals electronically and to provide geo-referenced digital data, and (7) its ability to be effective under night conditions and in bad weather.

Chapter 4 TE-CHI RESERVOIR WATERSHED

4.1 Geography

Te-Chi Reservoir Watershed is a sub-watershed located at the headstream of the Ta-Chia River basin in the Central Mountain Range of Taiwan. The area is about 601.61 square kilometers (Anonymous, 1996d). The watershed has a heart type in shape. Figure 4.1 shows the country of Taiwan, Republic of China. Figure 4.2 shows the location of the Te-Chi Reservoir Watershed.

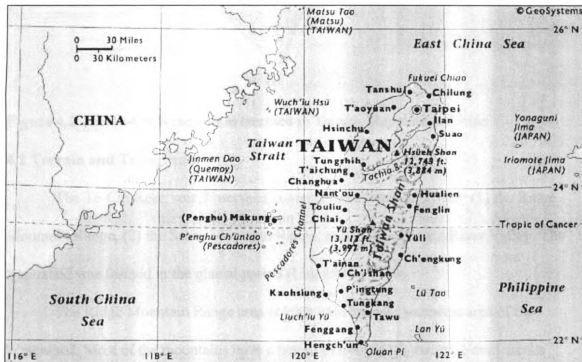


Figure 4.1 Taiwan, Republic of China.

Data source: Compton's Interactive Encyclopedia Deluxe, 1998.



Figure 4.2 The Te-Chi Reservoir Watershed in Taiwan, Republic of China

4.2 Terrain and Topography

The Te-Chi Reservoir Watershed contains three types of terrain: (1) the Ridge Mountain Range, (2) the Snow Mountain Range, and (3) the Central River Valley. The watershed was formed in the glacial period (Lin, 1974).

The Ridge Mountain Range area is located in the east/southeast area of the Watershed. Most of the mountains have a height of over 3,000 meters. Small creeks zigzag through this area, and stream into an over-a-hundred-meter-deep gorge.

The Snow Mountain Range area is located in the northwest area of the Watershed. The mountains are between 3,600m and 3,800m in height. Snow Mountain has an elevation of 3,884meters and is the highest peak in the Watershed (He, 1982).

The Central River Valley of the Watershed consists of the upstream valley of the Ta-Chia River, a gorge-type valley, a horn-like valley, and the down stream multi-streamlet area. The whole valley is at an elevation of over 2,000m.

The average slope of the riverbeds in the Watershed has a gradient of 1/60, with a range of 1/90 to 1/36.

4.3 Geology

Taiwan is located on the Pacific Convergent Plate Boundary. The western part of the Central Mountain Range of Taiwan lies on the Eurasia Continental Plate, and the eastern part on the Pacific Oceanic Plate. The island of Taiwan was formed due to the orogeny caused by the collision of the two plates during the so-called Continental Collision (He, 1982).

Metamorphic and sedimentary rocks dominate the Watershed; the rocks are relatively soft, fractured, and weathered. Extensive erosion occurs because of the intense rainfall and the resulting floods. Frequent earthquakes occur which further undermine the stability of the hill slopes.

4.4 Rivers

The stream type in the Te-Chi Reservoir Watershed is short, steep, and ephemeral. The Ta-Chia river is the main stream. The Watershed contains nine tributaries: the Ho-Huan creek, the Bi-Lu creek, the Er-Wu creek, the Nan-Hu creek, the Si-Chi-Lang creek, the Xue-Shan creek, the Chi-Chia-Wan creek, the You-Sheng creek, and the Yi-Ka-Wan creek. The Yi-Ka-Wan creek is the main upstream tributary; it receives water from the eastern mountains of the Watershed (He, 1982).

4.5 Climate and Hydrology

The climate in the Te-Chi Reservoir Watershed is subtropical. The monsoon prevails from October to March. Orographic rain, torrential rain, typhoons, and thunderstorms cause abundant rainfall from May to September (Anonymous, 1996c).

The average annual precipitation in the total Watershed is over 2,500mm, but is over 3,000mm in the Ridge Mountain Range area. The rainfall from May to September accounts for about 76% of the total average precipitation. In 1996, a typhoon caused a total rainfall of 900mm in 9 hours, 1157mm in 12 hours, 1575mm in 18 hours, and 1749 mm in 24 hours. Comparing the 1749mm in 24 hours to the 2,500mm in an average year, points to the necessity of considering typhoons in the hydrological modeling of the Watershed (Anonymous, 1996c).

4.6 Land Use

The land use in the Te-Chi Reservoir Watershed is: (1) natural forests (coniferous forest, broadleaf forest, and mixed forest), 397km², 66.0%, (2) forest plantations, 108km², 18.0%, (3) fruit orchards, 34.5km², 5.7%, (4) vegetable culture, 3.4km², 0.6%, and (5) tea plantations, 0.2km², 0.03%. Agricultural use accounts for 6.34% of the total Watershed area (Anonymous, 1996d).

Chapter 5 METHODOLOGY

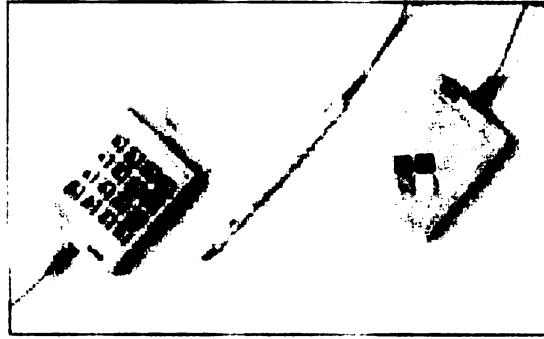
5.1 Hardware

5.1.1 GIS Digitizer System

The digitizer system consists of a GTCO AccuTab Surface-Lit LII Plus Digitizer with Mounting Base as shown in Figure 5.1. It includes: (1) a surface-lit tablet (model No: 2M-3648AL-16) with 91.44cm x 121.92cm active area, 0.00635mm as (150 lpmm) resolution, and +/- 0.0508mm accuracy, (2) a controller with standard firmware, RS-232 cable, and 9 to 25 pin adapter, (3) a 16-button cursor with 4-meter cable and glass reticule with ultra-fine etched crosshair as shown Figure 5.2, (4) a 3.5-inch disk with ADI, Windows, mouse and WINTAB drivers, and a self-diagnostic program for drive electronics and microprocessor, (5) a mounting base---Dakota Workstation with Monitor (model No: DKT-XJ1000A), and (6) a 120V power supply (Anonymous, 1996b).



Figure 5.1 The GTCO AccuTab Surface-Lit LII Plus Digitizer System



Choice of Pointing Devices

Figure 5.2 The GTCO 16-button pointing device (The most left one)

The altitude range of the digitizer system is between 0 and 3077 meters. The baud rate is between 1,200 and 34,400. The cursor switches use an elastomeric keypad. The system has to be operated at a temperature between 5° C and 46° C and at a humidity range between 10% and 90% (Anonymous, 1996b).

5.1.2 GPS Receiver

A DeLorme Tripmate GPS receiver has been employed in this study. A computer with an RS-232 interface with a NMEA-0183 (National Marine Electronics Association) protocol is used to transfer the GPS receiver data. The receiver has 12 channels and a GPS L1 C/A code generator. It has a cold start-up of about 3 minutes at 25° C and a warm start-up of about 1 minute. The unit can operate in the -10° C to 60° C temperature range and weighs (with batteries) is 0.27kg. (Anonymous, 1996a).

Using Street Atlas USA 4.0 software, the DeLorme Tripmate can display any location in the U.S. With AAA Map'n'Go 2.0 software, the DeLorme Tripmate can locate any place in the United States, Canada, Mexico and the Caribbean (Anonymous, 1996a).

The DeLorme Tripmate GPS receiver can track 12 satellites simultaneously. Its accuracy depends on several factors: (1) the atmosphere, (2) the ionosphere, and (3) the

position of the receiver sensor. Buildings, natural structures, and heavy foliage can obstruct the DeLorme Tripmate signals, and decrease the accuracy of the user position by preventing the satellite signals from reaching the receiver sensor (Anonymous, 1996a).

The DeLorme Tripmate GPS receiver is a SPS device. SA affects the accuracy of SPS (see section 3.4.1.6). With SA, SPS is to within 100m horizontally and 156m vertically.

5.2 Software

5.2.1 ArcView GIS 3.1 and Its Extension Programs

5.2.1.1 ArcView GIS 3.1

ArcView GIS 3.1 made by Environmental System Research Institute, Inc. (ESRI) has the ability to: (1) display data, (2) query data, (3) create data, and (4) use other types of data, e.g. CAD data.

ArcView GIS 3.1 displays data by creating a map in a variety of spatial data formats; e.g. the ARC/INFO spatial data formats. It can display tabular data about ground cover, land formation, and water quality to a map. The software is able to represent data on a map by symbolizing and charting the data, by labeling the map with text and graphics, and by choosing map projections. ArcView GIS 3.1 can also design and print various map layouts (Anonymous, 1996e).

The data-query function of ArcView GIS 3.1 is useful in obtaining information, and is an essential part of the software. Five sources of information are available to query: (1) *the attributes* of the features, (2) the features with particular attributes, (3) the features near other features, (4) the features that fall inside a polygon, and (5) the features of

special interest to the user (Anonymous, 1996e). All such data can be aggregated and summarized into relevant statistics, making the data easier to interpret.

ArcView GIS 3.1 can create new data by: (1) developing additional spatial data, (2) editing existing spatial data, and (3) digitizing a map. The software creates new spatial data either by developing a new point theme, line theme, or polygon theme, or by using a digitizing tablet to digitize a map into a point feature, a line feature, or a polygon feature. Editing spatial data can be done within certain themes.

ArcView GIS 3.1 data is compatible with several other data types, e.g. image-type data, Computer-Aided Design (CAD) data, Spatial Database Engine (SDE) data (Anonymous, 1996e). Image-type data includes scanned-map data, aerial-photograph data, and satellite-imagery data. CAD data are a set of non-GIS graphical data for engineering or architecture design, and can be employed as GIS data in ArcView GIS 3.1. With the spatial Database Themes extension of ArcView GIS 3.1, SDE data can be added to the database of a map in order to explore, query, and analyze the map data in ArcView (Anonymous, 1996e).

In this thesis, four additional software programs are used with basic ArcView GIS 3.1: (1) ArcView Spatial Analyst, (2) ArcView Tracking Analyst, (3) ArcView 3D Analyst, and (4) ArcView Image Analysis.

5.2.1.2 ArcView Spatial Analyst

The software ArcView Spatial Analyst can create, query, map, and analyze cell-based raster data and perform integrated vector-raster analyses. Its specific function is to provide solutions to problems that require distance modeling or other continuous-surface modeling. The software can generate surface representations from various data sources,

and develop new information from the overlaying of multiple theme types. The major functions of ArcView Spatial Analyst are (Anonymous, 1996f): (1) to convert feature themes (point, line, and polygon) to a grid theme, (2) to create raster buffers based on distance from feature or grid themes, (3) to create density maps from themes containing point features, (4) to create continuous surfaces from scattered point features, (5) to create contour, slope, and aspect maps and add hill-shades, (6) to perform Boolean queries and algebraic calculations on multiple grid themes, (7) to perform neighborhood and zone analyses, (8) to select a special interest grid on a feature, and (9) to produce a grid display.

5.2.1.3 ArcView Tracking Analyst

GPS technology offers an inexpensive, quick, and convenient way to collect data. The ArcView Tracking Analyst software can instantaneously display real-time GPS stream-data for temporal-data and spatial-data. The data which the Tracking Analyst software can import includes (Anonymous, 1998c): (1) real-time GPS tracking stream-data, (2) real-time logged-in data.

5.2.1.4 ArcView 3D Analyst

The ArcView 3D Analyst software can produce: (1) Triangulated Irregular Networks (TIN), (2) three-dimensional vector geometry, and (3) interactive perspective views. Specifically, the software is able: (1) to develop and modify surface models, (2) to develop 3D shapefile themes, (3) to edit TIN files, and (4) to planimetrically display surfaces (Anonymous, 1997c).

5.2.1.5 ArcView Image Analysis

The ArcView Image Analysis software processes and thereby enhances the display of an image, in particular: (1) satellite imagery, (2) aerial photography, and (3) remotely-sensed data such as infrared thermal imagery. The image processing can include: (1) image-to-map rectification, (2) spectral and color enhancement, (3) automatic feature boundary detection and extraction, (4) detection of the change in same-location images shot at different times, and (5) establishment of shapefiles by feature extraction (Anonymous, 1998 e).

5.2.2 Microsoft Excel 97

The dBASE file (dBASE III or dBASE IV) of Microsoft Excel 97 can be directly loaded into ArcView GIS 3.1. The dBASE files save only the text and data values contained in the cells of an active worksheet. The cell formatting, page-layout setting, graphics, and other Excel features are lost. Only the information stored in a limited number of columns is saved: (1) in dBASE III, 128 columns, and (2) in dBASE IV, 256 columns (Anonymous, 1996g).

In dBASE III and IV, only the range of cells called “Database” can be manipulated; it is necessary to redefine the range to include new cells. The values in the first row of data in Database determine the data type in each column. If the first cell in a row contains a blank value, all the cells in the row are read as text fields (Anonymous, 1996g).

5.3 Methods

Simulating the water runoff in a watershed requires the modeling of multiple “layers” of spatial and temporal data. In this thesis GIS, SVIS, DGPS, GPS, and RS are integrated with forest hydrology to simulate the water-runoff. The main steps are: (1)

digitize the watershed maps by GIS (Anonymous, 1996e), (2) modify the GIS maps by GPS and DGPS (Parkinson, 1996), (3) process the aerial photographs by GIS (Anonymous b, 1998), and (4) simulate the water runoff by GIS-SVIS (Arnell, 1995).

Digitizing the GIS watershed maps requires information on the watershed environment and properties. The maps should represent the topographical characteristics of the stream/water-body system, the topography, the soil type, the land use/cover, the geological properties, and the hydrological record. The digitizing of the Te-Chi Reservoir Watershed map is described in detail in Section 5.3.1.

To process the aerial photographs of Te-Chi Reservoir Watershed by GIS requires the integration of GIS into a desktop-mapping system. This provides a realistic backdrop for the geo-referenced database and updates the terrain environment and recent natural and man-made changes (Anonymous, 1998b). The details are given in Section 5.3.2.

To correct a GIS map by GPS an

121°26'29.82". The physical properties of the Watershed maps were obtained from the Water Resource Bureau, Ministry of Economic Affairs, Taiwan, Republic of China. The combined GIS maps digitized by ARC/INFO contain information on the topography, land use, streams and water bodies, geology, and the road features of the Watershed. The specifications of the digitized paper maps are listed in Table 5.1.

Table 5.1 Specifications of the Digitized Paper Maps of the Te-Chi Reservoir Watershed

Information Types	Information
Map Year	1985
Map Unit	Meter
Map Projection	Transverse Mercator*
Central Meridian	121°00'00"

* Transverse Mercator projection is similar to the Mercator projection except that the cylinder is longitudinal along a meridian instead of the equator. The zero elevation is at sea level in Keelung, Taiwan, Republic of China.

The cylindrical projection of the Transverse Mercator projection is longitudinal along a central meridian line and not along the equator. The result is a conformal projection. The central meridian is centered on the particular region which is to be highlighted. The centering on a specific region minimizes the distortion of the properties in the region. The north-to-south projection of the meridian is best for north-south landmasses (Anonymous, 1996e).

5.3.1.1 Preparing for Digitizing of A Watershed Map

The GTCO AccuTab Surface-Lit LII Plus digitizer (2M-3648AL-16) with Mounting Base (DKT-XJ1000A) and ArcView GIS 3.1 software are used to produce the digitized GIS maps. Before digitizing the maps in ArcView GIS 3.1, several steps are required: (1) setup the digitizer system, (2) prepare the paper map, (3) prepare the digitizing, and (4) register the coordinates of several points on the paper map.

The digitizer setup steps include: (1) check the compatibility of the digitizer system and the software, (2) install the up-to-date digitizer driver, (3) setup the driver control panel, and (4) configure the button of the digitizer puck-buttons (Anonymous, 1996e).

The latest version of the WinTab digitizer driver is used to operate the digitizer in the Microsoft Windows environment. It should be noted that ESRI successfully tested the digitizer system under ArcView GIS 3.1 (Anonymous, 1996 a; Anonymous, 1996b).

Configuring the digitizer puck buttons on the WinTab control panel under ArcView GIS 3.1 is an essential step. The GTCO digitizer has 16 puck-buttons which collectively act as the digitizer-pointing device. In order to configure the button properly, ArcView GIS 3.1 requires the digitizing tablet to be able to be toggled in two modes: (1) in absolute (digitizing) mode, and (2) in relative (mouse) mode.

In absolute mode, the location of the tablet is digitized to a specific location on the screen. The movement of the pointing device on the tablet surface causes the screen cursor to move to the same position as on the monitor. The ArcView GIS 3.1 user interface cannot select the menu choice, buttons, and tools when the screen cursor is locked in the drawing area of the View.

In relative mode, the tablet-pointing device functions like a mouse. However, there is no correlation between the position of the screen cursor and the surface of the digitizing tablet.

Preparing the paper map entails minimizing the map distortions. Two steps are needed to prepare a paper map: (1) select an reliable, up-to-date, and unfolded paper map, and (2) pre-choose the exact coordinates of at least four control points.

The preparation for digitizing requires loading of the Digitizer Extension programs, and proper selecting of the same map units and the same map projection (See Table 5.1) (Anonymous, 1996e).

Registering the paper map specifies the global location of any position on the map so that the desired features in geographical space are digitized (Anonymous, 1996 a; Anonymous, 1996 e). There are two conditions for registering a paper map: (1) digitize at least four-control points on the map when it is first registered, and (2) use the TIC files (tic.dbf) of ARC/INFO software to register the control points on the map. In this thesis, thirty-eight corner points (i.e. the points intersected by the straight lines of latitude and longitude on the map) and forty-eight mountain-peak points are saved in a TIC ARC/INFO file in order to register the map (see Table 6.3 in Appendix E).

5.3.1.2 Digitizing the Features of the Watershed Paper Map

ArcView GIS 3.1 allows the user to digitize a feature on a watershed paper map in three different ways: (1) by digitizing a feature, i.e. a point, a line, or a polygon feature into a new theme, (2) by editing an existing theme and make it active, and (3) by adding specific information to the View. Each feature can be digitized into two modes: (1) by the point mode, and (2) by the stream mode (Anonymous, 1996e).

In the ArcView GIS 3.1 interface, a certain shape feature can be developed and saved into a shape file by combining the “Editing and Drawing” tools with a certain shape theme, such as a point, a line, or a polygon theme. Each shape file contains only one feature. The “Shape Properties” setting can be used to view or edit a shape property of any selected feature.

5.3.1.3 Correcting the Digitizing Errors

The digitized spatial data needs to be confirmed and rectified. By using the programs in the ARC/INFO software, the digitizing errors can be identified and corrected, and the topology can be reconstructed (Anonymous, 1997a). The details of the correction are contained in the user guide of ARC/INFO.

5.3.2 Modifying GIS Maps by GPS, DGPS, and Relative Positioning Surveying

The digitized GIS map can be modified: (1) by the Total Stations and Relative Positioning Surveying option, or (2) by the GPS, DGPS, and Relative Positioning Surveying option. The second method is used to modify the digitized GIS maps, because the GPS receiver is cheaper, slighter, and more convenient to use for a steep and mountainous watershed (See Section 3.4) than the Total Station option.

Employing GPS and DGPS to modify the GIS maps is a challenge because the DGPS service regions do not include Taiwan. However, the GPS do receivers still receive the signals of the GPS-satellites. Two identical DeLorme Tripmate GPS receivers, DGPS technology, and Relative Positioning surveying technology are used to modify the GIS maps. The objectives are: (1) to cancel the errors common to both GPS receivers, (2) to find the bias of each GPS receiver, and (3) to find the relative positions of the measured points (Capaccio, 1997; Leick, 1995). Section 3.4.2 elaborates the details.

Microsoft Excel 97 is used to develop the statistical program (See Table 6.4 in Appendix F) and ArcView GIS 3.1 is to represent the modified points on the GIS map.

The statistical program uses the difference of n-variables in a normal distribution to calculate the bias of the GPS receivers and the differential values of the input coordinates of the digitized maps. The numbers of sampled points (N) should be at least

thirty points. The degree of free (df) is equal to $N-2$. In this thesis, there are two variables X and Y , and thus the df is $N-2$.

The two-dimensional sexagesimal-notation coordinates are latitude (X) and longitude (Y) and are measured by the GPS receivers A (X_A, Y_A) and B (X_B, Y_B). They are input into the statistical program which automatically converts the sexagesimal-notation coordinates into decimal notation and calculates the mean ($U_{X(XA-XB)}, U_{Y(YA-YB)}$), variance ($Var_{X(XA-XB)}, Var_{Y(YA-YB)}$), and standard deviation ($StD_{X(XA-XB)}, StD_{Y(YA-YB)}$). The program also calculates the probability-fluctuation in N trials at the 95% confidence level (i.e. $U_{X(XA-XB)} \pm 2StD_{X(XA-XB)}$ and $U_{Y(YA-YB)} \pm 2StD_{Y(YA-YB)}$).

Twenty-four points containing one of the registered control points (corner point 1) (See Table 6.3 in Appendix E) are measured. The positions of these points are along the roads, in particular about Province Highway No. 7 and Province Highway No. 8. The steps in the correction measurements are:

(1) cancel the errors that are common to both GPS receivers:

- (a) find the known coordinates of locations points P (reference point) and Q (remote point). The control points registered on the GIS map can be used if the distance between the two control points is less than 30km.
- (b) use two identical GPS receivers A and B and simultaneously measure the three-dimensional coordinates (latitude (X), longitude (Y)) of the point P at least thirty times. Each measurement should be the same GDOP values from the same satellites.

(2) find the bias of each GPS receiver:

- (a) input the measured data into the statistical program to find the mean, variance, and standard deviation of the latitude (X) and longitude (Y) of both GPS receivers.
 - (b) use receivers A and B to simultaneously measure once the three-dimensional coordinates of points P and Q. Both GPS receivers should have the same GDOP values for the same satellites.
 - (c) input the measured data into the statistical program to find the bias of receiver A.
- (3) find the relationship of the relative positions for the measured points:
- (a) use the bias of GPS receiver A to predict the coordinates of point Q measured by receiver B.
 - (b) find the Differential Value between the predicted coordinates of point Q and the known coordinates of point Q.

5.3.3 Processing the Aerial Photographs by GIS

According to the land-use GIS map, the areas along the Te-Chi Reservoir and its neighboring streams have variable land uses, i.e. orchards, vegetable farms, farms, and tea plantations (Anonymous, 1996d). The watershed contains slopes between 53% and 75% (Lin, 1974) which have a large affect on the water runoff. The black and white aerial photographs of these areas will update the geo-information, i.e. the changes in the land use.

The representative fraction of the black-and-white aerial photographs is 1:10,000. The latitude of the merged aerial photograph is between 121°09'00" and 121°15'00". The longitude of the merged aerial photograph is between 24°15'00" and 24°18'00". The

aerial photographs were shot in the 1987 by the Food Agency, Taiwan Province Government, Taiwan, Republic of China. A UMAX ASTRA 2400S scanner was used to scan these aerial photographs at a 100% scan size with 2,400.5dpi resolution; the information was saved in a TIFF file. Adobe PhotoDelux Business Edition 1.0 was used to merge the photography files into an aerial photograph file. ArcView GIS 3.1 and its Image Analysis extension software were used to process the merged aerial photograph files.

The Histogram Stretching program in Image Analysis adjusts the distribution of pixels to clearly display the appearance of a photo file in order to better visually interpret and evaluate the information. The Pyramid Layer program in Image Analysis converts the photo file into an IMG file for quickly display. The size of the merged photo file is about 23MB. The Seed Tool program in Image Analysis extracts the features of the aerial photograph in order to identify a similar area (Anonymous, 1998b).

The Interpretation Factors are used to interpret the extracted features of the merged aerial photograph. The digitized GIS land-use maps, i.e. the tea plantations map, fruit orchards map, vegetable field map, and the farms map are overlaid by ArcView GIS 3.1 and are used for comparison with the merged aerial photograph in order to update the land-use information.

5.3.4 Simulating Water Runoff of A Watershed by GIS-SVIS

Watershed factors affecting runoff are watershed size, shape, orientation, topography, and geology (Schwab, 1993). The topography takes the slope and land use/cover into account in the simulation of the water runoff in the Te-Chi Reservoir Watershed.

“Quadtree” is the essential concept used to simulate the runoff flow direction. A quadtree data structure, i.e. an organized hierarchical structure recursively divides a square cell into four equal sub-square cells until each sub-square either contains only one object or distributes the intensity uniformly (Chrisman, 1997). It is considered to apply to the RS image processing and to the grid GIS map.

Applying quadtree to simulate the runoff movement, the proper water quantities in a square cell need to be found, i.e. cell flow in millimeter. The cell flow is used to make a choropleth map for showing the spatial grid distribution of the Watershed. From the choropleth map, the flow paths, flow accumulation, and the flow length of the runoff over the watershed and the loading points along the water bodies can be predicted (Arnell, 1995).

5.3.4.1 Used Data and Software

The simulation of the runoff movement depends on the characteristics of the watershed, and the collected river-flow data (Kovar and Nachtnebel, 1996). The characteristics of the watershed are discussed in Chapter 4. The hydrological data from 1970 to 1996 is shown in Table 5.2 (See Appendix A) in terms of the annual runoff (cms-day) and drainage area (km²) recorded at seven hydrological stations over the Te-Chi Reservoir Watershed (Anonymous, 1970 ~ 1996c). The GIS land-use map and GIS hydrological stations-distribution map in polygon feature and in point feature, are used to simulate the runoff movement.

ArcView GIS 3.1 and its extension software Spatial Analyst and 3D Analyst along with Microsoft Excel 97 are used to simulate the runoff. ArcView GIS 3.1 and its extension software are used to process the GIS maps and produce the GIS-SVIS

choropleth map. The Microsoft Excel 97 is used to calculate the hydrological data and tabulate the GIS data.

According to the descriptions of the characteristics of the watershed in Chapter 4, the main factors to affect the runoff movement are topography and wind.

Table 5.3 Area Proportion of the Over 30% Slope

Slope Types	30% ~ 40%	40%~53%	53%~75%	> 75%
Area (m ²)	54993274	46811393	181139023	257071232
Percentage of the Total Area	9.14%	7.78%	30.11%	42.73%

According to Table 5.3, the area of the over 30% slope accounts for about 90% of the total watershed area. The steep slopes increase the water velocity and results in changes of flow direction and flow length (Hudson, 1981; Kirkby and Morgan, 1980). The land use/cover mainly affects the runoff movement and the flow accumulation although at times a typhoon and the monsoon from the Pacific Ocean also strongly affect it (Anonymous, 1970 ~ 1996c). Note: typhoon and monsoon affect are not considered in this thesis.

Due to the long rainy season and ample precipitation in the Watershed, the soil frequently approaches the water saturation status (Anonymous, 1970 ~ 1996c). The valleys have thicker topsoil than the peaks in the high mountain areas. Most of the topsoil in the valleys readily reaches the saturation status and thus rarely affects the runoff movement in the Watershed (Hudson, 1981; Kirkby and Morgan, 1980). The soil factor rarely affects the runoff movement in this watershed.

Most of land in the Watershed is in the forest land. Considerable evapotranspiration occurs in the forests resulting in the high humidity. The high humidity results in the higher pressure of the water vapor in the air because the air is saturated with

water vapor (Merva, 1995). The evaporation of the runoff is little affected in this watershed.

5.3.4.2 Cell Runoff (mm)

The cell runoff (mm) is obtained by using the area-weighted method, which measures the stream-flow as a volume per unit time (cms-day) (Arnell, 1995). The steps to find the cell runoff (mm) are:

(1) find the cell flow (mm) of the average annual runoff (cms-day):

(a) determine the runoff generated by the drainage measured at the hydrological station (i.e. by subtracting the volume of runoff measured at the upstream station). See Table 5.2 in Appendix A.

(b) select the average of the annual runoff (cms-day) of each station and use the method of the area-weighted cell runoff to find the cell runoff (mm). The cell runoff (mm) is of Type A.

(2) find the cell flow (mm) of the median annual runoff (cms-day):

(a) find the frequency histogram of the average annual runoff (cms-day) for each hydrological station from Table 5.2 (See Appendix A).

(b) select the median number of the maximum frequency range of the annual runoff (cms-day) of each station.

(c) find the cell runoff (mm) by the method of the area-weighted cell runoff by using the median number of the maximum frequency range of the annual runoff (cms-day). The cell runoff (mm) is of Type B.

(3) find the cell flow (mm) of the maximum daily runoff (cms-day):

(a) select the maximum daily runoff (cms-day) of each hydrological station from

Table 5.4 (See Appendix B).

(b) find the cell runoff (mm) by using the method of the area-weighted cell runoff (mm). The cell runoff (mm) is of Type C.

(4) compare the cell runoff (mm) of type A, type B, and type C.

(5) use ArcView GIS 3.1 and its extension software to produce the grid cell map, the flow directions map, the flow accumulation map, and the flow length map.

5.3.4.3 Cell Size (m)

A cell size should be at least one quarter of the minimum mapping unit in order to simulate the runoff movement of a certain landform with the smallest area. The minimum mapping unit can be found in the attribute table of the land-use in the Watershed (See Section 6.2).

Chapter 6 RESULTS AND DISCUSSION

6.1 GIS Watershed Maps

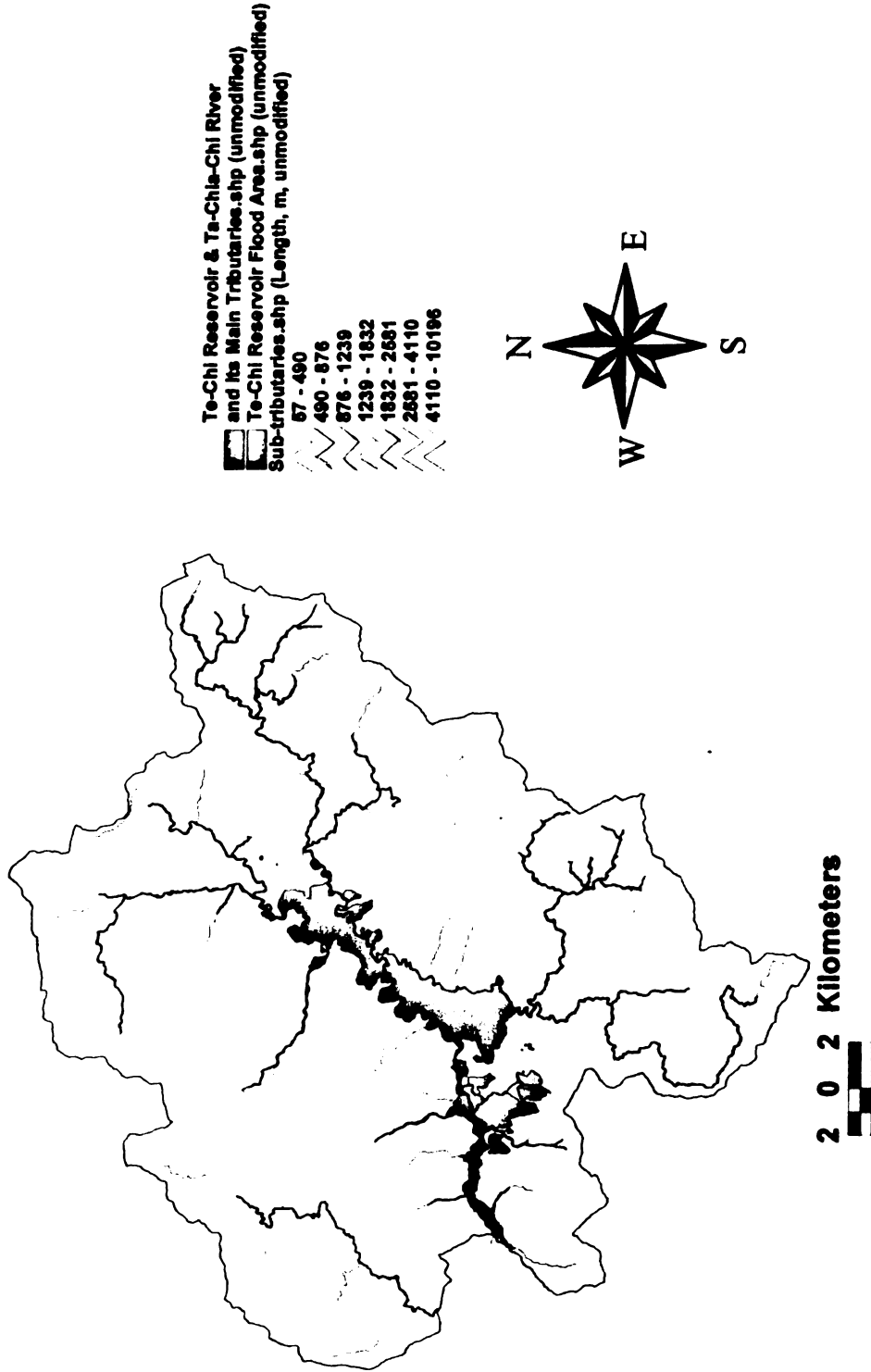
6.1.1 Unmodified GIS Watershed Maps

The GIS digitizing of the Te-Chi Reservoir Watershed created five ArcView shapefiles which contain the spatial data of the vector or raster data type. The shapefiles are non-topological files in which the geometric locations with their attribute information and geographic features are stored. The information in the files defines the geometry and the attributes of the geo-referenced features. The file extensions of the five shapefiles are: (1) shp, (2) shx, (3) dbf, (4) sbn and sbx, and (5) ain and aih (Anonymous, 1996 a).

The “shp” files store the geometric features of the Watershed area. The “shx” files contain the index of the area. The “dbf” files are the dBASE files which store the attribute information of the features (the data can be displayed as a feature table). The “sbn” and “sbx” files store the spatial indices of the features and are created when the “theme on theme selection”, “spatial join”, or “create theme” is chosen and is executed in the Shape field. The “ain” and “aih” files store the attribute indices of the active fields in a theme-attribute table and are created when the “Link on the tables” is executed (Anonymous, 1996e).

The unmodified GIS map of the water bodies in the Te-Chi Reservoir Watershed is digitized in line feature as shown as Figure 6.1. The flow directions of the streams are from north to south except that the streams in the south are from south to north. The map shows: (1) the network of the streams, (2) the stream lengths of sub-tributaries, and (3) the flooded areas of the Te-Chi Reservoir. Its attribute database is contained in the

**Figure 6.1 The Unmodified GIS Map of Water Bodies
in the Te-Chi Reservoir Watershed
(Line & Polygon Features)**



“aat.dbf” file, i.e. the Arc Attribute Table (aat) the “dbf” file format. The “aat” table of the Watershed is presented in Table 6.1 (See Appendix C).

The unmodified GIS map of the vegetable fields in the Watershed is shown in point feature in Figure 6.2 and in polygon feature in Figure 6.3. Their attribute database is contained in “pat.dbf”, i.e., the Point / Polygon Attribute Table (pat) in the “dbf” file format. The map shows the various vegetable farms. The database contains information on both point and polygon features (See Table 6.2 in Appendix D). Figure 6.2 indicates the center and size of a particular area, and Figure 6.3 shows its shape.

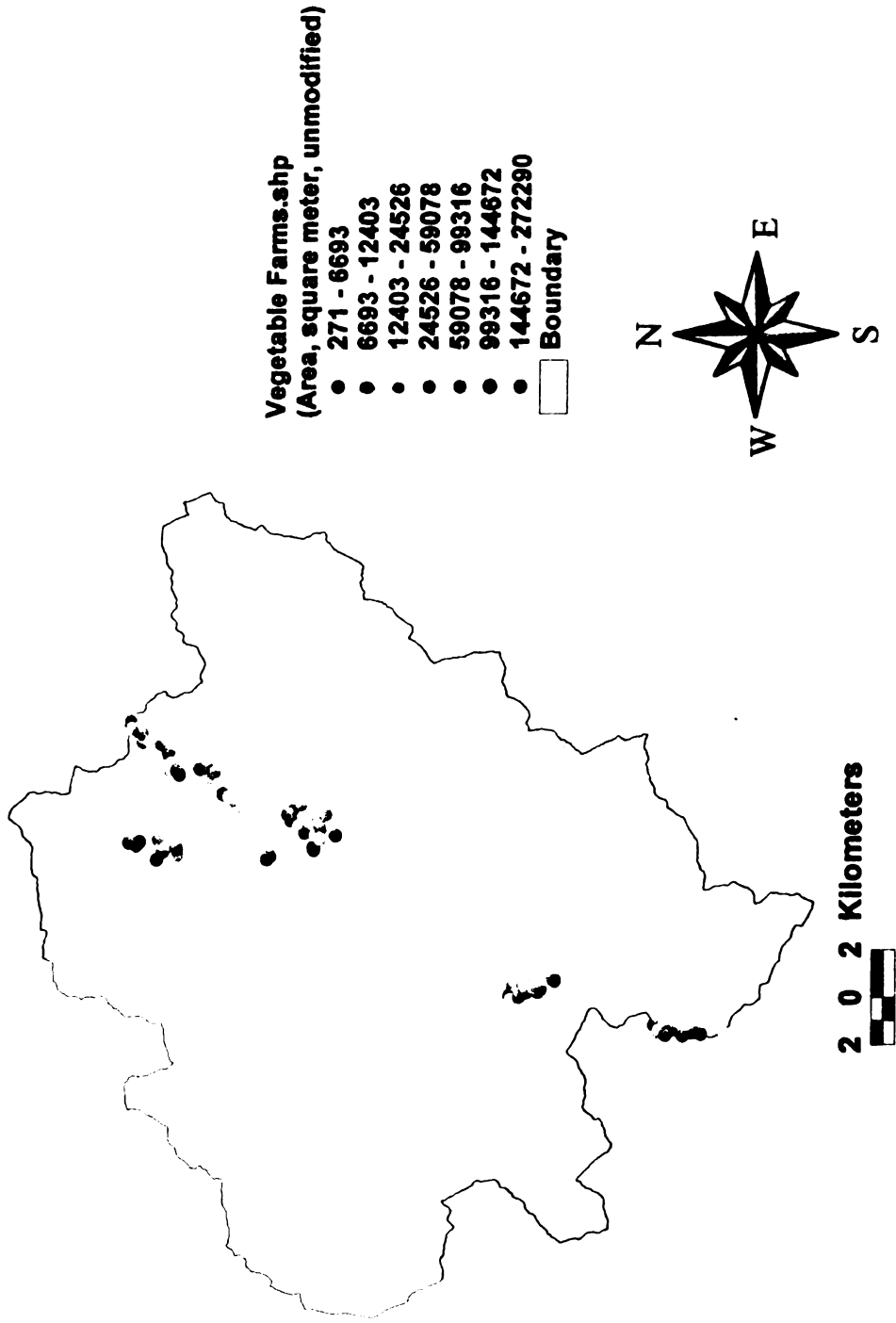
Combining Figures 6.1 and 6.3 results in Figure 6.4. It shows that the vegetable fields are distributed along the main tributaries of the Ta-Chia-Chi River in the Central River Valley area (See Section 4.2).

Figure 6.5 shows the unmodified GIS map of the cultivated agricultural areas in the Watershed, i.e. the tea plantations, fruit orchards, vegetable fields, and farms which cover the regions adjacent to the Te-Chi Reservoir flood area.

6.1.2 Modified GIS Watershed Maps

The twenty-four measured points which are registered on the digitized GIS maps are shown in Table 6.3 (See Appendix E). Their locations are quantified at least thirty times, and were statistically analyzed to establish the biases of the GPS receivers. The biases were used to find the relative positions of a group of points. The author developed a unique method to represent the corrected location-coordinates with statistics in Table 6.4 (See Appendix F) (See Section 5.3.2). The method is explained in the next paragraph. The modified GIS map of water bodies and vegetable fields in the Watershed is shown in

**Figure 6.2 The Unmodified GIS Map of Vegetable Farms
in the Te-Chi Reservoir Watershed
(Point Feature)**



**Figure 6.3 The Unmodified GIS Map of Vegetable Farms
in the Te-Chi Reservoir Watershed
(Polygon Feature)**

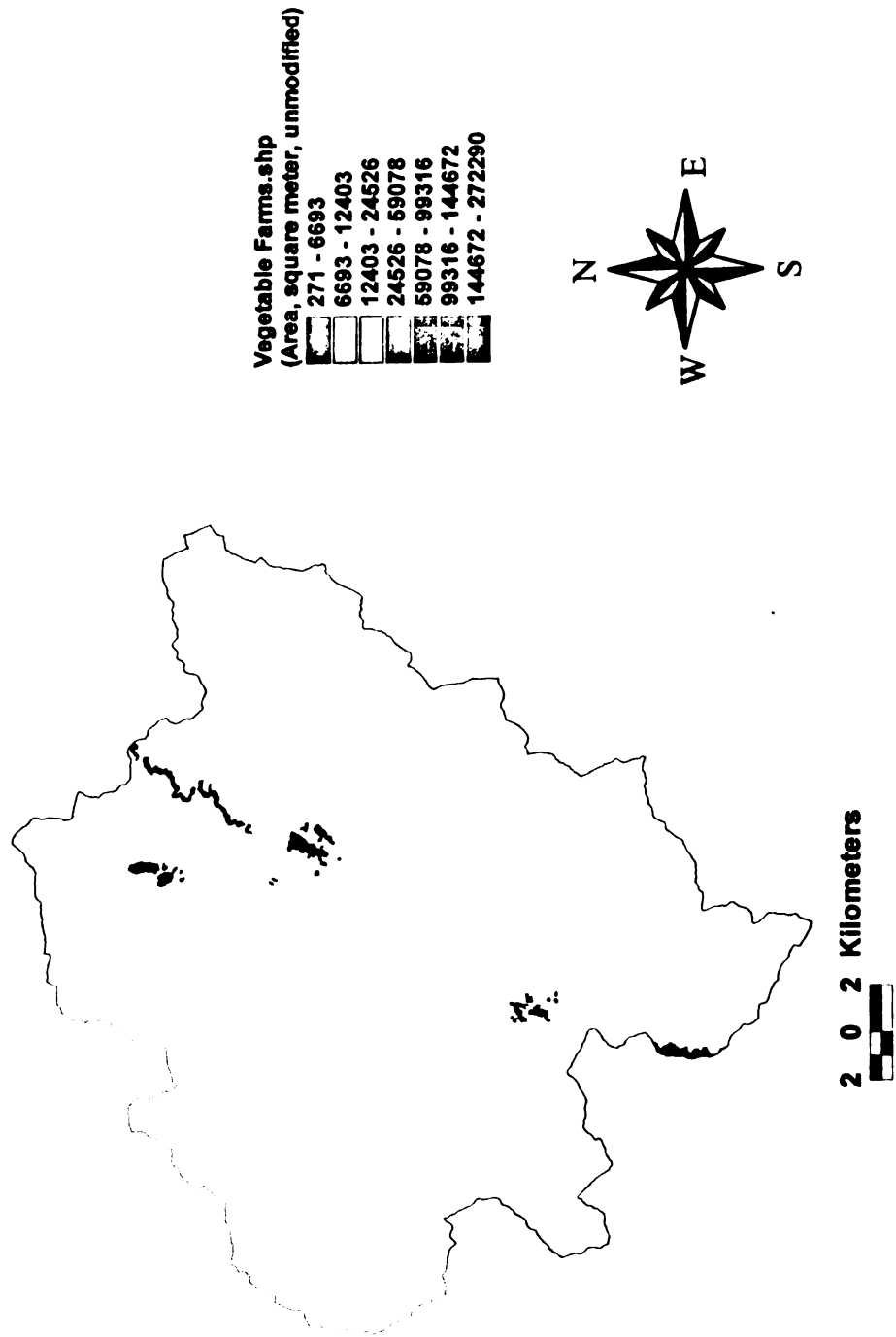
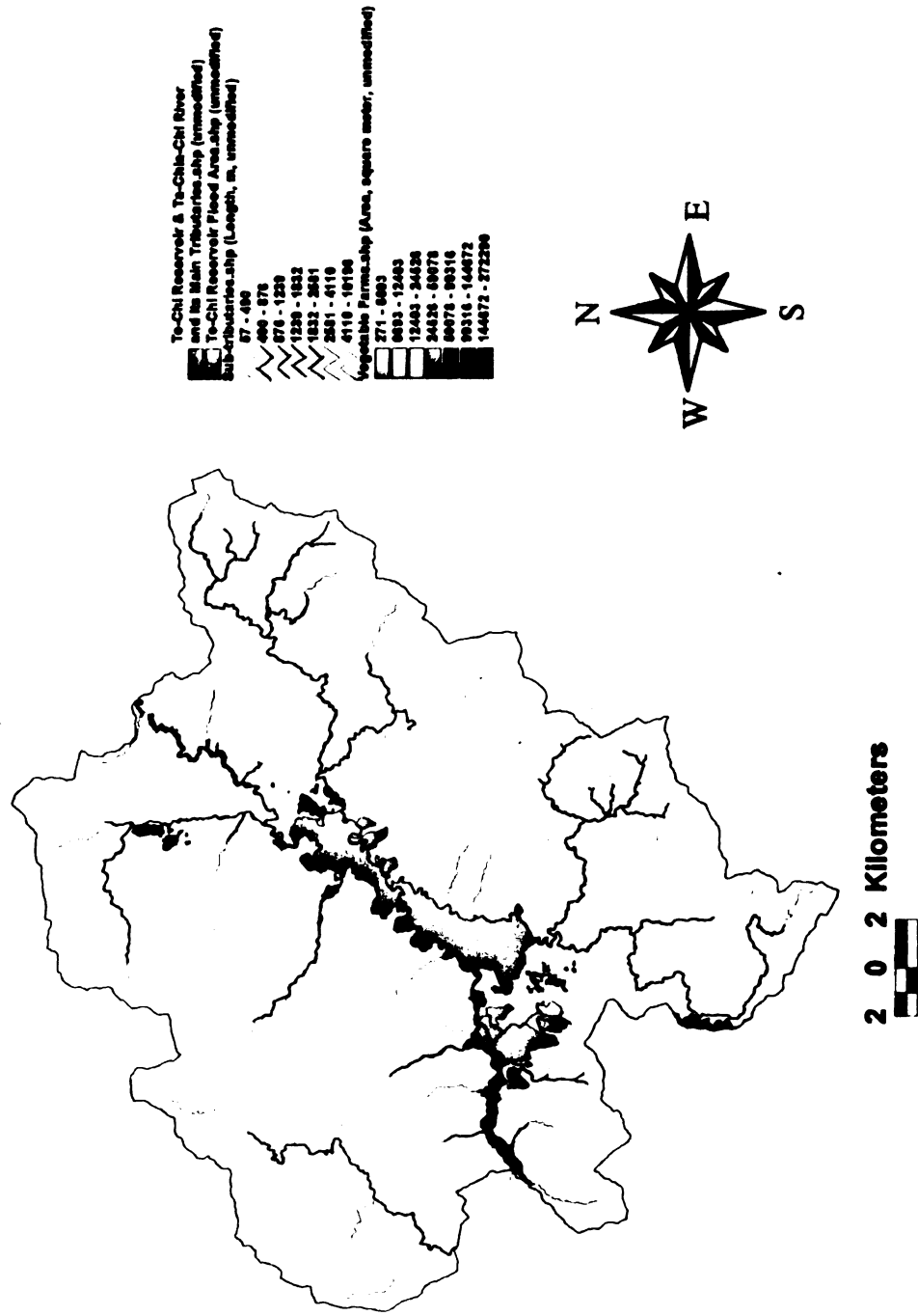


Figure 6.4 The Unmodified GIS Map of Water Bodies and Vegetable Farms in the Te-Chi Reservoir Watershed (Line & Polygon Features)



**Figure 6.5 The GIS Map of the Cultivated Agricultural Areas
in the Te-Chi Reservoir Watershed
(Line and Polygon Features)**

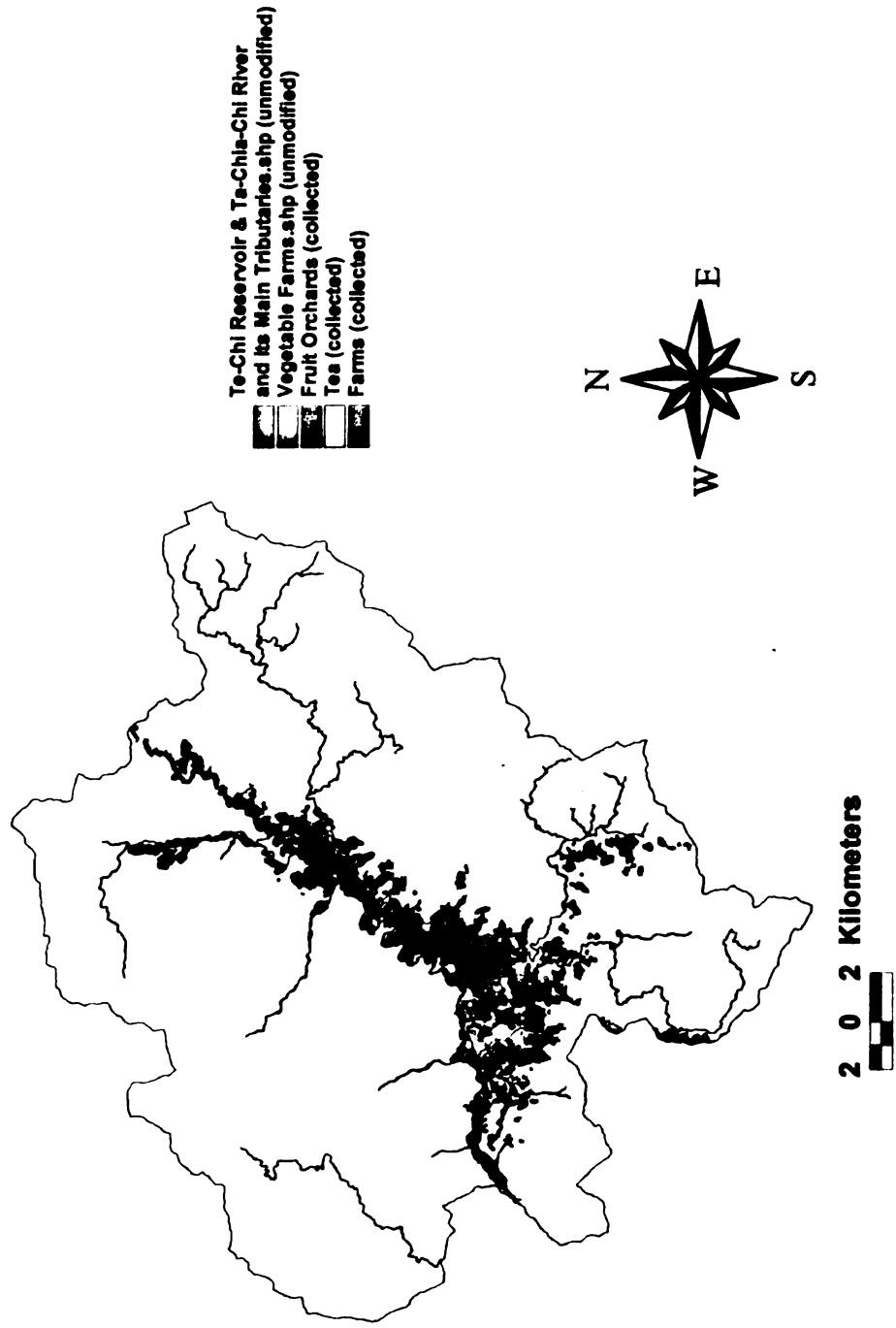


Figure 6.6. The difference between Figures 6.4 and 6.6 cannot be distinguished visually but is obvious from the data in Table 6.3 (See Appendix E).

Assigning units and applying conversion factors is done in the Representative Fraction (RF). The scale of the digitized maps is 1:25,000, and therefore 1cm on the map equals 250m in the Watershed. Also on the map, 2'30" latitude (X) equals 16.9cm and 2'30" longitude (Y) equals 18.45cm. Thus, each 1" latitude (X) equals 28.17m within the watershed and each 1" longitude (Y) equals 30.75m. According to the differential distances in Table 6.3 (See Appendix E), the maps do not represent the actual locations very well unless corrections are made in the coordinates values.

The RMS error is the distance between the starting location and the actual location of a position (Anonymous, 1996e). It is calculated for at least four sets of two control points defined in the Image Analysis theme and in the corresponding feature theme. In ArcView GIS 3.1, an acceptable RMS error is lower than 1. The RMS error represents the accuracy of the digitized map but not the accuracy of the actual location. Thus, map corrections are necessary.

6.1.3 Aerial Photographs Processed into GIS-SVIS Maps

Figure 6.7 shows an aerial photograph of the Te-Chi Reservoir and the surrounding area; the figure is made up of forty individually-scanned aerial photographs which have been merged and saved as a TIFF file. ArcView GIS 3.1 along with the Image Analysis software was used to process the aerial photographs in Figure 6.7 into a GIS-SVIS image theme (See Figure 6.8).

With the application of the Seed Tools program in the Image Analysis software (Anonymous, 1998b) and the Interpretation Factors, four types of the landform can be

Figure 6.6 The Modified GIS Map of Water Bodies and Vegetable Farms in the Te-Chi Reservoir Watershed (Line and Polygon Features)

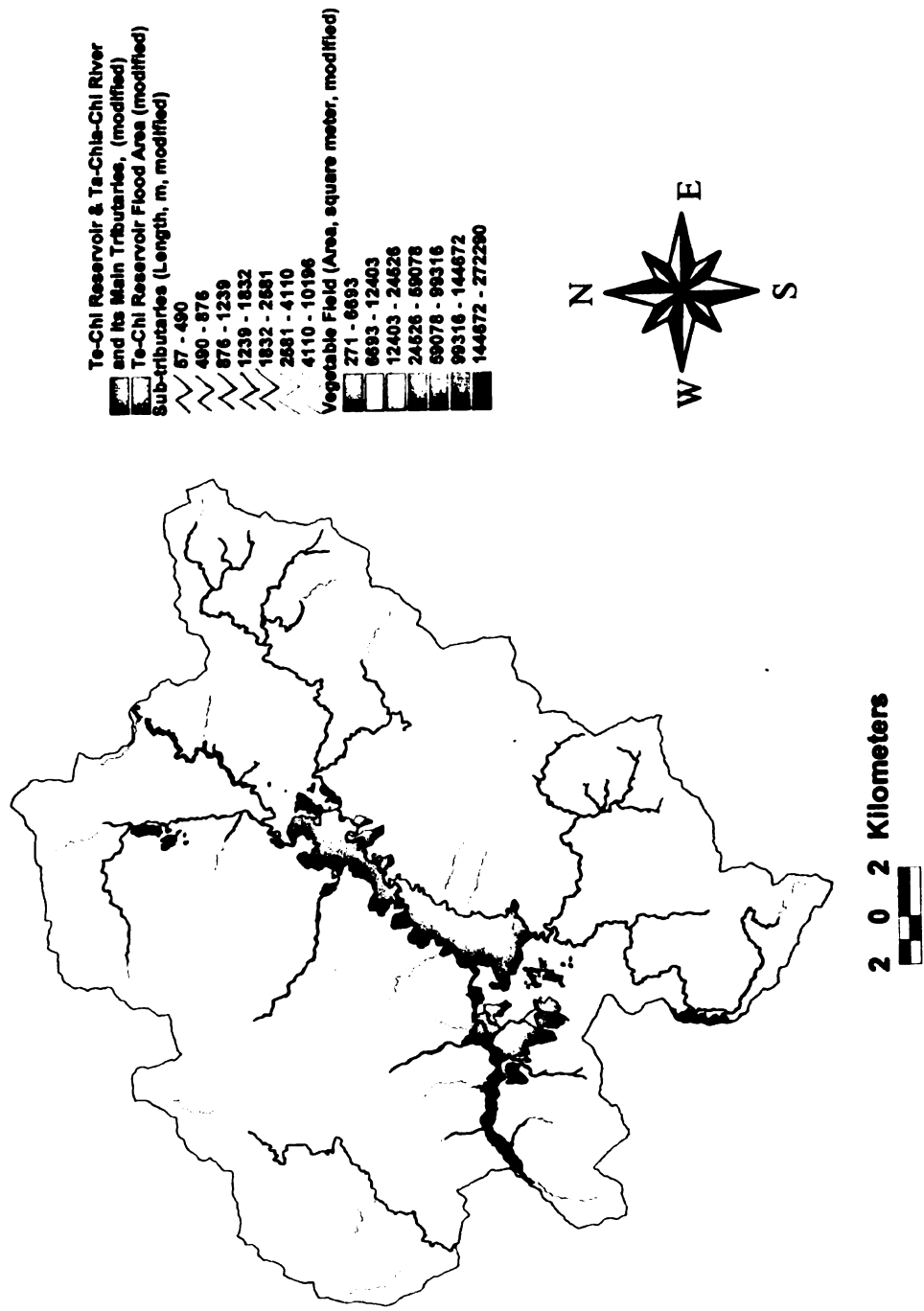
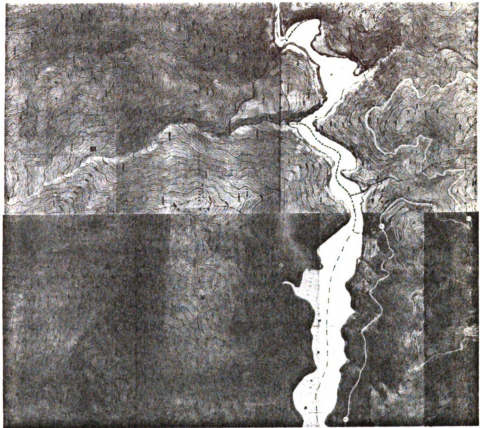


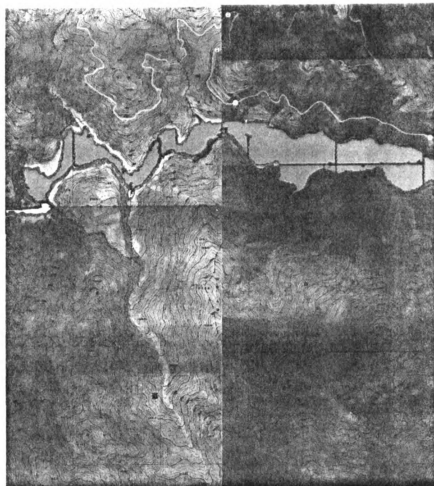
**Figure 6.7 The Aerial Photograph of
the Te-Chi Reservoir Watershed
and Its Surroundings**



Smoothnew_dele1.img
:Layer_3
:Layer_2
:Layer_1



**Figure 6.8 The Aerial Photograph of the Te-Chi Reservoir Watershed
Processed by GIS-SVIS**



distinguished in Figure 6.8: (1) the blue region of the Te-Chi Reservoir and the Ta-Chia-Chi River, (2) the curved grayish black lines of the terraces along the Reservoir (Paine, 1981), (3) the curved white lines of the tributaries flowing into the Reservoir and the River, and (4) the regions of the various vegetation types (Ulliman, 1995). The gray-toned irregular patterns represent the coniferous forest lands, and the grayish white regular areas represent the broadleaf forest lands (Avery and Berlin, 1992).

Comparing the conditions of the cultivated agricultural areas between Figure 6.5 (Year 1985) and Figure 6.8 (Year 1987), no change is seen.

6.2 GIS-SVIS Maps Illustrating Water Runoff

In a watershed with steep slopes, the choice of the cell size should be such that the runoff movement can be simulated for the smallest area of a specific type of land use and land cover, i.e. a cell size with at least a quarter of the minimum mapping unit can simulate the runoff movement in a certain landform with the smallest area. According to Table 6.5, a fruit orchard accounts for the smallest area, i.e. 137.38m² (11.7m x 11.7m). Therefore, the grid size is set equal to 5.86m for producing the slope grid map and the land-use grid map.

Table 6.5 The Smallest Area of the Various Types of Land-Use in the Te-Chi Reservoir Watershed

Type of Land Use	Farm	Forest	Landslide	Orchard	Tea Plantation	Vegetable Field
Area (m ²)	1601	1601	287	137	1364	271

The cell size of 5.86m-by-5.86m is small compared to other grid maps using, e.g. the USGS DEM map, which uses a cell-size of 2km-by 2km. A small cell-size is more precise in simulating water runoff in a steep, high-elevation watershed than a large cell-size.

Figure 6.9 The Annual Runoff in the Hydrological Stations of the Te-Chi Reservoir Watershed

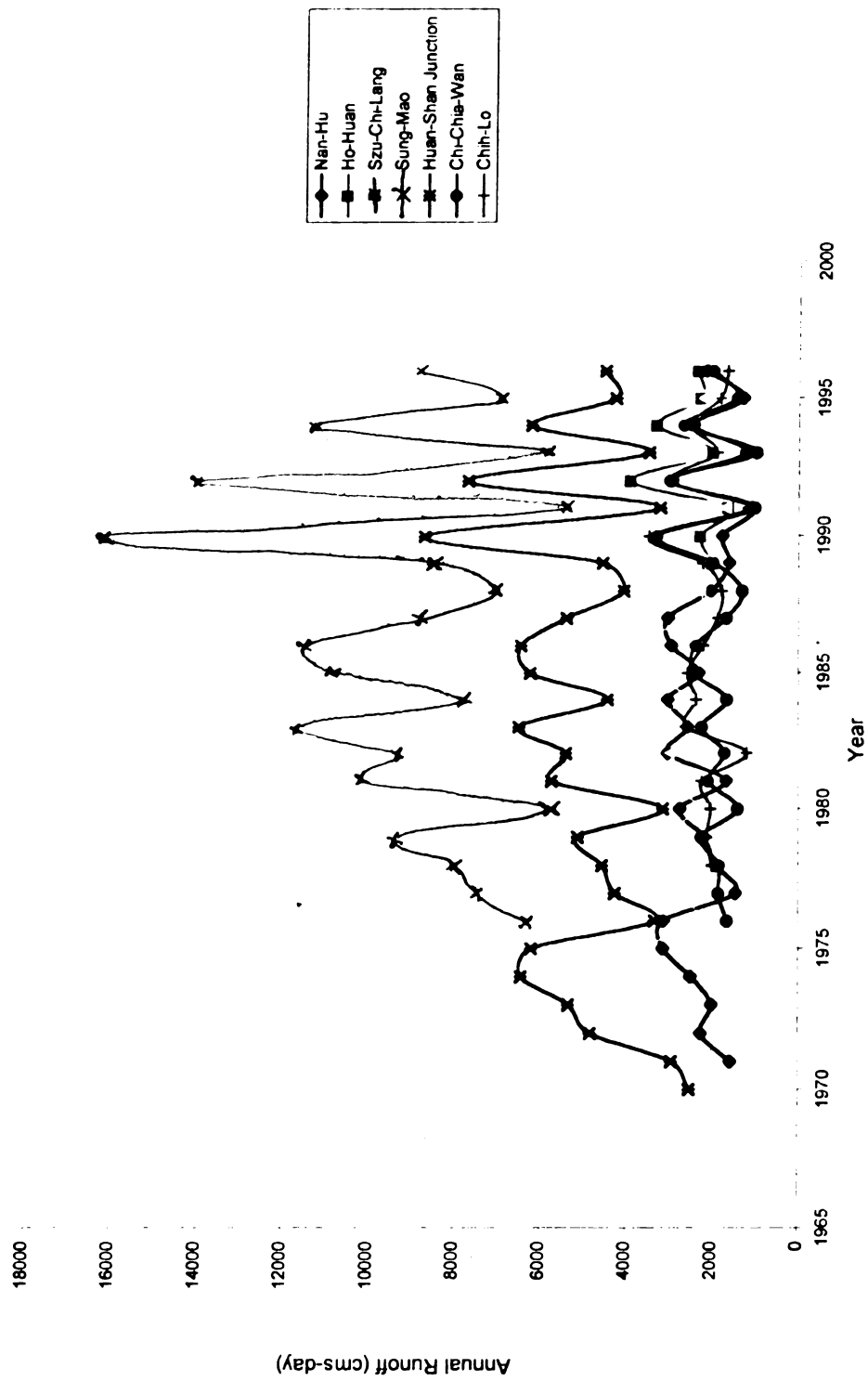


Figure 6.10 The Locations of the Hydrological Stations in the Te-Chi Reservoir Watershed

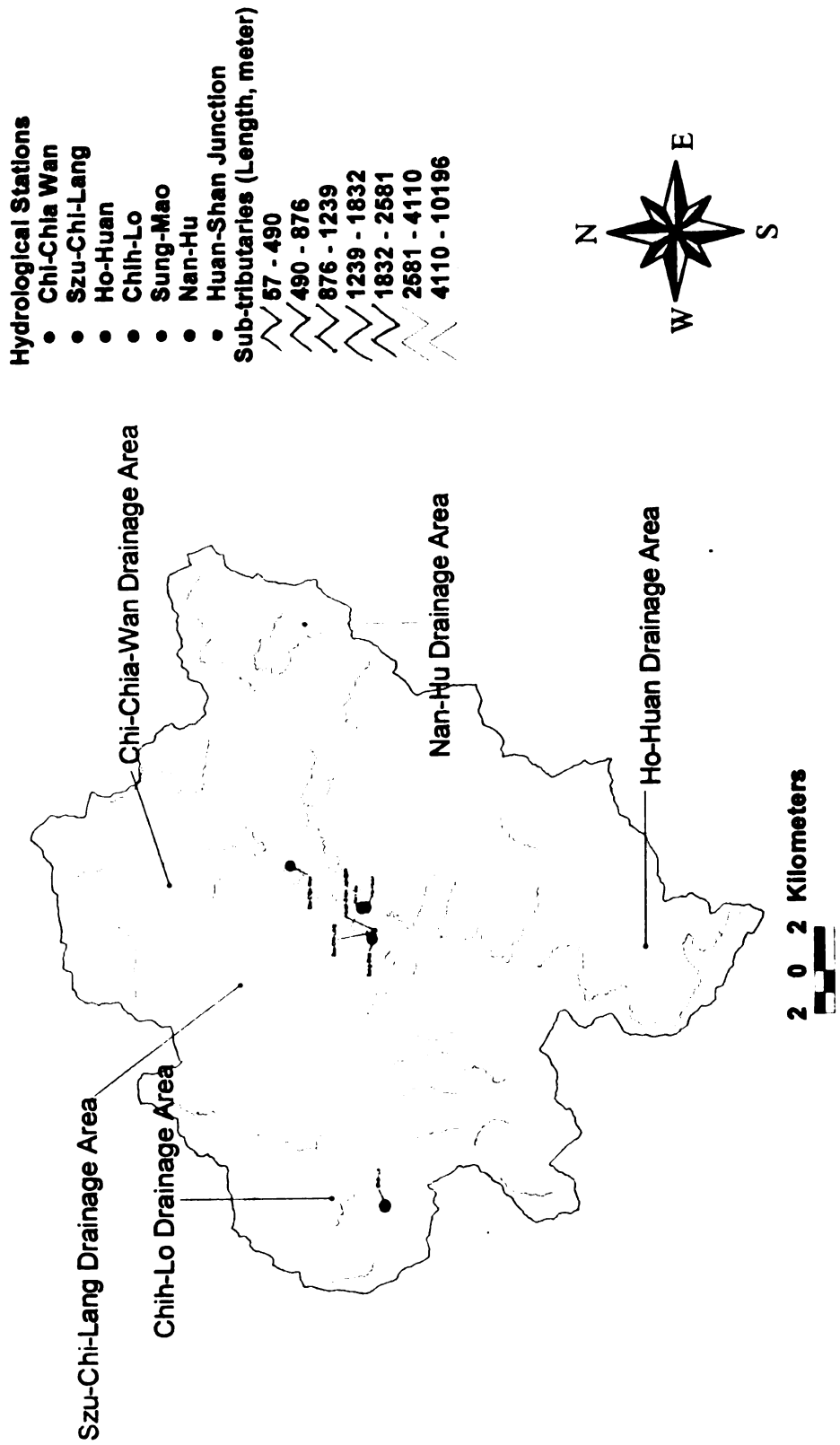
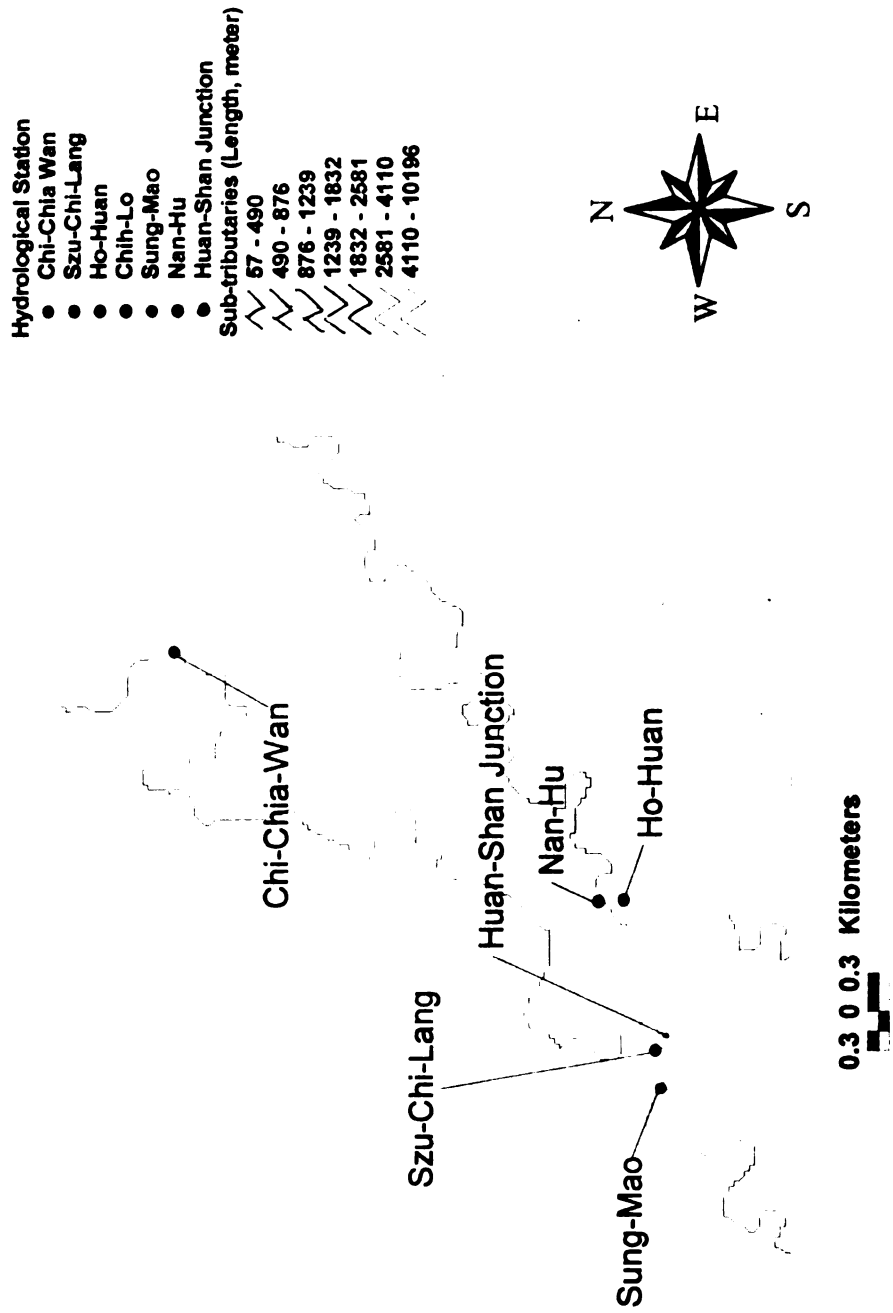


Figure 6.11 The GIS Map of the Hydrological Stations in the Te-Chi Reservoir Watershed



The runoff data over a twenty-seven-year period in seven hydrological stations in the Te-Chi Reservoir Watershed is tabulated in Table 5.2 (See Appendix A) and is illustrated in Figure 6.9. The data indicates the average annual runoff (cms-day) and its frequency of occurrence. Figures 6.10 and 6.11 show the locations of the hydrological stations.

Table 6.6 Average Annual Runoff (mm) (Type A) in Seven Drainage Areas in the Te-Chi Reservoir Watershed

Hydrological Station	Drainage Area (km ²)	Average Annual Runoff (cms-day)	Area Measured by Gauging Station (km ²)	Runoff in Measured Area (cms-day)	Runoff (mm)
Chih-Lo	77	2147	77	2147	2396
Chi-Chia-Wan	111	1948	111	1948	1520
Szu-Chi-Lang	156	3208	46	1261	2379
Nan-Hu	126	2240	126	2240	1540
Ho-Huan	129	2465	129	2465	1657
Huan-Shan Junction	258	5019	4	314	7456
Sun-Mao	417	9078	3	850	26796

Table 6.7 Medium Annual Runoff (mm) (Type B) in Seven Drainage Areas in the Te-Chi Reservoir Watershed

Hydrological Station	Drainage Area (km ²)	Maximum Frequency range of Annual Runoff (cms-days)	Area Measured by Gauging Station (km ²)	Runoff in Measured Area (cms-day)	Runoff (mm)
Chih-Lo	77	1900~2300	77	2203	2457
Chi-Chia-Wan	111	1300~1700	111	1440	1124
Szu-Chi-Lang	156	3300~3700	46	2035	3841
Nan-Hu	126	3000~3100	126	3045	2094
Ho-Huan	129	1500~2000	129	1637	1100
Huan-Shan Junction	258	6000~6600	4	1547	36729
Sun-Mao	417	9300~11300	3	430	13599

Table 6.8 Maximum Daily Runoff (mm) (Type C) in Seven Drainage Areas in the Te-Chi Reservoir Watershed

Hydrological Station	Drainage Area (km ²)	Maximum Daily Runoff (cms-day)	Area Measured by Gauging Station (km ²)	Runoff in Measured Area (cms-day)	Runoff (mm)
Chih-Lo	77	191	77	191	213
Chi-Chia-Wan	111	181	111	181	141
Szu-Chi-Lang	156	267	46	85	161
Nan-Hu	126	214	126	214	147
Ho-Huan	129	149	129	149	100
Huan-Shan Junction	258	640	4	276	6552
Sun-Mao	417	904	3	48	1521

Table 6.9 Three Types of Area-weighted Runoff (mm) in the Te-Chi Reservoir Watershed

Cell Runoff Type	Type A	Type B	Type C
Cell Runoff (mm)	1961	2156	200

Type A: Average Annual Runoff

Type B: Medium Annual Runoff

Type C: Maximum Daily Runoff

The elevation of the Te-Chi Reservoir Watershed is between 2,000m and 3,884m (Lin, 1974). The orographic rains and the local thunderstorms occur frequently (Anonymous, 1996d), and therefore the use of microclimatological data is essential for hydrological simulations. Table 6.6 shows the average annual runoff (Type A), Table 6.7 the median annual runoff (Type B), and Table 6.8 the maximum daily runoff (Type C) of the seven stations. Figure 6.11 is a reference used to mark the boundaries of a particular hydrological station.

The area-weighted runoff method along with the information from Tables 6.6, 6.7, and 6.8 is used to calculate the three types of average runoff (mm) in the Te-Chi Reservoir Watershed. The results are shown Table 6.9.

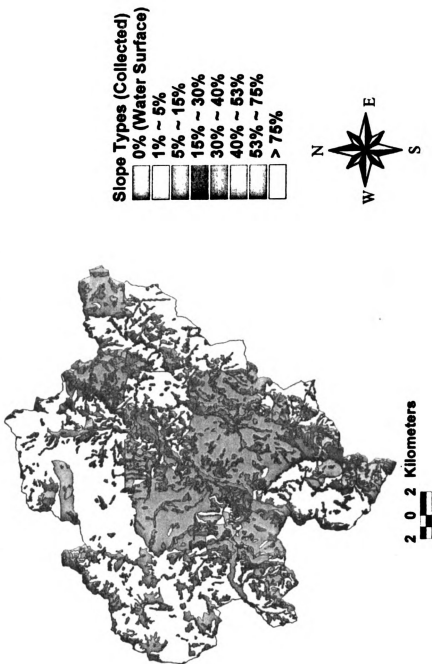
Type B runoff is larger than the runoff of Type A. Therefore, type A runoff can be ignored and type B runoff is used to simulate the water runoff movement in the Watershed.

Type C runoff (200.08mm) is a reflection of the maximum daily rainfall in the watershed. Therefore, when torrential rain is simulated, the simulation uses the runoff of type C.

The slope-type and land-use are two topographical factors affecting the water-runoff in the Watershed. For the design of the watershed-runoff system, an in-depth analysis of the water-runoff in the watershed has to be made. Thus, the GIS-SVIS maps of the slope-type and of land-use of the water-runoff in the watershed have to be available.

6.2.1 Slope-Type Factor

**Figure 6.12 The GIS Map of Slope-Type
in the Te-Chi Reservoir Watershed**



The two-dimensional GIS map of slope-type in Figure 6.12 was used with ArcView GIS 3.1 to produce the three-dimensional GIS-SVIS map of slope sun-shade in Figure 6.13. The GIS-SVIS map of slope sun-shade (Figure 6.13) was combined with the GIS map of slope-type (Figure 6.12) to make the three-dimensional GIS-SVIS map of slope-type shown in Figure 6.14. By employing the GIS-SVIS maps of slope-type (Figure 6.14), water runoff was depicted by four GIS-SVIS maps: (1) the three-dimensional GIS-SVIS map of flow directions in Figure 6.15, (2) the three-dimensional GIS-SVIS map of sinkholes in Figure 6.16, (3) the three-dimensional GIS-SVIS map of flow accumulation in Figure 6.17, and (4) the three-dimensional GIS-SVIS maps of upstream flow-length in Figure 6.18 and of downstream flow-length in Figure 6.19.

6.2.1.1 Slope Sun-Shade GIS-SVIS Map

The results of the computation of the sun-shade in the Watershed were used to illustrate the hypothetical illumination of a surface on a graphical display. For analysis, the display can be used to determine the length of time and intensity of the sun at a particular location. The brightness of the graphical display is an indication of the type of weather.

The elevation data of 271 mountain-peaks collected from the contour maps of the Watershed were added into the tabular elevation-data (48 mountain-peaks) of the GIS map of slope-type (Figure 6.12). These 319 mountain-peak elevation data were used to achieve the different effects by tentatively adjusting the azimuth and altitude parameters. An azimuth at 315° (the position of the sun in the northwest of the Watershed) and an altitude at 25° (the sun shadow computed at 4:20 PM) were used to produce the GIS-SVIS sun-shade map.

**Figure 6.13 The GIS-SVIS Map of Slope Sun-Shade at 4:20 PM
in the Te-Chi Reservoir Watershed
(Position of the Sun: in the Northwest of the Watershed)**

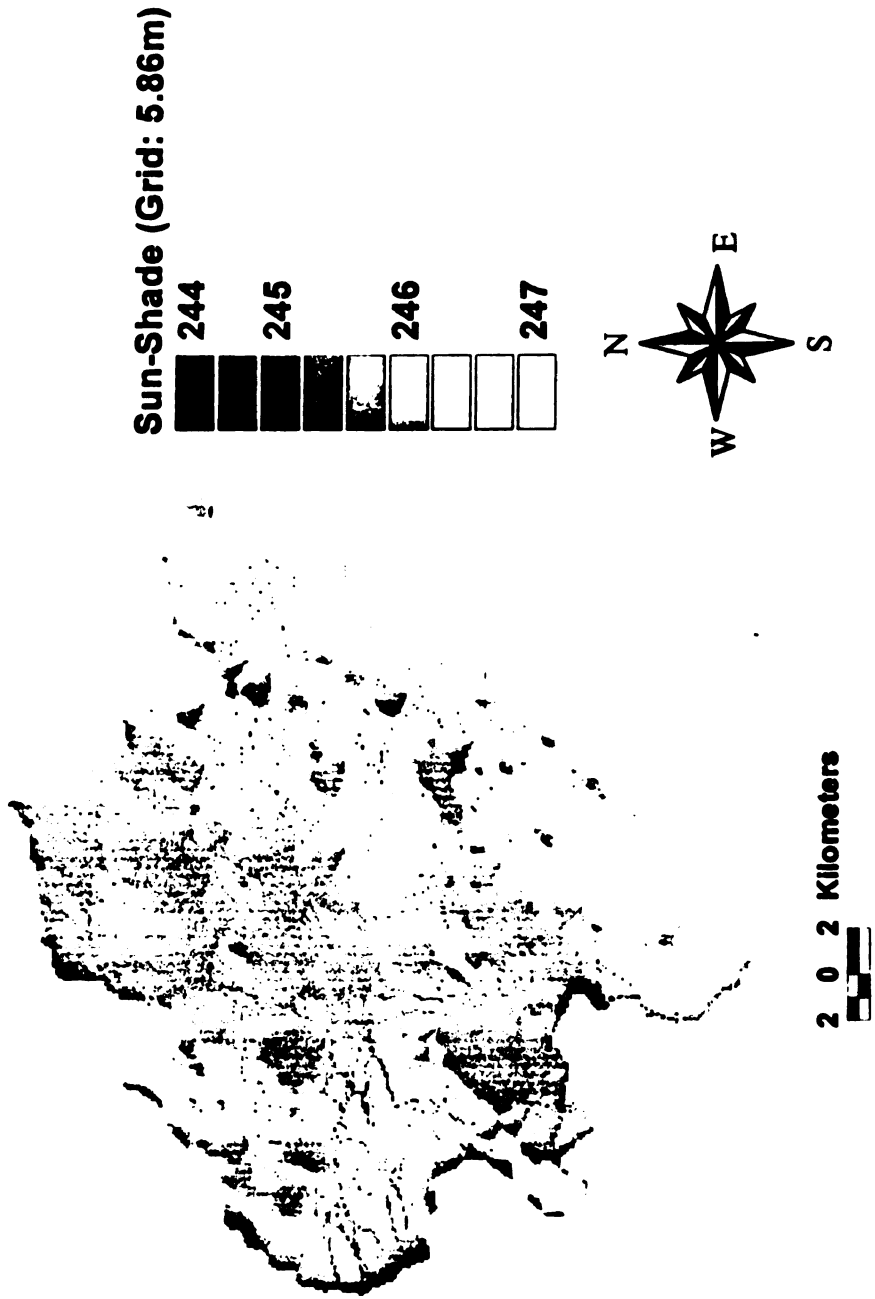


**Figure 6.14 The GIS-SVIS Map of Slope-Type
in the Te-Chi Reservoir Watershed**

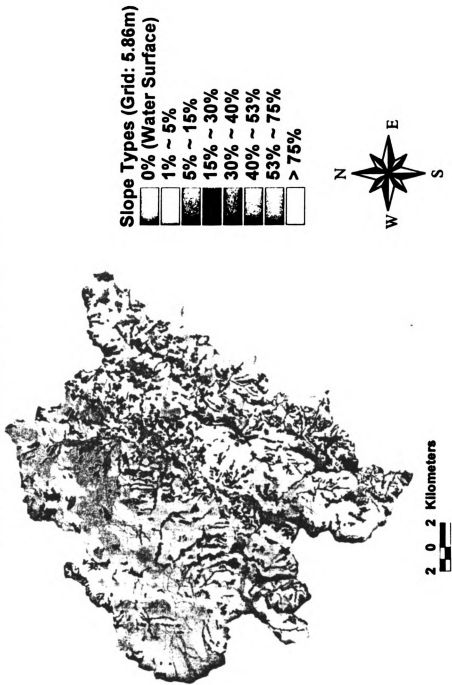


**Figure 6.15 The GIS-SVIS Map of Relative Elevation
in the Te-Chi Reservoir Watershed**

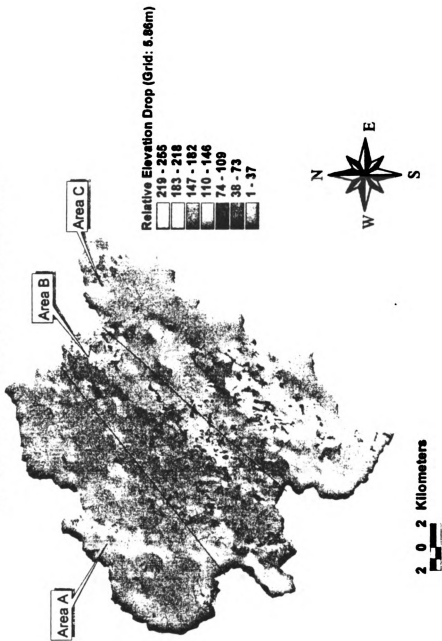


**Figure 6.16 The GIS-SVIS Map of Stream-Source Areas and Relative Elevations
in the Te-Chi Reservoir Watershed**

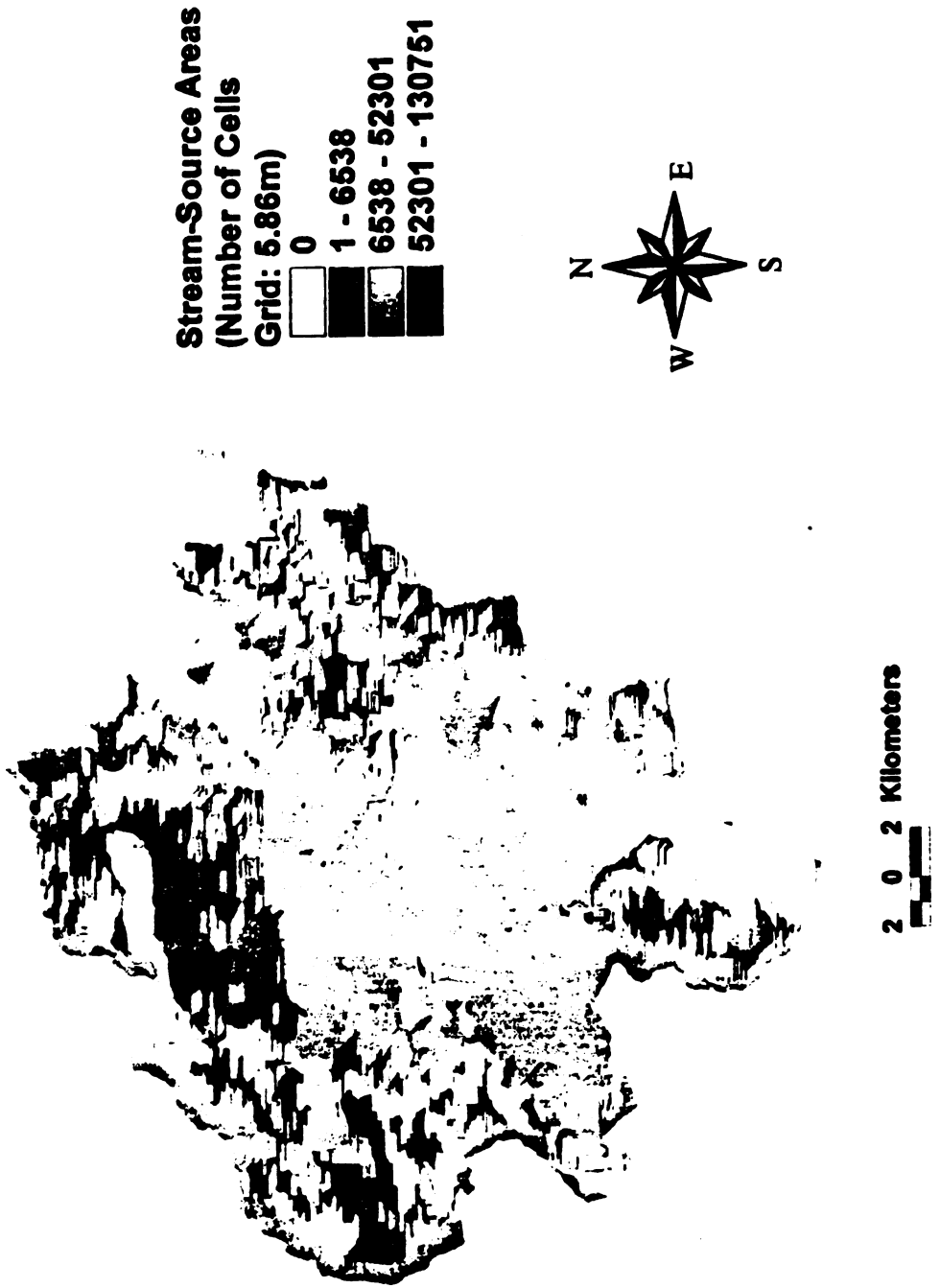


**Figure 6.17 The GIS-SVIS Map of Flow-Length
in the Te-Chi Reservoir Watershed**

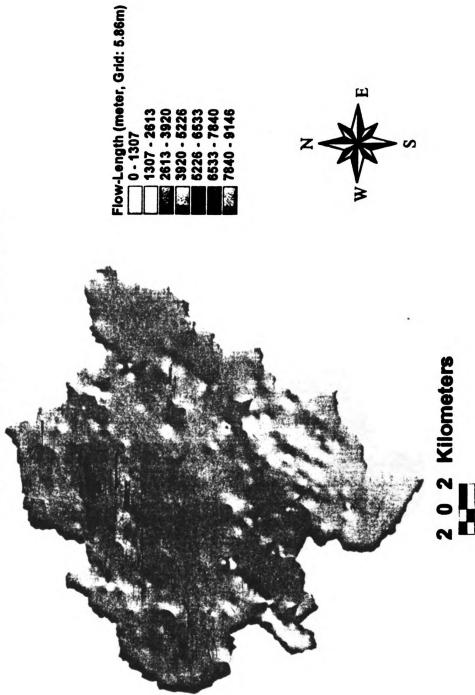


**Figure 6.18 The GIS Map of Land-Use
in the Te-Chi Reservoir Watershed**



Landuse Types (Collected)	
	Coniferous Forest
	Broadleaf Forest
	Mixed Forest
	Forest Plantation
	Fruit Orchard
	Tea Plantation
	Grassland
	Vegetable Field
	Exposed Arable
	Fire-Prevention Line
	Streams & Reservoir
	Construction Site
	Landslide Area
	Road

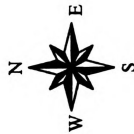
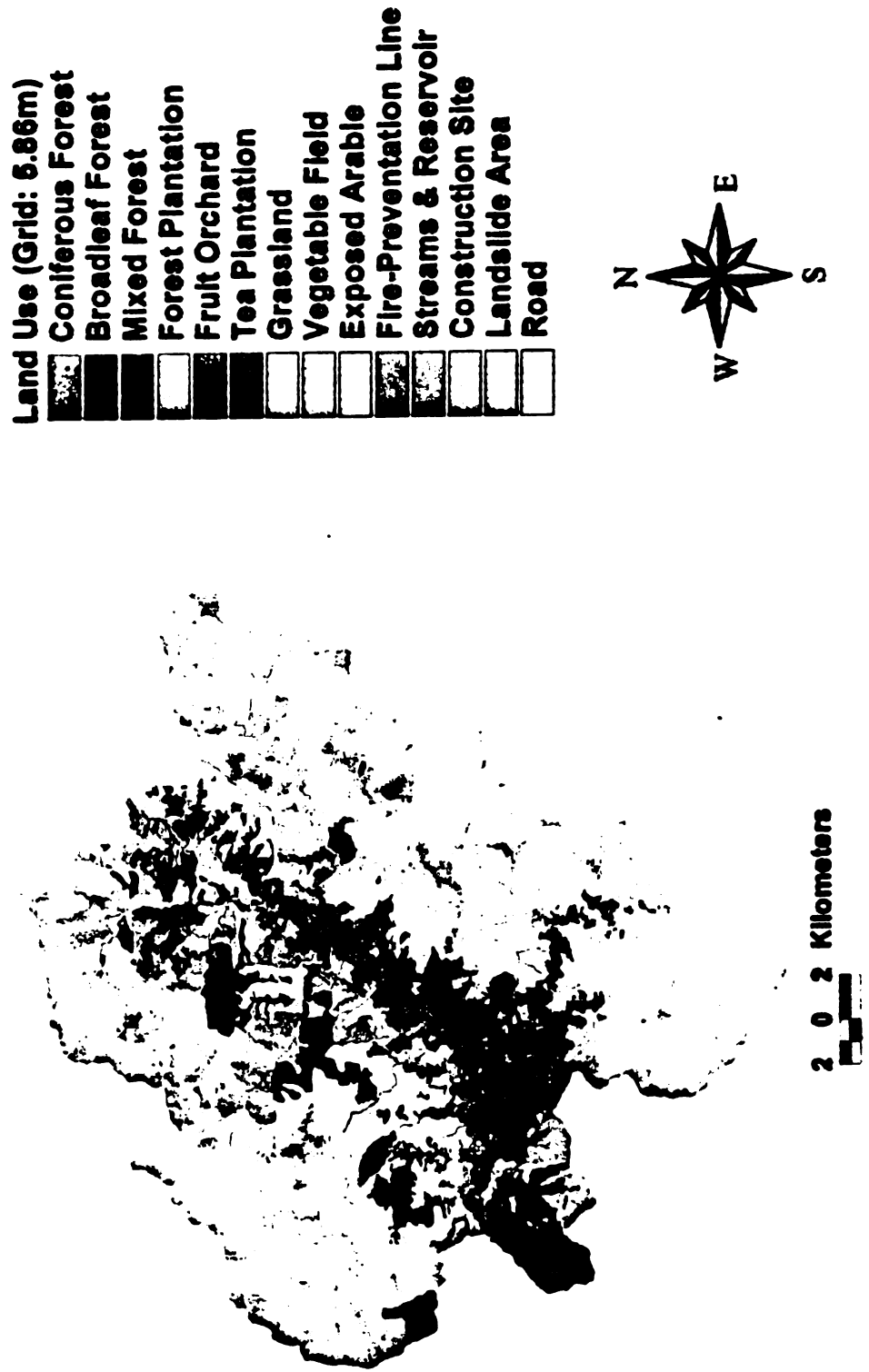


**Figure 6.19 The GIS-SVIS Map of Land-Use
in the Te-Chi Reservoir Watershed**



The azimuth angle, altitude angle, and representative-fraction size were used to display the virtual reality of a GIS-SVIS map. By changing the angles of the azimuth and altitude, the three-dimensional visualization of a watershed could be displayed. Also, by changing the scale of a GIS-SVIS map, the far-and-near distances to an object were visualized, i.e. the smaller the scale, the larger an object (See Section 3.3).

In Figure 6.13, the fine black lines with a shade index above 245 are streams. The remaining areas with a shade index between 245 and 246 are the high-mountain areas an elevation between 2,000m and 3,884m.

6.2.1.2 Relative-Elevation GIS-SVIS Map

The flow direction in a cell was calculated from its relative elevation viz a viz eight surrounding cells, using the relationship: $\text{drop} = \frac{\text{changed elevation (Z)}}{\text{distance}} \times 100$. Distance is equal to the distance between two cell centers, i.e. since the cell size is set to 5.86m, the distance between two orthogonal cells is 5.86m and between two diagonal cells is 8.29m. If the gradients to the adjacent cells are the same, then the water runoff to the neighboring cells will be the same. If the gradients to the adjacent cells are dissimilar, the water will flow to the neighboring cell at the lowest elevation (Greenlee, 1987).

The GIS-SVIS relative-elevation map in Figure 6.15 was used to calculate the flow-directions of the water in a central cell to its eight-neighboring cells. Each cell is assigned a Z value, which ranges from 1 (the lowest elevation) to 255 (the highest elevation). If a central cell is lower than its eight-neighboring cells, then it is given a value lower than its eight-neighboring cells, and the flow direction is thus towards this cell. If multiple-neighboring cells of a central cell have the same low value, these cells

are still assigned the lowest value, i.e. then a central cell has the same Z value in multiple directions, and thus the occurrence of a one- or multiple-cell sinkhole is eliminated (See Section 6.2.1.3) (Anonymous, 1996f).

The water flow in the Te-Chi Reservoir Watershed depends mainly on the topography of: (1) the Ridge Mountain Range (area A), (2) the Central River Valley (area B), and (3) the Snow Mountain Range (area C) (See Section 4.2). Figure 6.15 shows the topography of the three areas.

The total area of the pink regions (drop value between 219 and 255) in Figure 6.15 represents the largest area in the Watershed (it accounts for about 70% of the total area). The pink regions are distributed over the entire watershed.

The area of the yellowish brown regions (drop value between 183 and 218) is the second largest area in the Watershed (it accounts for about 14% of the total area). These regions located at the second highest elevation in the watershed receive the water runoff from the pink regions and move their runoff toward the green-, blue-, purple-, or red-colored regions.

The red-colored regions (drop value between 1 and 37) constitute the third largest area in the Watershed (these account for about 12% of the total area). Thus, the water runoff in the areas A and C flows toward area B, i.e. to the southeast of the Watershed.

By comparing Figure 6.14 with Figure 6.15, some regions represent an abnormal phenomenon because it applies that water in some areas flows from areas with a lower slope toward areas with a higher slope. The sinkholes cause this “phenomenon” (see next section).

6.2.1.3 Sinkhole-Areas and Relative-Elevation GIS-SVIS Map

A sinkhole occurs when all neighboring cells are higher than the central cell or multiple central cells (Anonymous, 1996f). Water is contained in a sinkhole, and does not flow anywhere (except may be into the ground).

There are 228 sinkholes in the Watershed. Each sinkhole is assigned a unique number from 1 to 228. Table 6.10 (See Appendix G) shows the size of each sinkhole. The largest sinkhole, No. 26, covers 18,346 hectares, and is located in areas A, B, and C.

In Figure 6.15, it shows the flow-direction of the water in some lower elevations toward the higher elevations. This phenomenon is caused because a sinkhole-area in a lower-slope location stores the water from the streams, the runoff, and the groundwater, and this water can flow out when the water pressure of the surface water bodies is lower than the water pressure of the sinkhole-areas during a drought. During a rainy period, the water pressure in a sinkhole-area is lower than the water pressure in a surface water-body, and thus either the water is restricted in the sinkhole-area or the surface water can flow into a sinkhole-area when the water pressure of the surface water body is much higher. Therefore, during a dry period, a sinkhole should be taken into account in calculating the runoff. During the rainy season, the sinkhole-area fills up first.

To develop an accurate representation of flow-direction and flow accumulation, a data set free of sinkhole-areas is required. The naturally-occurring sinkhole-areas in a data set with cell sizes of over 10 meters are rare (Mark, 1988) except for the glacier- and heart-type topographies in a watershed. Otherwise, the sinkhole-areas are considered the data errors. The sinkhole-areas in the Te-Chi Reservoir Watershed were caused by the glaciation (Lin, 1974), and thus the sinkhole-areas occurring in the Watershed dataset are correct.

6.2.1.4 Stream-Source Areas and Relative Elevation GIS-SVIS Map

The accumulated water-runoff in a down-slope cell was calculated by weighing the relative elevation of the cells surrounding it (except for the sinkholes, see Section 6.2.1.3). The accumulated water is dependent on the number of surrounding cells and their tendency to pass on accumulated water (Anonymous, 1996f).

A stream area is an area of concentrated water-runoff accumulation. Mountain ridges do not accumulate the water; i.e., the cells in a high topographical area have zero flow accumulation.

The GIS-SVIS map in Figure 6.16 shows the areas of the flow-accumulation in the Watershed; the map also shows the relative elevation of the stream-source areas. The mountain ridges (light-gray-colored areas) account for the largest area of the Watershed. The remaining colored areas in the Watershed are the stream-source areas, i.e. the water sources of the stream.

6.2.1.5 Slope Flow-Length GIS-SVIS Map

Figure 6.17 is the GIS-SVIS map of the flow-length distribution in the Watershed. The distance of the flow path of each cell is calculated in order to find the length of the longest flow path within the Watershed. It was used to calculate the time required for water to flow from the most remote point in the area to the outlet of the watershed, i.e. the time of concentration (in minutes).

Most of the mountain ridges in the watershed run in the north-south direction and thus the flow paths run in the east-west direction. The flow-lengths are much longer in regions A and C (which are over 2,000m in elevation) than in the valleys in area B. The

longest flow-lengths are in the northwest of the Watershed(they are colored red in Figure 6.17).

6.2.2 Land-Use Factor

The GIS-SVIS map of slope sun-shade (Figure 6.13) is combined with the GIS map of land-use (Figure 6.18) to produce the GIS-SVIS land-use map shown in Figure 6.19. There are fourteen types of land-use distributed in different topographies in the Watershed. Each land-use type results in a particular surface roughness, thus increasing or decreasing the velocity of the water runoff on the various slopes.

In Figure 6.19, the natural forests of coniferous trees, broadleaf trees, and mixed trees account for the largest area in the watershed. In the agricultural regions of area B, the water-runoff-driven erosion has caused nutrient and sediment loading and eutrophic conditions in the main reservoir (Anonymous, 1996d).

Water erosion in the watershed is affected by the interaction of torrential rainfall, water runoff, steep slopes, land-use conditions, and underground geological features. The kinetic energy resulting from the velocity of the water runoff becomes the power source driving other erosion factors in causing the considerable soil losses, decreased water storage, degraded water quality, and nutrient-related algae blooms which release dangerous toxins into the reservoir and surrounding streams. It is essential to control the flow-velocity of the water runoff in a certain locations of the Watershed.

6.2.3 Slope-Type and Land-Use Factors

The mountain slopes affect the flow direction, accumulation, flow length, and the velocity of the water runoff in the Watershed. The land-use also influences the velocity of the water runoff. For the design of the hillside soil-conservation construction and

practices, the velocity of the water runoff is an essential input because it is the major driving force causing the soil erosion.

To cultivate an agricultural crop on a hillside, the relationships between the physical properties of the water-runoff and the types of land-use should be considered in order to reduce the water-quality deterioration and the soil erosion. Figure 6.20 depicts the slopes of the terrain which are smaller than 30% and greater than 30%. When a slope is smaller than 30%, the velocity of the water runoff in an agricultural area should be reduced to less than 1.5 m/sec. When a slope is greater than 30% no agriculture should be practiced, one should adhere to the criteria for slope-land cultivation (Anonymous, 1990), and one should practice soil conservation, e.g. bench terracing and hillside ditching. In Figure 6.8 (Section 6.1.3), some bench terraces are shown to be along the main reservoir.

Figure 6.21 shows that some agriculture is still practiced on slopes greater than 30%, in particular fruit orchards, vegetable fields, and tea plantation. Figure 6.21 also shows where landslides have occurred in the agriculture areas.

Figure 6.22 depicts the location of a typical 21.8ha vegetable field located in a mountainous area (slopes over 30%) beside a large stream-source. The vegetable field does not conform to the criteria for slope-land cultivation.

Figure 6.23 is a detailed map of the vegetable field and its surroundings. It is located in the drainage area of the Chi-Chia-Wan hydrological station. The water from the vegetable field and the surrounding area collects in the southwest corner of the vegetable field. This lowest point receives the water from 33,325 cells (114ha). The calculation of the flow rate in the lowest-elevation cell per unit time is described below.

6.2.4 Calculation of Flow Rate

Figure 6.20 The GIS-SVIS Map of Areas of Slope < 30% and Slope \geq 30% in the Te-Chi Reservoir Watershed

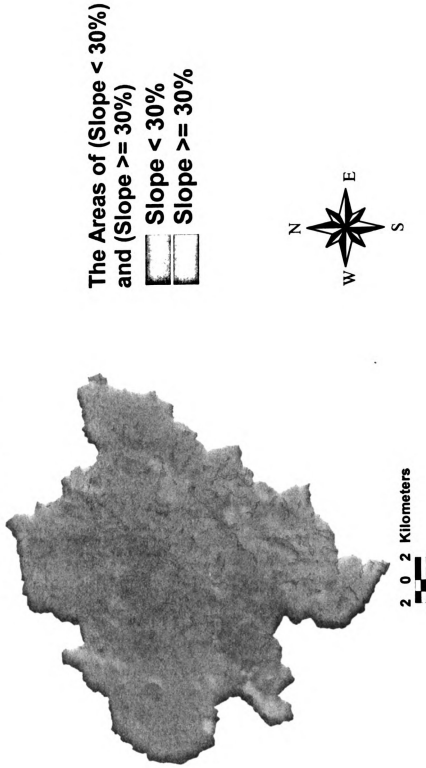


Figure 6.21 The GIS Map of Areas (Slope > 30%) of Cultivation, Roads, and Landslides in the Te-Chi Reservoir Watershed

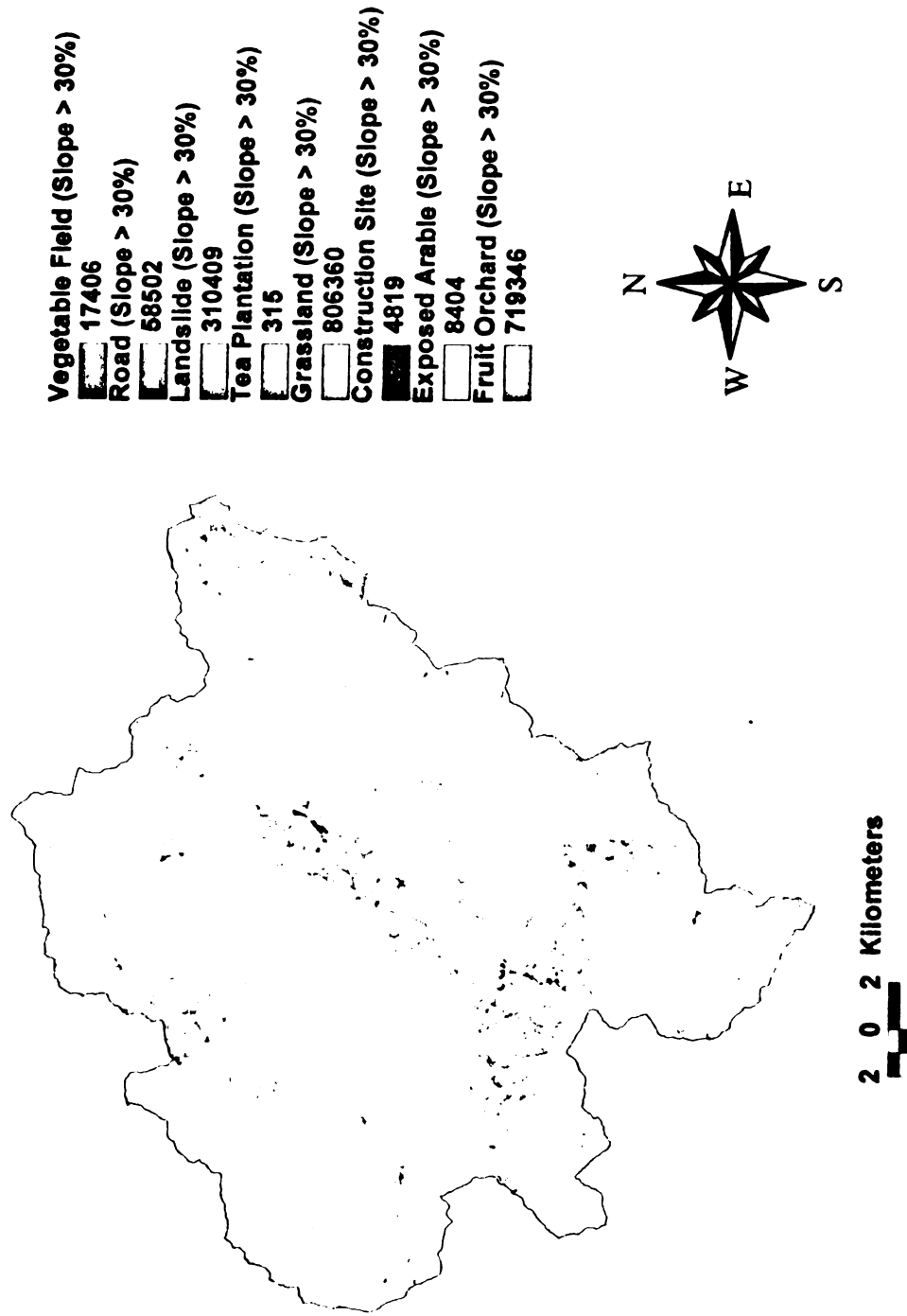
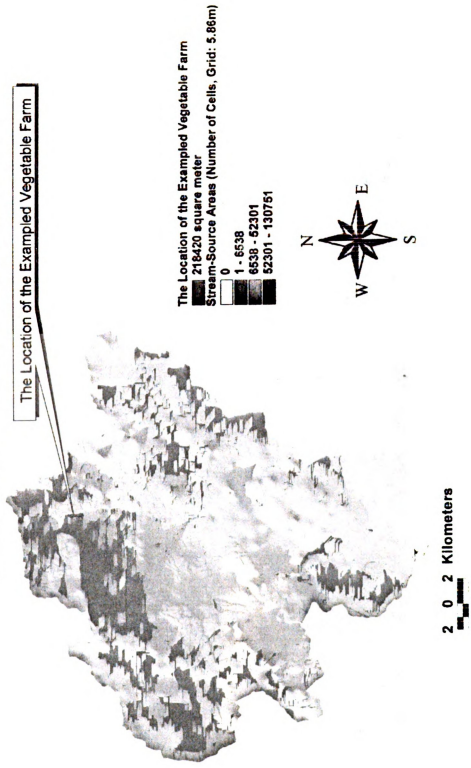


Figure 6.22 The Location of the Exemplified Vegetable Farm Area in the Te-Chi Reservoir Watershed



**Figure 6.23 The Location of the Exemplified Vegetable Farm
in the Te-Chi Reservoir Watershed**



The accumulated water in a cell (m^3) can be calculated by using the following of relationship: [area (m^2) of the cell] x [number of cells located above the cell] x [annual cell runoff (mm)]. The area (m^2) of a cell is $34.3396m^2$ [$5.86m \times 5.86m$]. In Figure 6.16, by using the “Identify” tool, the number of cells located above any cell is found. The annual runoff (mm) can be either the average annual runoff (Type A), the medium annual runoff (Type B), or the maximum daily runoff (Type C), for the total watershed (see Table 6.9, Section 5.3.4.3, and Section 6.2) or for a particular drainage area in the Watershed (see Tables 6.6, 6.7, and 6.8). The calculations are shown below and the results of the accumulated water in a cell are shown in Table 6.11.

6.2.5 Flow Rate in the Drainage Area of the Chi-Chia-Wan Hydrological Station

6.2.5.1 Average Annual Runoff (Type A)

The average annual cell runoff for the total watershed is 1,961mm (see Table 6.9) and thus the flow rate is:

$$(34.34m^2) \times 33,325 \text{ cells} \times 1,961mm = 2,244,264m^3 \text{ of water per year}$$

The average annual cell runoff for the drainage area of the Chi-Chia-Wan hydrological station is 1,520mm (see Table 6.6) and thus the flow rate is:

$$(34.34m^2) \times 33,325 \text{ cells} \times 1,520mm = 1,739,438m^3 \text{ of water per year}$$

6.2.5.2 Medium Annual Runoff (Type B)

The medium annual cell runoff for the total watershed is 2,156mm (see Table 6.9) and the flow rate is:

$$(34.34m^2) \times 33,325 \text{ cells} \times 2,156mm = 2,466,809m^3 \text{ of water per year}$$

The medium annual cell runoff for the drainage area of the Chi-Chia-Wan hydrological station is 1,124mm (see Table 6.7) and thus the flow rate is:

$$(34.34\text{m}^2) \times 33,325 \text{ cells} \times 1,124\text{mm} = 1,286,269\text{m}^3 \text{ of water per year}$$

6.2.5.3 Maximum Daily Annual Runoff (Type C)

The maximum daily annual cell runoff for the total watershed is 200mm (see Table 6.9) and thus the flow rate is:

$$(34.34\text{m}^2) \times 33,325 \text{ cells} \times 200\text{mm} = 228,965\text{m}^3 \text{ of water per day}$$

The value should be used in the design of erosion-prevention systems.

The maximum daily annual cell runoff for the drainage area of the Chi-Chia-Wan hydrological station is 141mm (see Table 6.8) and thus the flow rate is:

$$(34.3396\text{m}^2) \times 33,325 \text{ cells} \times 141\text{mm} = 161,356\text{m}^3 \text{ of water per day}$$

Table 6.11 Predicted Flow Rate ($\text{m}^3/\text{unit time}$) in the Drainage Area of Chi-Chia-Wan Hydrological Station

Cell Runoff Type	Accumulated Water ($\text{m}^3/\text{unit time}$)
Total Watershed of Type A	2,224,4264 m^3/year
Chi-Chia-Wan Drainage Area (Type A)	1,739,438 m^3/year
Total Watershed of Type B	2,422,809 m^3/year
Chi-Chia-Wan Drainage Area (Type B)	1,286,269 m^3/year
Total Watershed of Type C	228,965 m^3/day
Chi-Chia-Wan Drainage Area (Type C)	161,356 m^3/day

6.2.5.4 Flow Rate Conclusions

1. The annual and maximum water flow rates ($\text{m}^3/\text{unit time}$) in the Te-Chi Reservoir Watershed are larger than in the Chi-Chia-Wan drainage area.
2. The predicted flow rates in Table 6.11 did not take into account some extraneous influences (infiltration, evapotranspiration, human/animal use) but can be considered as reasonably accurate estimates of the water runoff in a particular region (i.e. a vegetable farm) of the Watershed.
3. The water infiltration and evapotranspiration can decrease the predicted flow rates in Table 6.11 by 10% ~ 30%.

4. In considering soil-erosion prevention and stream-source protection for a particular farm in the Watershed, the maximum daily runoff in its drainage area should be used (e.g. $161,356\text{m}^3/\text{day}$ for the vegetable farm in the Chi-Chia-Wan drainage area).

Chapter 7 CONCLUSIONS

- (1) GIS maps were developed of the vegetable fields and the water bodies in the Te-Chi Reservoir Watershed in Taiwan.**
- (2) The annual and maximum daily water flow rates in the Watershed were calculated, and the water-runoff GIS-SVIS maps were developed.**
- (3) The water flow rates on a vegetable farm in the Chi-Chia-Wan drainage area in the Watershed were calculated assuming that the drainage area is homogenous.**

Chapter 8 RECOMMENDATIONS FOR FURTHER STUDY

Listed below are some recommendations for future study:

1. The newly-developed design tool can be applied to the production of additional GIS-SVIS maps, e.g. road maps, street maps, in the Te-Chi Reservoir Watershed, or in other watersheds.
2. The design tool can be applied in Precision Agriculture.
3. The design tool can be used to simulate and/or monitor the water-quality pollution from non-point sources and point sources in the Te-Chi Reservoir Watershed.

Chapter 9 REFERENCES

- Anonymous.** 1999. Deep Computing Institute, IBM Corporation.
http://www.research.ibm.com/dci/dx_releases.html. May 24, 1999.
- Anonymous.** 1998a. *Compton's Interactive Encyclopedia Deluxe (in CD form)*. TLC Properties Inc., Cambridge, MA.
- Anonymous.** 1998b. *Using ArcView Image Analysis*. ERDAS, Inc., Atlanta, GE.
- Anonymous.** 1998c. *Using ArcView Tracking Analyst*. TASC, Inc., Reading, MA.
- Anonymous.** 1997a. *Understanding GIS-The ARC/INFO Method*. 4th ed. Environmental Systems Research Institute, Inc., Redlands, CA.
- Anonymous.** 1997b. Radio Technical Commission for Aviation Services Incorporated, Aeronautical Spectrum Planning For 19972010, DO-237, SC-185.
- Anonymous.** 1997c. *Using ArcView 3D Analyst*. Environmental Systems Research Institute, Inc., Redlands, CA.
- Anonymous.** 1996a. *Delorme Tripmate User's Guide*. DeLorme Inc., Freeport, ME.
- Anonymous.** 1996b. *GTCO AccuTab Surface-Lit LII Plus Digitizer User's Manual*.
- Anonymous.** 1970 ~ 1996c. *Hydrological Year Book of Taiwan, Republic of China*. Water Resources Bureau, Ministry of Economic Affairs, Taiwan, Republic of China.
- Anonymous.** 1996d. *The Planning for the Investigation of the Non-point Sources Pollution and the Control Tactics for Te-Chi Reservoir watershed*. Environmental Protection Bureau, Taichung Hsien, Taiwan, Republic of China.
- Anonymous.** 1996e. *Using ArcView GIS*. Environmental Systems Research Institute, Inc., Redlands, CA.
- Anonymous.** 1996f. *Using the ArcView Spatial Analyst*. Environmental Systems Research Institute, Inc., Redlands, CA.
- Anonymous.** 1996g. *Microsoft Excel 1997 User's Guide*. Microsoft Corporation.
- Anonymous.** 1995a. *Global Positioning System Standard Positioning Service Specification*. 2nd ed. United States Coast Guard Navigation Center.
- Anonymous.** 1995b. Radio Technical Commission for Aviation Services Incorporated. Minimum Aviation System Performance Standards DGNSS Instrument Approach System: Special Category 1 (SCAT I). DO-217. SC-159. April 19, 1995.

- Anonymous.** 1995c. *The Third Period of Integral Policy Making, Water Quality Monitoring, and Managing Modeling for Te-Chi Reservoir Watershed II.* Final Report. Te-Chi Reservoir Committee, Taiwan, Republic of China. p100.
- Anonymous.** 1994a. *Content Standards for Digital Geospatial Metadata.* Federal Geographic Data Committee (FGDC), U. S. Geological Survey, Washington, D.C.
- Anonymous.** 1994b. *Radio Technical Commission for Maritime Services.* RTCM Recommended Standards for Differential NAVSTAR GPS Service - Version 2.1. RTCM Special Committee No. 104. January 3, 1994.
- Anonymous.** 1994c. *The Setup of Information System and Landuse/cover Change Analysis of Te-Chi Reservoir Catchment.* Final Report, ERL Report 06-3-84-0020. Te-Chi Reservoir Committee, Taiwan, Republic of China. p185.
- Anonymous.** 1993. *Global Positioning System monographs.* The Institute of Navigation. Washington, D.C.
- Anonymous.** 1991. *ICD-GPS-200: GPS Interface Control Document.* GPS Joint Program Office. ARINC Research.
- Anonymous.** 1990. *Soil Conservation Handbook.* Soil and Water Conservation Service, Taiwan, Republic of China.
- Anonymous H.** 1984. *Standards and Specifications for Geodetic Control Networks.* Federal Geodetic Control Committee. National Geodetic Information Branch. Maryland, USA.
- Anonymous.** 1981. *Standard Specifications and Recommended Practices for Horizontal and Vertical Control Surveys.* 3rd Edition: Special Publication 1. National Mapping Council of Australia. Canberra: National Mapping Council of Australia.
- Anonymous.** 1978. *Specifications and Recommendations for Control Surveys and Survey Markers.* Surveys and Mapping Branch, Ottawa, Canada: nergy, Mines and Resources Canada.
- Armstrong, A.P., P.A. Collier, and F.J. Leahy.** 1992. *Leveling Using the Global Positioning System.* Urban Water Research Association of Australia, Research Report No. 47, Department of Surveying and Land Information, The University of Melbourne.
- Arnell, N.W.** 1995. *Grid Mapping of River Discharge.* Journal of Hydrology. 167 (1995) 39-56.
- Asrar, G. (ed).** 1989. *Theory and Applications of Optical Remote Sensing.* John Wiley and Sons, Inc. New York, NY.

- Avery, T.E., and G.L. Berlin.** 1992. *Fundamentals of Remote Sensing and Airphoto Interpretation*. 5th edition. Macmillan Publishing Company, New York, NY.
- Axelrad, P. & Brown, R. G.** 1996. *GPS: Theory and Applications Volume 1: GPS Navigation Algorithms*. Astronautics and Aeronautics. 163: 409-434.
- Blanchard, W.** November 1996. *The Global Nav. The Situation Up To Now. NAV96: Global Navigation Systems Where are we now*. International Conference of the Royal Institute of Navigation, London. pp.1.1-1.18.
- Brodin, G.** 1996. *GNSS Code and Carrier Tracking in the Presence of Multipath*. Proceedings of the 9th International Technical Meeting of the Satellite Division of the Institute of Navigation GPS-96, Kansas City, September 17-20 1996. p1389-1398.
- Capaccio, S., D.M.A. Walsh, D.Lowe, P.Daly.** *GLONASS as an Accompaniment to the GPS Satellite System*. Surveying in the Offshore Oil & Gas Industry Technology Seminar, The Hydrographic Society in Scotland, (Aberdeen, UK), April 3, 1997.
- Capaccio, S., and D.M.A. Walsh.** 1996. *Results of GPS and GLONASS real-time differential positioning over a 370km baseline*. Civil Aviation Authority Institute of Satellite Navigation, (Leeds, UK), Jan., 1996.
- Capaccio, S., D. Lowe, D.M.A. Walsh, P.Daly, G.Richards, A.Wolfe, and H.Mistry.** February 1997. *GPS/GLONASS LAAS and RAAS En-route Positioning and CATI Precision Approach with FMS Integration: Demonstration and Evaluation (Project Boscombe)*. Institute of Satellite Navigation.
- Capaccio, S., D.M.A. Walsh, D.Lowe, P.Daly.** *GLONASS as an Accompaniment to the GPS Satellite System*. Surveying in the Offshore Oil & Gas Industry Technology Seminar, The Hydrographic Society in Scotland, (Aberdeen, UK), April 3, 1997.
- Capaccio, S., and D.M.A. Walsh.** 1996. *Results of GPS and GLONASS real-time differential positioning over a 370km baseline*. Civil Aviation Authority Institute of Satellite Navigation, (Leeds, UK), Jan., 1996.
- Capaccio, S., D. Lowe, D.M.A. Walsh, P.Daly, G.Richards, A.Wolfe, and H.Mistry.** February 1997. *GPS/GLONASS LAAS and RAAS En-route Positioning and CATI Precision Approach with FMS Integration: Demonstration and Evaluation (Project Boscombe)*. Institute of Satellite Navigation.
- Capaccio, S., D.M.A. Walsh, D. Lowe, and P. Daly.** 1997. *Real-time differential GPS/GLONASS trials in Europe using all-in-view 20-channel receivers*. Journal of Navigation, p193-208.

- Chrisman, N.R.** 1997. *Exploring Geographic Information Systems*. John Wiley & Sons, Inc., New York, NY.
- Clarke, D.** 1963. *Plane and Geodetic Surveying; Volume II*. Constable and Company Ltd. London, UK.
- Congalton, R.G. and K. Green.** 1995. *Wetland and Environmental Application of GIS: The ABCs of GIS: An Introduction to Geographic Information System*. CRC Press, Inc., Boca Raton, FL.
- Denzer, R.** 1993. Graphics for Environmental Decision-Making. *IEEE Computer Graphics & Applications*, 13 (3): 58-64.
- Dueker, K.J. and D. Kjerne.** 1989. *Multipurpose Cadastre: Terms and Definitions*. ASPRS and ACSM, Falls Church, VA.
- Doebelin, E.** 1990. *Measurement Systems Application and Design*. 4th ed. McGraw-Hill Company. New York, New York.
- Domik, G.O.** 1994. *Visualization Education*. *Computers & Graphics*, 18 (3): p277-280.
- Greenlee, D. D.** 1987. *Raster and Vector Processing for Scanned Linework, Photogrammetric Engineering and Remote Sensing*. October 1987. 53 (10): 1383-1387.
- Guptill, S.C. (ed).** 1988. *A Process for Evaluating Geographic Information Systems*. US Geological Survey Open File Report 88-105. Reston, VA.
- Hearnshaw, H. M. and Unwin, D. J. (eds.).** 1994. *Visualization and GIS*. London: Wiley, Inc., London, UK.
- Ji, W. and L.C. Mitchell.** 1995. *Analytical Model-Based Decision Support GIS for Wetland Resource Management*. CRC Press, Inc., Boca Raton, FL.
- Evans, T. E.** May 1986. *Microwave Landing System*. *IEEE Aerospace and Electronic Systems Magazine*. pp. 6-9.
- Federal Aviation Authority.** October 21, 1996. *FAA National Airspace System (NAS) Architecture, version 2.0, ASD1*, Washington.
- Filatchenkov, S.** 1996. *NAV96: Global Navigation Systems: Where are we now. The Current Status and Future Plans for GLONASS*. International Conference of the Royal Institute of Navigation, London. November 5-6. 1996. pp.4.1-4.9.
- Halliday, D., R. Resnick, and J. Walker.** 1993. *Fundamentals of Physics*. 4th Edition. John Wiley & Son, Inc. New York, NY.

- Hartman, R.G., M.A. Brenner, and N.K. Kant.** 1991. *GPS/GLONASS Flight Test, Lab Test and Coverage Analysis Tests*. Proceedings of the Institute of Navigation GPS-91. Albuquerque, NEW MEXICO. September 11-13, 1991. pp.333-344.
- Harvey, B.R.** 1986. *Transformation of 3D Coordinates*. The Australian Surveyor 33(2): 105 - 125.
- He, Chun-Sun.** 1982. *Tectonic Evolution of Taiwan Explanatory Text of the Tectonic Map of Taiwan*. Central Geological Investigation Research Institute, Ministry of Economic Affairs, Taiwan, Republic of China.
- Hoffmann-Wellenhof, B., H. Lichtenegger, and J. Collins.** 1994. *GPS: Theory and Practice*. 3rd ed. New York: Springer-Verlag.
- Hudson, N.** 1981. *Soil Conservation*. London: B.T. Bastford Limited.
- Kaplan, E.D. (ed).** 1996. *Understanding GPS: Principles and Applications*. Artech House Publishers. Boston, MA.
- Kayton, M.** 1989. *Introduction to Aircraft Navigation, Navigation: Land, Sea, Air & Space*. IEEE Press. pp.229-244.
- Kelly, R. J. and E.F.C. LaBerge.** 1990. *MLS: A Total System Approach*. IEEE Aerospace and Electronic Systems Magazine. May, 1990. 5: 27-39.
- Keller, P.R., Keller, M.M.** 1992. *Visual Cues: Practical Data Visualization*. IEEE Computer Society Press, Inc., Los Alamitos, CA.
- Kirkby, M.J. and R.P.C. Morgan.** 1980. *Soil Erosion*. New York, NY: John Wilry & Sons, Inc.
- Kovar, K. and H.P. Nachtnebel.** 1996. *Application of Geographic Information Systems in Hydrology and Water Resources Management*. Oxfordshire, UK: International Association of Hydrological Sciences. Institute of Hydrology Press.
- Kromer, D. and J. Landis.** 1992. *GPS Interface Control Document*. ICD-GPS-200, IRN200B-PROOJ, Rev.B-PR. U.S. Air Force. July1, 1992.
- Kuranov, V.** *Global Navigation Satellite Systems Panel (GNSSP)*. Montreal, CANADA: GLONASS - Interface Control Document. November. 14-24.
- Langley, R. B.** 1997. *GLONASS: Review and Update*. GPS World. July, 1997. pp.46-51.
- Leick, A.** 1995. *GPS Satellite Surveying*. 2nd ed. John Wiley & Sons, Inc. New York, New York.

- Lee, C.** and S. Marsh. 1995. *The Use of Archival Landsat MMS and Ancillary Data in a GIS Environment to Map Historical Change in an Urban Riparian Habitat*. CRC Press, Inc., Boca Raton, FL.
- Lee, K.H.** and R.S. Lunetta. 1995. *Wetland and Environmental Application of GIS: Wetlands Detection Methods*. CRC Press Inc., Boca Raton, FL.
- Lin, Chao-Chi.** 1974. *Taiwanese Topography*. Central Geological Investigation Research Institute, Ministry of Economic Affairs, Taiwan, Republic of China.
- Lyon, J.G.** and J. McCarthy (ed). 1995. *Wetland and Environmental Application of GIS: Introduction to Wetland and Environmental Application of GIS*. CRC Press Inc., Boca Raton.
- Lyon, J.G.** and J. McCarthy (ed). 1995. *Wetland and Environmental Application of GIS: Water Resource Engineering Application of Geographic Information System*. CRC Press Inc., Boca Raton, FL.
- Lyon, J.G.** and J. McCarthy (ed). 1995. *Wetland and Environmental Applications of GIS: Introduction to Other Issues and Applications*. CRC Press, Inc., Boca Raton, FL.
- Mark, D. M.** 1988. *Network Models in Geomorphology, Modeling in Geomorphologic Systems*. John Wiley and Sons, Inc. New York, NY.
- Merva, G.E.** 1995. *Physical Principles of the Plant Biosystem*. St. Joseph, MI: American Society of Agricultural Engineers.
- Misra, P., R.I. Abbot, E.M. Gaposchkin.** 1996. *Integrated Use of GPS and GLONASS: Transformation Between WGS84 and PZ-90*. Proceedings of the 9th International Technical Meeting of the Satellite Division of the Institute of Navigation GPS-96. Kansas City. September 17-20. 1996. pp.307-314.
- Misra, P.** et al. 1993. *SGS85 - WGS84 Transformation: Interim Results*. MIT ATC Project Memorandum 42PM-SATNAV-0004. Feb 1993.
- Muehrcke, P.C.** 1986. *Map Use: Reading, Analysis, Interpretation*. JP Publication, Madison, WI.
- Ohanian, H.C.** 1985. *Physics*. 1st ed. W.W. Norton & Company, Inc. New York, NY.
- Paine, D.E.** 1981. *Aerial Photography and Image Interpretation for Resource Management*. John Wiley and Sons, Inc. New York, NY.
- Parker, H.D.** (ed). 1989. *The GIS Sourcebook*. GIS World, Inc., Fort Collins, CO.

- Parkinson, B. W. 1996. *GPS: Theory and Applications Volume 1: Introduction and Heritage of NAVSTAR, the Global Positioning System*. Astronautics and Aeronautics. 163: 3-28.
- Parkinson, B. W. 1996. *GPS: Theory and Applications Volume 1--- GPS Error Analysis*. Journal of Astronautics and Aeronautics, 163: 469-483.
- Parkinson, B.W. and J.J. Spilker. (ed). 1996. *Global Positioning System: Theory and Practice. Volumes I*. American Institute of Aeronautics and Astronautics, Inc., Washington, DC.
- Parkinson, B.W. and J.J. Spilker. (ed). 1996. *Global Positioning System: Theory and Practice. Volumes II*. American Institute of Aeronautics and Astronautics, Inc., Washington, DC.
- Parkinson, B. W. and J.S. James (ed). 1996. *Global Positioning System: Theory and Practice. Volumes I and II*. American Institute of Aeronautics and Astronautics, Inc. Washington, DC.
- Pierce, J.A. 1946. *An Introduction to LORAN*. Proceedings of the IRE and Waves and Electronics. 34: 216-234.
- Raby, P. 1994. *Integrating Signal Information from GPS and GLONASS*. Department of Electronic and Electrical Engineering, The University of Leeds. August 1994.
- Raper, J. (ed). 1989. *Three Dimensional Applications in Geographic Information Systems*. Taylor & Francis, Inc., Philadelphia, PA.
- Robinson, A.H. and B.B. Petchenik. 1976. *The Nature of Maps*. University of Chicago Press, Chicago, IL.
- Rosbach, U., H. Habrich, and N. Zarraoa. *Transformation Parameters Between PZ-90 and WGS-84*. Proceedings of the 9th International Technical Meeting of the Satellite Division of the Institute of Navigation GPS-96. Kansas City. September 17-20, 1996, pp.279-285.
- Rowson, S, et al. 1994. *Performance of Cat III B Automatic landings Using C/A code Tracking Differential GPS*. Journal of the Institute of Navigation. 1994, pp127-144.
- Serway, R.A. 1992. *Physics for Scientists & Engineers with Modern Physics*. 3rd ed. Saunders College Publishing. Orlando, FL.
- Schwab, G.O, D.D. Fangmeier, W.J. Elliot, and R.K. Frevert. 1993. *Soil and Water Conservation Engineering*. 4th Edition. New York, NY: John Wiley & Sons, Inc.
- Stevens, S.S. 1946. *On the Theory of Scales of Measurement*. Science 103: 677-680.

- Synder, J.P. 1987. *Map Projections-A Working Manual*. USGS Professional Paper 1395. U.S. Government Printing Office. Washington, D.C.
- Thompson, M.M. 1988. *Maps for America*. U.S. Government Printing Office. Washington, D.C.
- Van Graas, F, et al. 1995. *FAA/Ohio University/UPS Autoland Flight Test Results", Navigating the 90's: Technology, Applications and Policy*. Proceedings of the National Technical Meeting, Institute of Navigation. Anaheim. January 18-20, 1995. pp.145-166.
- Ulliman, J. J. 1995. *Aerial Photo Interpretation of Renewable Natural Resources: Course Notes and Workbook*. Department of Forest Resources, University of Idaho. 83844. Moscow, Idaho.
- Walsh, D.M.A. 1995. *A feasibility study of Category III Precision Approach and Landing using GPS, GLONASS and Pseudolites*. CAA Institute of Satellite Navigation. Leeds, UK. May, 1995.
- Wells, D. (ed). 1989. *Guide to GPS positioning*. Fredericton. Canadian GPS Associates. NB, Canada.
- Wolf, P.R. 1983. *Elements of Photogrammetry with Air Photo Interpretation and Remote Sensing*. 2nd ed. McGraw-Hill Book Company. New York, N.Y.
- Worboys, M.F. 1995. *GIS: A Computing Perspective*. Taylor & Francis, Inc., Bristol, PA.
- Yu, Chia-Yii. 1997. *Remote Sensing of the Environment: Course Note*. Department of Agricultural Engineering, Michigan State University, East Lansing, MI.

APPENDICES

APPENDIX A

Table 5.2 The Annual Runoff Data over 27-Year Period in Seven Hydrological Stations in the Te-Chi Reservoir Watershed

HYDROLOGICAL STATIONS									
Average Annual Runoff (cms-day)	Nan-Hu	Ho-Huan	Szu-Chi-Lang	Sung-Mao	Huan-Shan Junction	Chi-Chia-Wan	Chih-Lo		
Year									
1996	2165.11000	2341.67000	3024.98000	8799.80000	4494.15000	1990.75000	1660.27000		
1995	1303.27000	2274.80000	2208.39000	6938.37000	4262.44000	1440.31000	1833.17000		
1994	2449.86000	3303.32000	3989.17000	11267.87000	6215.33000	2671.82000	2526.99000		
1993	1233.73000	1989.48000	1736.97000	5784.59000	3473.64000	985.85000	1895.22000		
1992	2942.70000	3906.40000	5340.20000	14019.81000	7687.57000	2997.42000	2992.12000		
1991	1088.98000	1637.12000	1702.79000	5390.44000	3221.00000	1019.20000	1177.07000		
1990	=====	=====	5902.24000	16166.70000	8688.59000	3285.81000	3482.16000		
1989	1782.85000	2277.14000	3182.02000	8514.26000	4553.17000	1982.84000	2215.44000		
1988	1618.90000	1990.59000	2276.69000	6993.91000	4063.03000	1303.20000	1785.66000		
1987	2043.67000	=====	2588.18000	8751.65000	5388.49000	1668.80000	1880.19000		
1986	3043.34000	=====	3841.67000	11474.77000	6444.53000	2384.75000	2202.90000		
1985	2959.55000	=====	3793.68000	10876.57000	6229.90000	2448.84000	2578.90000		
1984	2309.67000	=====	2504.70000	7687.27000	4438.22000	1665.04000	=====		
1983	3045.39000	=====	4127.11000	11669.63000	6492.54000	2248.79000	=====		
1982	2576.75000	=====	3005.14000	9314.63000	5396.82000	1714.91000	2370.90000		
1981	3039.95000	=====	3416.28000	10135.22000	5739.23000	2091.98000	2617.93000		
1980	1675.13000	=====	2204.47000	5686.22000	3149.84000	1405.04000	1194.78000		
1979	2759.83000	=====	3471.52000	9343.28000	5129.93000	2242.16000	2249.16000		
1978	2189.25000	=====	2781.85000	7965.99000	4554.05000	1842.10000	2024.95000		
1977	1907.00000	=====	2476.31000	7507.47000	4264.88000	1856.12000	2124.03000		
1976	1456.43000	=====	2497.50000	6340.84000	3331.83000	1654.74000	1989.10000		
1975	3137.87000	=====	3475.31000	=====	6210.14000	=====	=====		
1974	3144.83000	=====	3388.39000	=====	6443.97000	=====	=====		
1973	2509.91000	=====	2552.91000	=====	5338.07000	=====	=====		
1972	2021.99000	=====	3364.33000	=====	4836.30000	=====	=====		
1971	2263.89000	=====	4156.16000	=====	2944.06000	=====	=====		
1970	1577.53000	=====	3615.85000	=====	2534.08000	=====	=====		
Drainage Area (Km²)	125.65	128.56	156.49	417.08	257.85	110.71	77.45		

IP PR -- I I DR D I

APPENDIX B

Table 5.4 The Maximum Daily Runoff Data Over 27-Year Period in Seven Hydrological Stations in the Te-Chi Reservoir Watershed

HYDROLOGICAL STATIONS										
Year	Non-Hs	Hs-Huan	Yue-Chi-Leng	Sung-Miao	Huan-Shan Junction	Chi-Chia-Wan	Chih-Li			
1996	184.79000	134.81000	266.50000	648.40000	340.67000	181.12000	76.22000			
1995	20.92000	35.37000	26.12000	85.68000	48.98000	18.57000	37.68000			
1994	25.93000	52.80000	45.23000	146.59000	85.54000	17.38000	47.82000			
1993	132.75000	148.84000	216.68000	583.42000	277.00000	131.81000	191.14000			
1992	89.66	104.75	230.22	488.21	218.24	167.98	44.16			
1991	24.82000	63.88000	40.46000	130.50000	97.89000	19.74000	41.32000			
1990	87.98000	120.40000	217.62000	954.34000	639.61000	133.51000	119.42000			
1989	120.40000	78.71000	243.95000	560.93000	315.27000	175.28000	77.38000			
1988	17.69000	25.32000	27.67000	86.77000	49.42000	12.76000	35.84000			
1987	70.72000	65.89000	61.38000	319.67000	215.49000	48.08000	23.49000			
1986	98.16000	144.85000	144.85000	491.96000	238.46000	78.34000	51.34000			
1985	65.36000	96.64000	96.64000	224.25000	133.03000	61.75000	82.60000			
1984	71.48000	54.27000	54.27000	168.33000	101.18000	36.41000	27.55000			
1983	97.95000	71.91000	71.91000	253.72000	165.56000	42.05000	61.74000			
1982	196.45000	87.38000	87.38000	512.97000	396.07000	68.83000	77.13000			
1981	110.18000	104.10000	104.10000	390.47000	237.02000	78.60000	100.33000			
1980	96.24000	135.40000	135.40000	318.61000	168.42000	94.66000	90.91000			
1979	126.32000	77.47000	77.47000	236.88000	172.88000	57.90000	46.70000			
1978	51.34000	38.45000	38.45000	172.60000	92.67000	28.79000	39.35000			
1977	79.83000	94.52000	94.52000	252.44000	128.09000	75.53000	142.38000			
1976	54.71000	89.48000	89.48000	186.47000	123.23000	82.02000	38.62000			
1975	165.21000	105.71000	105.71000	291.46000	120.00000	320.00000	320.00000			
1974	92.52000	44.50000	44.50000	349.25000	200.00000	200.00000	200.00000			
1973	214.45000	82.68000	82.68000	220.00000	318.40000	318.40000	318.40000			
1972	103.90000	182.80000	182.80000	200.00000	101.47000	101.47000	101.47000			
1971	176.48000	200.08000	200.08000	954.34000	639.61000	181.12000	191.14000			
1970	214.45000	148.84000	148.84000	266.50000	417.08	110.71	77.45			
	125.65	128.56	156.49	417.08	257.85	110.71	77.45			
	Area (Km ²)									

APPENDIX C

Table 6.1 The "aat.dbf" file of the Water Bodies Map of the Te-Chi Reservoir Watershed

FNODE_	TNODE_	LPOLY_	RPOLY_	LENGTH	STREAM_	STREAM_ID
0	0	0	0	1238 823000	1	19
0	0	0	0	2790.783000	2	27
0	0	0	0	1278 823000	3	29
0	0	0	0	346.274200	4	45
0	0	0	0	802 842700	5	52
0	0	0	0	802 842700	6	53
0	0	0	0	936.568500	7	54
0	0	0	0	1911.960000	8	61
0	0	0	0	1198 823000	9	63
0	0	0	0	2037 646000	10	69
0	0	0	0	1071 960000	11	71
0	0	0	0	459 411300	12	79
0	0	0	0	915 979800	13	84
0	0	0	0	1325 686000	14	86
0	0	0	0	1408 528000	15	90
0	0	0	0	1325 686000	16	91
0	0	0	0	216.568500	17	93
0	0	0	0	1629 117000	18	94
0	0	0	0	2827 940000	19	104
0	0	0	0	320 000000	20	105
0	0	0	0	969 705600	21	107
0	0	0	0	2305 097000	22	108
0	0	0	0	1971 372000	23	122
0	0	0	0	2161.666000	24	124
0	0	0	0	2458.234000	25	126
0	0	0	0	433.137100	26	127
0	0	0	0	329 705600	27	131
0	0	0	0	2981 077000	28	132
0	0	0	0	200 000000	29	133
0	0	0	0	2950 783000	30	134
0	0	0	0	1019 411000	31	138
0	0	0	0	193 137100	32	142
0	0	0	0	1235 980000	33	143
0	0	0	0	2074 803000	34	144
0	0	0	0	629.116900	35	147
0	0	0	0	2397.646000	36	158
0	0	0	0	1525 686000	37	166
0	0	0	0	193 137100	38	171
0	0	0	0	819.411300	39	174
0	0	0	0	1302.254000	40	175
0	0	0	0	859 411300	41	184
0	0	0	0	113 137100	42	188
0	0	0	0	1066 274000	43	189
0	0	0	0	942 254000	44	215
0	0	0	0	1831 960000	45	1
0	0	0	0	2710.783000	46	2
0	0	0	0	1085 686000	47	3
0	0	0	0	1132 548000	48	4
0	0	0	0	2221 077600	49	5
0	0	0	0	1775 391000	50	6
0	0	0	0	1678 823000	51	7
0	0	0	0	1891 372000	52	8
0	0	0	0	3709 606000	53	9
0	0	0	0	2164 509000	54	10
0	0	0	0	1235 980000	55	11
0	0	0	0	2185 097000	56	12
0	0	0	0	346 274200	57	13
0	0	0	0	802 842700	58	14

0	0	0	0	4417 057000	59	15
0	0	0	0	1382.254000	60	16
0	0	0	0	1358 823000	61	17
0	0	0	0	1911 960000	62	18
0	0	0	0	1102 254000	63	20
0	0	0	0	739 411300	64	21
0	0	0	0	1425 097000	65	22
0	0	0	0	1365 686000	66	23
0	0	0	0	80 000000	67	24
0	0	0	0	3370 195000	68	25
0	0	0	0	869 116900	69	26
0	0	0	0	699 411300	70	28
0	0	0	0	273 137100	71	30
0	0	0	0	602 842700	72	31
0	0	0	0	2041 666000	73	32
0	0	0	0	1085 685000	74	33
0	0	0	0	2787 940000	75	34
0	0	0	0	1695 391000	76	35
0	0	0	0	296 568500	77	36
0	0	0	0	1358 823000	78	37
0	0	0	0	1874 803000	79	38
0	0	0	0	402 842700	80	39
0	0	0	0	998 822500	81	40
0	0	0	0	442 842700	82	41
0	0	0	0	5098 722000	83	42
0	0	0	0	2154 803000	84	43
0	0	0	0	1391 960000	85	44
0	0	0	0	2775 392000	86	46
0	0	0	0	675 979800	87	47
0	0	0	0	2025 097000	88	48
0	0	0	0	426 274200	89	49
0	0	0	0	5655 878000	90	50
0	0	0	0	2907 940000	91	51
0	0	0	0	369 705600	92	55
0	0	0	0	675 979800	93	56
0	0	0	0	1731 371000	94	57
0	0	0	0	249 705600	95	58
0	0	0	0	1422 254000	96	59
0	0	0	0	706 274200	97	60
0	0	0	0	1398 823000	98	62
0	0	0	0	715 979800	99	64
0	0	0	0	1012 548000	100	65
0	0	0	0	1938 234000	101	66
0	0	0	0	402 842700	102	67
0	0	0	0	136 568500	103	68
0	0	0	0	273 137100	104	70
0	0	0	0	1349 117000	105	72
0	0	0	0	2374 215000	106	73
0	0	0	0	513 137100	107	74
0	0	0	0	489 705600	108	75
0	0	0	0	2147 940000	109	76
0	0	0	0	2867 940000	110	77
0	0	0	0	193 137100	111	78
0	0	0	0	1985 097000	112	80
0	0	0	0	612 548300	113	81
0	0	0	0	2517 646000	114	82
0	0	0	0	1212 548000	115	83
0	0	0	0	2547 940000	116	85
0	0	0	0	2368 529000	117	87

0	0	0	0	1342 254000	118	88
0	0	0	0	2550 783000	119	89
0	0	0	0	1422 254000	120	92
0	0	0	0	369 705600	121	95
0	0	0	0	466 274200	122	96
0	0	0	0	5722 152000	123	97
0	0	0	0	892 548300	124	98
0	0	0	0	336 568500	125	99
0	0	0	0	2505 097000	126	100
0	0	0	0	659 411300	127	101
0	0	0	0	1318 823000	128	102
0	0	0	0	369 705600	129	103
0	0	0	0	4057 057000	130	106
0	0	0	0	2781 077000	131	109
0	0	0	0	2328 529000	132	110
0	0	0	0	579 411300	133	111
0	0	0	0	2081 666000	134	112
0	0	0	0	369 705600	135	113
0	0	0	0	313 137100	136	114
0	0	0	0	3993 626000	137	115
0	0	0	0	482 842700	138	116
0	0	0	0	4109 606000	139	117
0	0	0	0	826 274200	140	118
0	0	0	0	902 254000	141	119
0	0	0	0	2431 960000	142	120
0	0	0	0	369 705600	143	121
0	0	0	0	1311 960000	144	123
0	0	0	0	5682 151000	145	125
0	0	0	0	2581 077000	146	128
0	0	0	0	1492 549000	147	129
0	0	0	0	2783 920000	148	130
0	0	0	0	3167 352000	149	135
0	0	0	0	336 568500	150	136
0	0	0	0	1575 391000	151	137
0	0	0	0	3477 646000	152	139
0	0	0	0	1099 411000	153	140
0	0	0	0	1578 234000	154	141
0	0	0	0	1514 803000	155	145
0	0	0	0	4476 468000	156	146
0	0	0	0	702 254000	157	148
0	0	0	0	506 274200	158	149
0	0	0	0	482 842700	159	150
0	0	0	0	1391 960000	160	151
0	0	0	0	3773 038000	161	152
0	0	0	0	682 842700	243	243
0	0	0	0	1075 980000	244	244
0	0	0	0	2027 940000	245	245
0	0	0	0	1591 960000	246	246
0	0	0	0	692 548300	247	247
0	0	0	0	56 568540	248	248
0	0	0	0	369 705600	249	249
0	0	0	0	932 548300	250	250
0	0	0	0	562 842700	251	251
0	0	0	0	1299 411000	252	252
0	0	0	0	96 568540	253	253
0	0	0	0	176 568500	254	254
0	0	0	0	1231 960000	255	255
0	0	0	0	2347 940000	256	256
0	0	0	0	1365 686000	257	257

0	0	0	0	626 274200	258	258
0	0	0	0	4729 016000	259	259
0	0	0	0	955 979800	260	260
0	0	0	0	3160 489000	261	261
0	0	0	0	2378 234000	262	262
0	0	0	0	1069 117000	263	263
0	0	0	0	120 000000	264	264
0	0	0	0	2281 666000	265	265
0	0	0	0	273 137100	266	266
0	0	0	0	1485 686000	267	267
0	0	0	0	689 705600	268	268
0	0	0	0	862 254000	269	269
0	0	0	0	892 548300	270	270
0	0	0	0	3393 626000	271	271
0	0	0	0	1601 666000	272	272
0	0	0	0	160 000000	273	273
0	0	0	0	3207 352000	274	274
0	0	0	0	972 548300	275	275
0	0	0	0	909 116900	276	276
0	0	0	0	553 137100	277	277
0	0	0	0	732 548300	278	278
0	0	0	0	1598 823000	279	279
0	0	0	0	1069 117000	280	280
0	0	0	0	256 568500	281	281
0	0	0	0	1278 823000	282	282
0	0	0	0	682 842700	283	283
0	0	0	0	932 548300	284	284
0	0	0	0	772 548300	285	285
0	0	0	0	1135 391000	286	286
0	0	0	0	2844 509000	287	287
0	0	0	0	1405 686000	288	288
0	0	0	0	1191 960000	289	289
0	0	0	0	1975 392000	290	290
0	0	0	0	2481 666000	291	291
0	0	0	0	120 000000	292	292
0	0	0	0	1035 980000	293	293
0	0	0	0	369 705600	294	294
0	0	0	0	10195 770000	295	295
0	0	0	0	5086 173000	296	296

FNODE_ = Internal node number for the beginning of an arc (from-node)

TNODE_ = Internal node number for the end of an arc (to-node)

L.POLY_ = Internal number for the left polygon

R.POLY_ = internal number for the right polygon

LENGTH = Length of each arc measured in coverage units

STREAM_ = Internal arc number

STREAM_ID = Stream-ID

APPENDIX D

Table 6.2 The "pat.dbf" File of the Vegetable Farms Map of the Te-Chi Reservoir Watershed

AREA	PERIMETER	VEGETABL_	VEGETABL_I	LANDUSE
-3450228.000000	99084.590000	1	0	
218419.600000	4272.860000	2	148	V
140387.100000	4405.426000	3	149	V
45748.260000	1860.044000	4	153	V
21941.220000	1300.698000	5	156	V
3267.586000	313.867500	6	0	
1434.078000	156.931000	7	164	V
191938.600000	6947.825000	8	184	V
2992.098000	265.325300	9	188	V
15202.320000	720.244000	10	194	V
6693.203000	416.664100	11	195	V
10947.520000	517.653000	12	214	V
5606.078000	529.838100	13	0	
1883.910000	173.225900	14	0	
125944.500000	1708.999000	15	236	V
75221.720000	1552.847000	16	241	V
10552.500000	488.069000	17	262	V
9652.672000	536.769800	18	263	V
3917.730000	324.581100	19	264	V
4464.117000	253.600500	20	275	V
3210.680000	282.950200	21	302	V
14519.820000	838.644700	22	304	V
5626.805000	428.397000	23	312	V
15168.610000	799.490100	24	314	V
15876.130000	669.432900	25	317	V
8857.430000	479.950100	26	326	V
31064.940000	1665.745000	27	334	V
39703.670000	2107.025000	28	345	V
13986.750000	536.834000	29	353	V
5798.848000	345.574100	30	354	V
7027.563000	443.014300	31	411	V
24525.730000	724.898700	32	438	V
16005.360000	831.753500	33	443	V
43331.460000	1044.744000	34	449	V
43056.790000	1536.946000	35	500	V
91423.470000	3302.516000	36	501	V
15926.810000	714.944400	37	526	V
2382.055000	241.309000	38	539	V
7912.422000	535.533000	39	556	V
51675.950000	1485.429000	40	577	V
9174.590000	550.438700	41	599	V
13738.550000	616.008600	42	619	V
15478.710000	664.878200	43	644	V
14725.780000	1253.900000	44	676	V
10727.830000	969.223300	45	680	V
4952.457000	481.682300	46	810	V
6285.234000	541.026900	47	825	V
272289.900000	3633.878000	48	920	V
143989.600000	2699.589000	49	927	V
4582.969000	292.213900	50	929	V
11064.800000	470.469200	51	979	V
46968.000000	1326.083000	52	983	V
10513.080000	494.719100	53	1016	V
5621.020000	310.408200	54	1017	V
99315.940000	2203.641000	55	1034	V
13869.540000	543.890300	56	1037	V

APPENDIX D

Table 6.2 The "pat.dbf" File of the Vegetable Farms Map of the Te-Chi Reservoir Watershed

90333 860000	1536 558000	57	1042	V
13654 100000	525 920100	58	1047	V
6382 988000	355 964300	59	1050	V
39876 820000	2020 862000	60	1062	V
2448 105000	205 553700	61	0	
8519 871000	369 342100	62	1065	V
46884 680000	1152 359000	63	1075	V
21150 510000	705 015200	64	1076	V
4625 586000	281 015700	65	1079	V
36106 410000	1683 497000	66	1099	V
271 035200	65 770700	67	0	
6001 016000	314 600900	68	1153	V
11961 050000	483 464200	69	1926	V
5524 781000	326 440200	70	1934	V
9070 816000	675 668900	71	1950	V
96563 470000	1738 859000	72	1959	V
48086 140000	1340 978000	73	1986	V
32276 780000	931 959200	74	2000	V
3566 344000	302 925300	75	2045	V
59078 020000	1494 687000	76	2048	V
1088 961000	129 836200	77	2067	V
5513 660000	323 885200	78	2069	V
141578 700000	3108 471000	79	2078	V
12403 340000	618 908600	80	2097	V
5048 609000	321 336400	81	2107	V
2561 602000	297 405900	82	0	
4525 387000	341 265300	83	2113	V
370 035200	80 694260	84	2143	V
12110 700000	481 349300	85	2153	V
3607 371000	305 305000	86	2194	V
9901 199000	514 192700	87	2199	V
5118 652000	297 398800	88	2205	V
32968 050000	1127 395000	89	2609	V
15627 980000	690 046700	90	2617	V
230521 900000	3367 702000	91	2620	V
2339 871000	192 154100	92	0	
31598 280000	1345 450000	93	2633	V
2103 922000	179 481600	94	0	
144672 100000	4061 283000	95	2659	V
48339 030000	1138 529000	96	2665	V
81900 440000	2322 125000	97	2683	V
67621 200000	2067 832000	98	2687	V
9730 125000	636 985200	99	2704	V

AREA = Area of each polygon measured in coverage units
 PERIMETER = Length of each polygon boundary measured in coverage units
 VEGETABL_ = Internal polygon number
 VEGETABL_I = Vegetable-ID
 LANDUSE = Mark of a type of land use (vegetable farm)

APPENDIX F

Table 6.4 Statistical Programs for Modification of the GIS Map
(Measured Points: 2P / 2Q)

ID 2P / 2Q	GPS Receiver A Latitude (XA)			Decimal Notation	Longitude (YA)			Decimal Notation
	Sexagesimal Notation	Sexagesimal Notation	Sexagesimal Notation		Sexagesimal Notation	Sexagesimal Notation	Sexagesimal Notation	
Item	Degree	Minute	Second	Degree	Degree	Minute	Second	Degree
1	120	59	58	120 9994444	24	15	0	24 25
2	121	0	1	121 0002778	24	14	58	24 24944444
3	121	0	1	121 0002778	24	14	59	24 24972222
4	120	0	2	120 0005556	24	14	57	24 24916667
5	121	0	0	121	24	14	58	24 24944444
6	121	0	1	121 0002778	24	14	58	24 24944444
7	121	0	0	121	24	15	0	24 25
8	121	0	0	121	24	15	0	24 25
9	120	59	59	120 9997222	24	15	1	24 25027778
10	121	0	1	121 0002778	24	15	2	24 25055556
11	120	59	59	120 9997222	24	15	0	24 25
12	120	59	59	120 9997222	24	15	2	24 25055556
13	121	0	0	121	24	15	1	24 25027778
14	121	0	1	121 0002778	24	15	1	24 25027778
15	120	59	59	120 9997222	24	14	59	24 24972222
16	120	59	59	120 9997222	24	14	59	24 24972222
17	120	59	59	120 9997222	24	15	0	24 25
18	120	59	59	120 9997222	24	14	59	24 24972222
19	120	59	57	120 9991667	24	15	0	24 25
20	120	59	58	120 9994444	24	15	1	24 25027778
21	121	0	2	121 0005556	24	15	1	24 25027778
22	121	0	3	121 0008333	24	15	1	24 25027778
23	121	0	1	121 0002778	24	15	2	24 25055556
24	121	0	1	121 0002778	24	14	59	24 24972222
25	121	0	0	121	24	15	0	24 25
26	120	59	58	120 9994444	24	14	59	24 24972222
27	121	0	0	121	24	15	0	24 25
28	120	59	58	120 9994444	24	15	0	24 25
29	121	0	3	121 0008333	24	15	1	24 25027778
30	121	0	1	121 0002778	24	15	1	24 25027778
31	121	0	1	121 0002778	24	15	2	24 25055556
32	120	59	59	120 9997222	24	15	1	24 25027778
33	120	59	58	120 9994444	24	15	2	24 25055556
34	121	0	0	121	24	14	59	24 24972222
35	121	0	0	121	24	14	59	24 24972222
36	121	0	0	121	24	15	0	24 25
37	121	0	1	121 0002778	24	15	1	24 25027778
38	121	0	2	121 0005556	24	15	1	24 25027778
39	121	0	1	121 0002778	24	15	2	24 25055556
40	121	0	2	121 0005556	24	14	59	24 24972222
41	121	0	3	121 0008333	24	15	0	24 25
42	120	59	59	120 9997222	24	14	58	24 24944444
43	120	59	58	120 9994444	24	14	58	24 24944444
44	121	0	1	121 0002778	24	14	59	24 24972222
45	121	0	1	121 0002778	24	14	59	24 24972222
46	120	59	59	120 9997222	24	15	0	24 25
47	120	59	58	120 9994444	24	15	1	24 25027778
48	121	0	2	121 0005556	24	14	59	24 24972222
49	121	0	1	121 0002778	24	15	0	24 25
50	121	0	1	121 0002778	24	15	1	24 25027778

GPS Receiver B Latitude (XB)			Longitude (YB)				
Sexagesimal Notation			Decimal Notation	Sexagesimal Notation			Decimal Notation
Degree	Minute	Second	Degree	Degree	Minute	Second	Degree
121	20	1	121.3336111	24	22	30	24.375
121	20	1	121.3336111	24	22	31	24.37527778
121	20	2	121.3338889	24	22	31	24.37527778
121	20	1	121.3336111	24	22	31	24.37527778
121	20	3	121.3341667	24	22	30	24.375
121	20	1	121.3336111	24	22	30	24.375
121	20	2	121.3338889	24	22	30	24.375
121	20	1	121.3336111	24	22	30	24.375
121	19	59	121.3330556	24	22	29	24.37472222
121	19	58	121.3327778	24	22	29	24.37472222
121	20	2	121.3338889	24	22	29	24.37472222
121	19	58	121.3327778	24	22	30	24.375
121	20	1	121.3336111	24	22	30	24.375
121	20	1	121.3336111	24	22	30	24.375
121	20	1	121.3336111	24	22	29	24.37472222
121	19	58	121.3327778	24	22	29	24.37472222
121	19	59	121.3330556	24	22	28	24.37444444
121	19	58	121.3327778	24	22	29	24.37472222
121	19	59	121.3330556	24	22	30	24.375
121	19	57	121.3325	24	22	31	24.37527778
121	19	57	121.3325	24	22	31	24.37527778
121	20	0	121.3333333	24	22	29	24.37472222
121	20	0	121.3333333	24	22	29	24.37472222
121	19	58	121.3327778	24	22	30	24.375
121	19	57	121.3325	24	22	31	24.37527778
121	20	1	121.3336111	24	22	30	24.375
121	20	1	121.3336111	24	22	30	24.375
121	19	2	121.3172222	24	22	29	24.37472222
121	20	3	121.3341667	24	22	29	24.37472222
121	19	58	121.3327778	24	22	30	24.375
121	20	59	121.3497222	24	22	29	24.37472222
121	20	2	121.3338889	24	22	29	24.37472222
121	19	58	121.3327778	24	22	30	24.375
121	19	59	121.3330556	24	22	30	24.375
121	20	1	121.3336111	24	22	30	24.375
121	19	59	121.3330556	24	22	29	24.37472222
121	20	0	121.3333333	24	22	29	24.37472222
121	20	0	121.3333333	24	22	30	24.375
121	20	0	121.3333333	24	22	30	24.375
121	20	0	121.3333333	24	22	30	24.375
121	20	1	121.3336111	24	22	31	24.37527778
121	19	59	121.3330556	24	22	32	24.37555556
121	19	58	121.3327778	24	22	33	24.37583333
121	19	58	121.3327778	24	22	32	24.37555556
121	20	1	121.3336111	24	22	33	24.37583333
121	20	2	121.3338889	24	22	32	24.37555556
121	19	59	121.3330556	24	22	30	24.375
121	19	59	121.3330556	24	22	29	24.37472222
121	20	1	121.3336111	24	22	28	24.37444444
121	20	2	121.3338889	24	22	27	24.37416667

Item	X(XA - XB)	X(XA - XB)^2	Y(YA - YB)	Y(YA - YB)^2	(X(XA - XB)-uX(XA - XB))^2	(Y(YA - YB)-uY(YA - YB))^2
1	-0.334166667	0.111667361	-0.125	0.015625	0.000365447	2.77778E-10
2	-0.333333333	0.111111111	-0.125833333	0.015834028	0.000398003	7.225E-07
3	-0.333611111	0.111296373	-0.125555556	0.015764198	0.000386996	3.27438E-07
4	-1.333055556	1.777037114	-0.126111111	0.015904012	0.959953607	1.27188E-06
5	-0.334166667	0.111667361	-0.125555556	0.015764198	0.000365447	3.27438E-07
6	-0.333333333	0.111111111	-0.125555556	0.015764198	0.000398003	3.27438E-07
7	-0.333888889	0.11148179	-0.125	0.015625	0.000376144	2.77778E-10
8	-0.333611111	0.111296373	-0.125	0.015625	0.000386996	2.77778E-10
9	-0.333333333	0.111111111	-0.124444444	0.01548642	0.000398002	2.90401E-07
10	-0.3325	0.11055625	-0.124166667	0.015417361	0.000431947	6.66944E-07
11	-0.334166667	0.111667361	-0.124722222	0.015555633	0.000365447	6.8179E-08
12	-0.333055556	0.110926003	-0.124444444	0.01548642	0.000409163	2.90401E-07
13	-0.333611111	0.111296373	-0.124722222	0.015555633	0.000386996	6.8179E-08
14	-0.333333333	0.111111111	-0.124722222	0.015555633	0.000398003	6.8179E-08
15	-0.333888889	0.11148179	-0.125	0.015625	0.000376144	2.77778E-10
16	-0.333055556	0.110926003	-0.125	0.015625	0.000409163	2.77778E-10
17	-0.333333333	0.111111111	-0.124444444	0.01548642	0.000398002	2.90401E-07
18	-0.333055556	0.110926003	-0.125	0.015625	0.000409163	2.77778E-10
19	-0.333888889	0.11148179	-0.125	0.015625	0.000376144	2.77778E-10
20	-0.333055556	0.110926003	-0.125	0.015625	0.000409163	2.77778E-10
21	-0.331944444	0.110187114	-0.125	0.015625	0.000455348	2.77778E-10
22	-0.3325	0.11055625	-0.124444444	0.01548642	0.000431947	2.90401E-07
23	-0.333055556	0.110926003	-0.124166667	0.015417361	0.000409163	6.66944E-07
24	-0.3325	0.11055625	-0.125277778	0.015694522	0.000431947	8.66975E-08
25	-0.3325	0.11055625	-0.125277778	0.015694522	0.000431947	8.66975E-08
26	-0.334166667	0.111667361	-0.125277778	0.015694522	0.000365447	8.66975E-08
27	-0.333611111	0.111296373	-0.125	0.015625	0.000386996	2.77778E-10
28	-0.317777778	0.100982716	-0.124722222	0.015555633	0.001260644	6.8179E-08
29	-0.333333333	0.111111111	-0.124444444	0.01548642	0.000398003	2.90401E-07
30	-0.3325	0.11055625	-0.124722222	0.015555633	0.000431947	6.8179E-08
31	-0.349444444	0.12211142	-0.124166667	0.015417361	1.47371E-05	6.66944E-07
32	-0.334166667	0.111667361	-0.124444444	0.01548642	0.000365447	2.90401E-07
33	-0.333333333	0.111111111	-0.124444444	0.01548642	0.000398003	2.90401E-07
34	-0.333055556	0.110926003	-0.125277778	0.015694522	0.000409163	8.66975E-08
35	-0.333611111	0.111296373	-0.125277778	0.015694522	0.000386996	8.66975E-08
36	-0.333055556	0.110926003	-0.124722222	0.015555633	0.000409163	6.8179E-08
37	-0.333055556	0.110926003	-0.124444444	0.01548642	0.000409163	2.90401E-07
38	-0.332777778	0.110741049	-0.124722222	0.015555633	0.000420478	6.8179E-08
39	-0.333055556	0.110926003	-0.124444444	0.01548642	0.000409163	2.90401E-07
40	-0.332777778	0.110741049	-0.125277778	0.015694522	0.000420478	8.66975E-08
41	-0.332777778	0.110741049	-0.125277778	0.015694522	0.000420478	8.66975E-08
42	-0.333333333	0.111111111	-0.126111111	0.015904012	0.000398002	1.27188E-06
43	-0.333333333	0.111111111	-0.126388889	0.015974151	0.000398003	1.97559E-06
44	-0.3325	0.11055625	-0.125833333	0.015834028	0.000431947	7.225E-07
45	-0.333333333	0.111111111	-0.126111111	0.015904012	0.000398003	1.27188E-06
46	-0.334166667	0.111667361	-0.125555556	0.015764198	0.000365447	3.27438E-07
47	-0.333611111	0.111296373	-0.124722222	0.015555633	0.000386996	6.8179E-08
48	-0.3325	0.11055625	-0.125	0.015625	0.000431947	2.77778E-10
49	-0.333333333	0.111111111	-0.124444444	0.01548642	0.000398003	2.90401E-07
50	-0.333611111	0.111296373	-0.123888889	0.015348457	0.000386996	1.19781E-06
Sum	-17.66416667	7.220515664	-6.249166667	0.781057485	0.980059983	1.5804E-05

N = 50
 df = 48
 ux(XA-XB) = -0.353283333 Var=(Sigma x(XA-XB))^2= 0.0196012
 uy(YA-YB) = -0.124983333 Var=(Sigma y(YA-YB))^2= 3.1608E-07
 StDX(XA-XB) = 0.000384207
 StDY(YA-YB) = 9.99067E-14
 ux(XA-XB) +/- 2 StDX(XA-XB) = -0.353283333 +/- 0.000768414 at 95% confidence
 uy(YA-YB) +/- 2 StDY(YA-YB) = -0.124983333 +/- 1.99813E-13 at 95% confidence
 Use Receiver A and Receiver B to measure point P and point Q, respectively:
 The coordinates of point P measured by Receiver A = (121.0002778 24.25027778)
 The coordinates of point Q measured by Receiver B = (120.9994444 24.29222222)

The landmarks' coordinates of point P and point Q
 point P = (121 24.25)
 point Q = (121 24.29166667)

Bias between the landmark's coordinates of point P and the measured coordinates of point P from Receiver A:
 =====> Bias = (-0.000277778 -0.000277778)

The predicted coordinates of point Q measured by Receiver B
 =====> Component X= 121.3530056 +/- 0.000768414 t 95% confidence
 Component Y= 24.41637222 +/- 1.99813E-13 t 95% confidence

The differential value between the predicted coordinates of point Q and the landmark coordinates by Receiver B =
 Component X = 0.353005556 +/- 0.000768414 at 95% confidence
 Component Y = 0.124705556 +/- 1.99813E-13 at 95% confidence

Convert to Sexagesimal notation:

	+/-	Degree	Minute	Second		Degree	Minute	Second
Component X =	-	0	0	0.488016	+/-	0	0	5.01937E-07
Component Y =	-	0	0	0.8799984	+/-	0	0	7.65418E-10

APPENDIX G

Table 6.10 The Area and Location of the Sinkholes in the Te-Chi Reservoir Watershed

Sinkhole ID	Area (hectare)	Location (arca)	Sinkhole ID	Area (hectare)	Location (arca)	Sinkhole ID	Area (hectare)	Location (arca)
1	112736 9068	A	79	123073 1264	A	157	55492 7936	C
2	25273 9456	A	80	82689 7568	B	158	2573134 907	A
3	102950 1208	A	81	50273 1744	A	159	29909 7916	A
4	74894 6676	A	82	108856 532	C	160	20054 3264	A
5	56694 6796	A	83	170015 3596	C	161	283095 6624	A
6	22561 1172	A	84	32553 9408	A	162	616601 8576	B
7	82724 0964	A	85	32622 62	A	163	609115 8248	B
8	36159 5988	A	86	25445 6436	A	164	44916 1968	A
9	99172 7648	A	87	37704 8808	A	165	20638 0996	A
10	12636 9728	A	88	2488899 868	A	166	61399 2048	A
11	21599 6084	A	89	80492 0224	C	167	184644 0292	A
12	123107 466	A	90	54187 8888	B	168	122248 976	A
13	460253 6588	A	91	1218025 612	A	169	198997 982	A
14	18096 9692	A	92	114556 9156	C	170	82449 3796	C
15	100924 0844	A	93	15075 0844	A	171	11435 0868	C
16	1875045 179	A	94	2963610 499	A	172	32107 526	C
17	19916 968	A	95	406477 8452	C	173	41791 2932	B
18	14800 3676	A	96	40417 7092	C	174	68747 8792	B
19	41653 9348	A	97	30562 244	C	175	29806 7728	B
20	28810 9244	A	98	205556 8456	C	176	42787 1416	C
21	144157 6408	A	99	1163185 271	A	177	12636 9728	B
22	5798207 12	A	100	186979 122	C	178	337901 664	B
23	55595 8124	A	101	68404 4832	A	179	61193 1672	B
24	2374068 246	A	102	339034 8708	C	180	13735 84	B
25	23556 9656	A & B	103	58205 622	C	181	22046 0232	B
26	183459038.3	A	104	28124 1324	C	182	34 3396	B
27	27368 6612	A	105	532984 9316	C	183	163010 0812	B
28	152742 5408	A	106	66412 7864	C	184	207170 8068	B
29	34511 298	A	107	67958 0684	C	185	60025 6208	B
30	1386907 765	A	108	39421 8608	C	186	34133 5624	B
31	72628 254	A	109	83548 2468	B	187	210433 0688	B
32	102709 7436	A	110	78431 6464	A	188	608429 0328	B
33	417123 1212	A	111	109371 626	B	189	108719 1736	B
34	11823948 43	C	112	36537 3344	A	190	413689 1612	B
35	114419 5472	C	113	827240 964	C	191	846436 8004	B
36	43714 3108	C	114	55252 4164	C	192	500602 6888	B
37	574123 7724	A	115	59750 904	C	193	119398 7892	B
38	67236 9368	C	116	396416 3424	A	194	87188 2444	B
39	15452 82	B	117	57896 5656	C	195	96356 9176	B
40	63459 5808	B	118	42237 708	C	196	85608 6228	B
41	30390 546	B	119	255314 926	A	197	407885 7688	B
42	52951 6632	B	120	2430934 624	C	198	120497 6564	B
43	32828 6576	A	121	27609 0384	C	199	157687 4432	B
44	5391 1172	A	122	70293 1612	C	200	105697 2888	C
45	81728 248	A	123	99869 746	C	201	290375 6576	C
46	75341 0824	C	124	35266 7692	C	202	111947 096	C
47	662891 6384	C	125	631505 244	B	203	161224 422	C
48	28398 8492	A	126	30493 5648	A	204	36983 7492	C
49	222245 8912	A	127	626869 398	A	205	53192 0404	C
50	27918 0948	B	128	18577 7236	C	206	67168 2576	C
51	300917 9148	B	129	21908 6648	C	207	149823 6748	C
52	40246 0112	B	130	28639 2264	C	208	1099176 256	C
53	120841 0524	B	131	140964 058	B	209	44092 0464	C
54	38322 9936	B	132	1439790 749	A	210	190344 4028	C
55	175818 752	B	133	61364 8652	C	211	41173 1804	C
56	1153776 22	A	134	183888 558	B	212	75753 1576	C
57	738644 796	A	135	75272 4032	B	213	4086 4124	C
58	49208 6468	A	136	204080 2428	A	214	28604 8868	C
59	38494 6916	C	137	241922 482	A	215	37121 1076	C
60	275369 2524	C	138	79015 4196	C	216	17890 9316	C
61	53020 3424	A	139	65485 6172	C	217	16757 7248	C
62	54909 0204	A	140	35644 5048	C	218	223379 0998	C
63	756467 0484	A	141	42031 6704	A	219	53672 7948	C
64	29532 056	A	142	579446 4104	A	220	32485 2616	C
65	77161 0812	A	143	18852 4404	A	221	40967 1428	C
66	378628 4296	A	144	549124 5436	A	222	172831 2068	C
67	100855 4052	A	145	69915 4256	A	223	80148 6264	C
68	30699 6024	B	146	310326 9652	C	224	10892992 21	C
69	72937 3104	B	147	11091 6908	C	225	93128 9952	C
70	14525 6508	C	148	65897 6924	C	226	94021 8248	C
71	103739 9316	C	149	49895 4388	A	227	36399 976	C
72	295457 9184	A	150	208235 3344	A	228	43576 9524	C
73	28913 9432	A	151	68026 7476	A			
74	90828 242	A	152	39112 8044	A			
75	68679 2	A	153	147179 5256	A			
76	41276 1992	A	154	17272 8188	C			
77	41962 9912	A	155	53981 8512	C			
78	110230 116	A	156	34373 9396	C			